Sediment Transport and Morphological Response of a Semi-Alluvial Channel

Insights from a Froude Scaled Laboratory Model

by

David Steven Luzi

MSc, The University of British Columbia, 2000

A THESIS SUBMITTED IN PARTIAL FULFILLMENT OF THE REQUIREMENTS FOR THE DEGREE OF

DOCTOR OF PHILOSOPHY

in

The Faculty Graduate and Postdoctoral Studies

(Geography)

THE UNIVERSITY OF BRITISH COLUMBIA

(Vancouver)

August 2014

Abstract

Laboratory physical models have been used in geomorphology for over a century. Physical models are a useful tool for understanding and observing phenomenon that are difficult or impossible to observe in the field. The objective of this study was to understand the long-term evolution of a semi-alluvial channel in terms of its morphology and sediment transport under various scenarios of constant sediment supply and discharge. Specifically, the research aimed to investigate (1) effects of various flows and sediment feed rates on surface textures and sediment output, (2) relationship between channel storage, and the (3) morphology and sediment transport sediment transport processes and pathways. These objectives were addressed by building a Froude scaled physical model based on the irregular meandering planform of Fishtrap Creek, and conducting ten experiments of varying temporal lengths, discharge and feed rates. The model successfully replicated pool-riffle and plane-bed morphologies.

The effects on the characteristics of the bed surface and transported sediment under differing regimes of discharge and sediment feed were investigated. Scaled formative flows ranging from 2-yr to over 150-yr return period events were employed. The results indicated that even with discharges exceeding the 10-yr event, full mobility was not observed. This slight but persistent size-selectivity produced long-term aggradation and surface coarsening.

The effects of varying sediment supply and discharge in channel storage and morphology were explored. Results showed that sediment transport rates varied both spatially and temporally. The variability was more dependent upon changes in channel morphology than adjustments in the grain size distribution of the surface. Cycles of aggradation-degradation were observed to occur without changes in sediment supply of discharge and that they tended to occur in periods when sediment output approximately equaled sediment feed rates.

Lastly, one experiment was selected to describe sediment transport processes and pathways. Primary information regarding sediment pathways was obtained through the observation of bedload sheet movement and migration during the experiments, as well as through subsequent review of videos made during the experiments. The behaviour of bedload sheets also shed new information on how sediment sorting through a pool varies.

Preface

This dissertation presents research conducted by David Luzi in collaboration with his supervisor, Dr. Brett Eaton. David Luzi was the primary investigator and responsible for the design of the research and the collection, analysis and interpretation of the data. Dr. Brett Eaton and Dr. Marwan Hassan provided analytical support and timely reviews throughout the research and the preparation of this dissertation.

Table of Contents

List of Tables

List of Figures

Acknowledgements

> *"By the time it came to the edge of the Forest, the stream had grown up, so that it was almost a river, and, being grown-up, it did not run and jump and sparkle along as it used to do when it was younger, but moved more slowly. For it knew now where it was going, and it said to itself, "There is no hurry. We shall get there some day." But all the little streams higher up in the Forest went this way and that, quickly, eagerly, having so much to find out before it was too late." Milne* (1928)

Numerous people have been involved in this project. My supervisor Brett Eaton encouraged me to return from the field and to explore the laboratory as another means of understanding fluvial processes. Marwan, although late to the official party, has been part of this endeavour since the beginning and has always been open to conversations on geomorphology.

I appreciate Drs. Dan Moore, Peter Ashmore and Sarah Gergel for reviewing the thesis, their comments resulted in a much improved final product.

I am thankful for the friendship from my fellow lab mates at the beginning of this journey, Ashley Perkins, Jeff Phillips, and Christie Andrews. I would also like to thank Andre Zimmermann for his help with coding Labview, troubleshooting problems and for being open and willing to help at many points along the way. Thanks also to Mike, Jen, Jaclyn, Michael, Dylan and Sarah for all of your help in conducting the experiments and sieving sediment.

This work could not have happened with out the support of my family. To my wife Marla, I hope to one day to repay the patience and understanding you have given me during this journey. To Ariel and Zoë, my amazing girls, whose arrival during this project showed me that being a father is the most important thing in life.

Chapter 1

Preamble

While sitting on the floodplain of Fishtrap Creek and observing how the channel was responding to a recent fire which devastated the riparian zone, I began to think of what happens to the channel during the 100 years or so between disturbances. During my earlier work at Carnation Creek, I found that, on average, channel disturbances, inferred by ages of log jams, occurred almost every 20 years and that the locations of same aged log jams were spatially distributed throughout the channel's length. Therefore, as one reach responded to some channel disturbance, another reach had a decade or two to adjust from the previous disturbance, and at another it may have been a century or two. At Carnation Creek, channel recovery appeared to occur relatively rapidly, and most of the time in any given reach of the river, the channel remained within its banks, which were in turn influenced by the forest that held them together and the size and quantity of sediment that composed the channel bed. This disturbance regime, seemed to be similar to what I was currently observing at Fishtrap Creek. From the age of the trees in the floodplain and the evidence of historical channel activity, Fishtrap Creek appeared to spend most of the time exhibiting long periods of relative lateral stability.

Once I had begun to realize that it was the longer time frame, the one which occurred in between disturbances, that held the more interesting questions and answers to river behaviour, I knew I must return from the field and head into the laboratory. Space for time studies are a common and useful tool in field based geomorphology, but sometimes can introduce more questions than answers. In the laboratory environment, one can control the forcing functions, and with proper scaling can observe morphological responses over much longer time scales than is achievable in the field.

1.1 Introduction

The main objective of this project is to provide a better understanding of the pathways, or process-form interactions responsible for channel response. Although advancements have been made in the understanding of how some channel characteristics react to changes in the governing conditions the broader understanding of channel form response is still limited. This limitation is partly due to limits of time and budgets for long-term field programs, but is also due to the use of overly simplistic channels in laboratory environments, where longer term channel morphodynamics can be investigated. Understanding the response mechanisms for mountain gravel-bed streams is of growing importance in regions such as British Columbia with large-scale industrial forest operations and where pressure to develop these systems for small scale power generation and impacts due to transmission lines, pipelines and mining is increasing.

1.2 Literature Review

1.2.1 Process Response Models

The character and behaviour of a stream at any particular location reflects the net effect of landscape, upstream, and local basin variables, referred to as governing conditions, that exert control on channel morphology. At the reach scale, the frequency, magnitude and duration of streamflow and the valley slope (which together determine transport capacity), the frequency, volume and size distribution of sediment input (i.e. sediment supply), and the boundary materials (including both alluvial and non-alluvial material and vegetation), determine dependent (response) channel variables, such as width, depth, bed slope, resistance and surface grain size. Engineers, geologists and geomorphologists have long pursued some methodology to explain and/or predict channel response to changes in governing conditions. However, it is important to determine at what temporal scale the information needed.

The importance of temporal scale in fluvial geomorphology is that it determines what the independent and dependent variables are, because at some point, over a long enough time span, most variables become dependent (*Schumm*, 1977). *Schumm and Lichty* (1965) proposed that three time scales exist in geomorphology:

- cyclic or geologic time — which is at the scale of landscape erosion cycles (millions of years);
- graded time — a shorter period than cyclic during which a graded condition or dynamic equilibrium exists (tens to hundreds of years); and,
- steady time — during this time a static equilibrium may exist (less than a month).

For the purposes of investigating channel response to changes in governing conditions, the graded time scale is the span of interest as at this scale channel morphology is dynamically dependent upon the specified governing conditions. However, an analysis at this temporal scale can not simply ignore the historical contingency or conditioning of the channel in understanding its response. Further, the assumption that the morphology of the channel and its governing conditions are 'causally independent of each other' is not necessarily true. Short-term, small scale processes can influence morphodynamics over the longer term and at larger spatial scales (*Lane and Richards*, 1997).

Schumm and Lichty (1965) referred to a graded condition or dynamic equilibrium that exists during graded time. *Mackin* (1948) defined a graded condition or a graded stream as one that, over time, has adjusted its slope to produce a velocity sufficient to transport the sediment supplied with the available discharge and channel characteristics. The graded stream, therefore, is a stream in equilibrium and any change in the governing conditions will result in adjustments in channel slope to absorb the effect of the change (*Mackin*, 1948). This definition overemphasized slope and ignored both adjustments in channel storage and transport capacity (*Lisle and Church*, 2002) amongst others (for example, width, grain size and armouring, and sinuosity). Dynamic equilibrium, discussed as early as *Gilbert* (1880), was defined by *Chorley and Kennedy* (1971) as a circumstance in which fluctuations are balanced about a constantly changing system condition which has a trajectory of unrepeated average states through time.

In the absence of data of a 'sufficient' nature to develop quantitative predictions of channel response to changes in governing conditions, *Lane* (1955) proposed a very general expression:

$$QS \propto Q_s D \tag{1.1}$$

where Q is discharge, S is channel gradient, Q_s is sediment flux of the bedload, and D is sediment size (for Lane it was indexed by the D_{50}). The expression describes the condition under which a river is in equilibrium with its imposed water and sediment fluxes. Here, discharge sets the scale of the channel, and together with gradient determines the rate of energy expenditure, and the morphology is then determined by the size and quantity of sediment delivered to the channel (*Church*, 2006). This equilibrium model then predicts that an increase in discharge can be offset with a decrease in channel gradient, i.e. degradation, or increase in the sediment flux or grain size. It would appear that one limitation in the relationship is that only Q and Q_s are independent variables, as the other variables can all be adjusted by the channel. Thus the equation can be rearranged to have independent (governing conditions) and dependent (response) variables on separate sides:

$$\frac{Q_s}{Q} \propto \frac{S}{D} \tag{1.2}$$

From above it can be seen that any changes in sediment supply or discharge are compensated for by adjustments in the bed slope or surface grain size. As with *Mackin* (1948), this model does not account for changes in the storage of sediment

Since Lane, many more functional relationships have been proposed based on the type and direction of change in sediment supply and/or discharge, and the response (expressed qualitatively as either an increase or decrease) of an expanded set of channel response variables, which may include meander wavelength (λ), channel sinuosity (L), which are both essentially slope metrics, mean depth (d), width (w), and the width-depth ratio (*Schumm*, 1969, 1977; *Nunnally*, 1985; *Simon and Hupp*, 1986; *Kellerhals and Church*, 1989; *Montgomery and Buffington*, 1998). One of the drawbacks of these types of models is they can be indeterminate. For example, the *Schumm* (1969) model indicates that decreasing discharge while increasing sediment supply will produce a decrease in channel depth and sinuosity but either increase or decrease channel width.

One of the main limitations with predicting channel response lies in the number of ways a channel can respond. The primary response modes that have been identified include:

- bed slope (*Mackin*, 1948; *Lane*, 1955);
- channel geometry and planform (*Schumm*, 1969);
- bed texture (*Lane*, 1937; *Dietrich et al.*, 1989); and,
- channel form and roughness (*Madej*, 2001; *Eaton et al.*, 2004; *Gran and Montgomery*, 2005).

Additionally, the nature of the response is contingent upon both historical and existing conditions (*Church*, 1995; *Brewer and Lewin*, 1998; *Eaton and Lapointe*, 2001; *Talbot and Lapointe*, 2002), channel sedimentology (*Simon*, 1992; *Gaeumann et al.*, 2005; *Bartley and Rutherford*, 2005), and sediment supply within a reach and from upstream sources (*Kasai et al.*, 2004; *Schuerch et al.*, 2006). The end result is that similar changes in governing conditions can produce very different channel responses, depending on the local conditions found in different reaches (*Madej and Ozaki*, 1996; *Carling*, 1988).

Although some insight has been gained from process response models, for example bed surface and slope response, a detailed understanding of reach scale response still remains illusive. Specifically, understanding how slope, grain size and bar forms adjust to changes in either sediment supply or discharge and how these adjustments are influenced by historic conditions of the channel. As there are a variety of channel types in a variety of environments, it is necessary to limit the scope of the research for brevity.

In the Pacific Northwest, intermediate-sized forested gravel-bed mountain streams are critical habitat for many aquatic species including salmonids, they supply clean water for downstream users, and are increasingly being utilized for small scale hydro generation. Increasing interest has been brought to these streams in British Columbia as companies search for systems suitable for small scale hydro, as well as attempting to assess impacts of forestry in a results based regulatory environment, and understanding the long-term effects of mining. In Washington, declining salmon stocks have renewed interest in habitat improvements, and thus renewed interest in improving our knowledge of how these systems respond to changes in discharge and sediment supply. The focus of this research is on intermediate-sized forested gravel-bed streams.

Church (1992) identified intermediate streams as having relative roughness (D/d) of 0.1 to 1.0 and channel widths of up to 30 m: the streams of interest here are those with widths between 10 and 20 m. In forested environments, bank strength is increased by root strength (*Millar and Quick*, 1993), which leads to channel stability. Lateral instability in forested channels appears to be related to either changes in the riparian vegetation, such as the result of logging (e.g. *Millar*, 2000) or due to in-channel aggradation of sediment (*Madej* *and Ozaki*, 1996; *Brummer et al.*, 2006). An improved understanding of how response to changes in governing conditions within the channel, may shed additional light on to mechanisms of lateral activity. Channel response can therefore be restricted to changes of variables within channel itself, such as bed topography and surface texture. Thus, in this study, attention will be given to changes in slope, depth, and sediment characteristics, which require measurements of changes in velocity, surface grain size distributions, and channel bedforms.

The type of channels investigated here have been further described as being threshold channels by *Church* (2006). In this channel type bedload transport characteristically occurs only at low intensity during high flows. Threshold channels are relatively stable for long periods of time, except during major floods or following development of in-channel log jams, which may induce local channel aggradation that can lead to lateral channel instability and/or avulsions. Additionally, instability may be related to changes in the boundary conditions either due to riparian disturbance or with an influx of sediment.

Intermediate (or threshold) channels can exhibit either plane-bed or pool-riffle morphologies (*Montgomery and Buffington*, 1997). A plane-bed channel is a largely featureless channel that lacks significant depositional structures, such as channel bars, and is most common at channel gradients of 0.01 to 0.03. Channel bars represent major storage places for bedload and are important flow resistance elements which may evolve in the short term in response to changing flow and sediment transport conditions; bars generally do not occur if the flow depth is less than three times the grain size (*Church and Jones*, 1982). Plane-bed channels commonly exhibit an armoured bed surface, which is indicative of transport capacity being greater the sediment supply (*Dietrich et al.*, 1989). In addition to armouring, bed structures, such as grain imbrication and grain clusters, are common in these streams, and can also lead to decreased sediment mobility (*Lane*, 1937; *Church*, 1998). In contrast to plane-bed channels, pool-riffle channels tend to have regularly occurring bedforms generated by local flow convergence and divergence and may be either freely formed by cross-stream flow and sediment transport, or forced by channel bends and obstructions (e.g. *Lisle*, 1986). This morphology tends to be more responsive to changes in sediment supply and discharge than plane-bed channels.

A brief review of the existing literature on channel response to changes in sediment supply and discharge is provided below.

1.2.2 Sediment Supply

A variety of research papers have documented the effects of sediment supply on channel morphology. The scales of response to changes in sediment supply have been investigated at the grain scale, the bedform scale and the reach scale, as such the research will be reviewed at these three scales.

The response of surface grains to changes in sediment supply has been the focus of much interest for over 20 years. To examine grain response to changes in supply, *Dietrich et al.*

(1989) used a plane-bed flume and observed that a 90% reduction in the feed rate resulted in a 32% increase in the median grain size of the surface. *Dietrich et al.* (1989) proposed $q*$, which is the ratio of sediment transport predicted with and without armouring of the bed surface:

$$q^* = [(\tau_b - \tau_{cs})/(\tau_b - \tau_{ct})]^{1.5} \tag{1.3}$$

in which q^* is the transport ratio, τ_b is the boundary shear stress determined with DuBoys shear stress estimate ($\rho g d S$, where ρ is the density of water and g is gravitational acceleration), τ_{cs} is the critical shear stress for the surface material, and τ_{ct} is the critical shear stress of the transported bedload (following *Hassan and Church*, 2000).

If $q^* = 1$ the sediment supply is so high that no armouring exists; when $q^* = 0$ no sediment is being transported. *Lisle et al.* (1993) observed similar but stronger textural adjustment in experiments using a wider flume with alternate bars. They noted that a 90% reduction in the feed rate resulted in a 62% increase in mean surface grain size. In the case with bars, the bed surface coarsening was accomplished by narrowing of the zone of active bedload transport, accretion of coarse particles onto emerging bar heads, and winnowing of fines in inactive areas of the bed (*Lisle et al.*, 1993). The variability of the active zone in sediment transport was previously noted by *Gilbert* (1914). These observations support the idea that pool-riffle channels may be more sensitive to changes in supply than plane-bed ones. This is likely related to both longitudinal and lateral variability (*Ferguson*, 2003) of the bed surface, which may allow a wider range of response as well as concentrating the effects over a much smaller area of the bed than under plane-bed conditions. The results of a numerical model presented in *Francalanci et al.* (2012) confirmed that the net effect of the variability in the bed surface was an increase in the transport rate over a plane-bed.

In addition to coarsening of the bed surface, decreases in sediment supply (or in the case of *Church et al.* (1998), the elimination of all sediment supply) may contribute to the development of bed surface structures. *Lane* (1937) noted that, over time, the surface of a channel can rearrange itself to become more stable. In follow up experiments to *Church et al.* (1998), *Hassan and Church* (2000) investigated low sediment feed rates over a previously armoured and structured bed and found that increased sediment supply resulted in a reduction in surface armouring but bed structures remained relatively similar. This suggests that bed structures may play a larger role in channel stability over a wider range of fluctuations in sediment supply than does armouring. It is uncertain at this point what effect the combination of bed structures and bars would have in terms of channel response.

Iseya and Ikeda (1987) and *Lisle et al.* (1991) observed that the bed surface became sorted into three distinct textural patches in response to local variations in sediment supply. The zones included a smooth zone of mostly sand over which gravel moved at high velocities, a congested zone of mostly stationary, interacting gravel, and a transitional zone (*Iseya and Ikeda*, 1987). Further *Iseya and Ikeda* (1987) found that varying the percentages of gravel and sand in their flume mixtures resulted in three different bed states, smooth (more sand), transitional and congested (more gravel). Field studies by *Dietrich et al.* (2005) observed much greater transport rates over fine patches than coarse patches. *Smith* (2004) observed a similar response in flume experiments, and noted that the greatest transport rates occurred when fine patches were longitudinally linked, rather than in distinct patches. At the grain scale, the channel can respond either by:

1. armouring;
2. developing surface structures; or,
3. developing patches.

Changes in sediment supply can be accommodated by one or all three of these mechanisms. In total they operate to stabilize the channel under changing sediment supply conditions.

Sediment supply to channels in mountainous regions is inherently stochastic and sediment supply to channels usually occurs as a complex series of pulses (*Benda and Dunne*, 1997a). *Lisle et al.* (1997) introduced a single pulse of sediment into a recirculating flume with migrating alternate bars. The initial response was adjustment in bed slope and no detectable differences in bars were identified. Sediment from the pulse appeared to overpass the bars without being deposited. *Madej and Ozaki* (1996) documented a large increase in sediment supply at Redwood Creek using 20 years of channel cross sectional changes. Channel response included channel widening, decreases in both pool spacing and depths, and persistently higher sediment yields. High sediment supply inhibits the development of armour layers and promotes surface fining (*Lisle*, 1982; *Lisle and Hilton*, 1992; *Madej and Ozaki*, 1996), which drowns out roughness associated with bars (*Lisle*, 1982; *Buffington and Montgomery*, 1999b; *Kasai et al.*, 2004), all of which lead to increased transport capacity (*Buffington and Montgomery*, 1999a; *Lisle and Church*, 2002). This suggests a strong linkage between channel response and channel resistance.

An additional linkage may exist between channel response and channel storage. *Lisle and Church* (2002) suggested that strong linkages exist between transport capacity and the volume of sediment stored in the channel. They proposed that changes in transport capacity reflect changes in channel planform, geometry, surface grain size, and surface structure, all of which have been shown to be directly linked to changes in sediment supply. In channels with either increasing or decreasing rates of sediment supply, two distinct phases of sediment transport exist. Phase I is an aggradation (transport-limited) phase where changes in sediment supply cause relatively small changes to sediment transport rate; transport in this phase is non-selective, and is accommodated by changes in storage. Phase II is a degradation (supply-limited) phase and is indicated by reduced sediment mobility, due to increased armouring and form roughness. However, there is no suggestion as to how channel response would be different due to changes in morphology.

Lisle et al. (2000) examined how a channel responds to changes in sediment supply at the reach scale and found that it is generally the result of interactions between channel form, local grain size, and local flow dynamics that govern bed mobility. Channels with high sediment supply have greater areas of their channel involved in full mobility, whereas low sediment supply channels had greater areas of partial mobility. However, under both supply rates, large areas of the channel exhibited little to no mobility. They also found that areas of finer bed material seem to be the most responsive to sediment supply changes, and the coarse areas of the channel created during some initial disturbance remain relatively static. Two reach scale parameters determined for bankfull stage (modified Shields number and Q^*) seemed to correlate reasonably well with sediment supply. The modified Shields number (θ), a ratio of tractive and gravitational forces acting on bed particles, is defined as:

$$\theta = pgdS_g/g(\rho_s - \rho)D_{50s} \tag{1.4}$$

where $pgdS_g$ represents a modified boundary shear stress (τ_b) where channel slope S is replaced with S_g which is the energy slope attributed to grain resistance, calculated following *Parker and Peterson* (1980), ρ_s is sediment density, and D_{50s} is the median particle size of the bed surface. Shields stress represents the ratio of tractive and gravitational forces acting on bed particles. *Lisle et al.* (2000) defined Q^*, modified from *Dietrich et al.* (1989), as the ratio of the mean predicted transport rate of the reach-averaged median particle size of the subsurface material (D_{50ss}) given the armouring measured by the surface particle size to the transport rate assuming there is no armouring (D_{50s}). Of the two reach scale parameters, they concluded that Q^* was the best choice in that it can be directly linked to changes in sediment supply, and therefore may have greater predictive capability of channel response (*Lisle et al.*, 2000). However, they also caution that it is unlikely that either of the metrics can predict response from anything smaller than a doubling of sediment supply.

A variety of field and experimental studies have investigated the impacts of changes in the size of the sediment supplied on channel response, more specifically sediment transport. *Gilbert* (1914) noted that the addition of fine sediment increased the mobility of coarser grains. Similarly, *Jackson and Beschta* (1984) increased the amount of sand in their flume experiments and noted increased rates in gravel transport and instability in previously stable riffles. *Wilcock et al.* (2001) also found increasing gravel transport rates with increasing sand content, even after the proportion of gravel on the bed had decreased. Their findings seem to indicate that the increased transport capacity due to the sand content can in turn limit the magnitude of channel response to large sediment inputs as the channel can evacuate the sediment much more quickly (*Wilcock et al.*, 2001). *Gran and Montgomery* (2005) observed channel recovery following fine lahar deposits from Mount Pinatubo, and observed the initial preferential transport of the finer material, followed by the development of bed structures amongst the larger classes and ultimately an increase in both form roughness and critical shear stress.

The response time to changes in sediment supply is also an important issue and depends on a variety of factors. *Parker* (1990) proposed that the time line for surface response is much quicker than other adjustments, and is therefore the primary response to changes in sediment supply. In a numerical model of the effects of sediment pulses *Cui and Parker* (2005) found that the transport capacity of the system, as well as the size of the pulse, determine the recovery time of the system. *Cui et al.* (2003) examined the effects of differing grain size in pulse material and found that finer grain sizes resulted in higher transport rates and faster recovery times than coarser material. Similar results were seen in the field by *Gran and Montgomery* (2005).

1.2.3 Discharge

Channel response to changes in discharge has also been investigated in the field and in the laboratory, as well as through the use of numerical models. As above, the research will be broken into three spatial scales (i.e. grain, bedform and reach scales).

At the grain-scale *Parker et al.* (2007a) employed a numerical model to investigate the effects of a sequence of repeated hydrographs on surface armouring. Their results suggested that gravel-bed rivers respond to repeated flood hydrographs by evolving a bed that changes little in terms of either elevation or surface size distribution as flow varies. As result, nearly all the variation in transport capacity was being absorbed by the bedload transport rate and bedload grain size distribution. This conclusion was later verified in flume experiments conducted by *Wong and Parker* (2006). Although both studies varied the hydrograph shape, the peak discharge was held constant, as was the sediment feed rate, which may have influenced their conclusions. In a field study, *Wittenberg and Newson* (2005) found that variability of the flow hydrograph was related to the variability of bed structure, and hence bed stability, and that peak discharges determined the rate of bed material transport, whereas the recession limb regulated the critical patterns of deposition. Additionally, they found that the legacy of the last flood, in terms of the nature and extent of bed clusters, determined the effectiveness of subsequent floods in terms of sediment transport (*Wittenberg and Newson*, 2005). Uncertainty still seems to exist in how flows alter surface grain sizes.

Hassan et al. (2006) investigated the effects of hydrograph shape on the armouring processes, and in particular, the effect of flashiness of the flood on armouring development. They hypothesized that hydrologic regimes characterized by relatively flat, long hydrographs can be associated with conditions that promote the development of armouring, whereas regimes characterized by short, peaky floods tend to subdue or destroy this armour. *Hassan et al.* (2006) concluded that sediment supply tends to dominate the development of bed surface armouring while hydrograph shape plays a secondary, but also important role.

Lewin (1976) found that the range of natural discharge values resulted in a variety of bedforms and that the channel at any point in time cannot be represented by a single discharge value. *Jones* (1977) found that the speed and magnitude of the change in discharge resulted in varying types of bedforms.

At the reach scale, establishing what discharge is related to equilibrium morphology has a long history of debate in geomorphology. The earliest work in quantifying a relationship between discharge and reach scale morphology was undertaken in order to design stable, unlined canals in India (*Kennedy*, 1895; *Lacey*, 1930; *Blench*, 1969). This work, referred as regime theory, empirically found that stable canal and river dimensions varied with discharge in the form:

$$w \propto Q^{0.5} \tag{1.5}$$

$$d \propto Q^{0.33} \tag{1.6}$$

Leopold and Maddock (1953) found similar hydraulic geometry relations from data obtained from gauged rivers in the midwestern United States:

$$w \propto Q^{0.5} \tag{1.7}$$

$$d \propto Q^{0.4} \tag{1.8}$$

The exponents found were very similar to the regime equations. The approach of *Leopold and Maddock* (1953), was similar to the regime approach, and the results are entirely empirical.

Although the original work of *Leopold and Maddock* (1953) incorporated a range of discharge frequencies in developing their relations, subsequent work has focused on the use of formative discharge (*Eaton*, 2013). *Wolman and Miller* (1960) concluded that equilibrium channel form appears to be related to flows at or near bankfull, rather than the rarer floods of unusual magnitude. *Ackers and Charlton* (1970) further found in their experimental channels that a steady discharge, equivalent to bankfull, produces that same meandering pattern as varying discharge. *Carling* (1987), however, noted that a threshold exists between flows that maintain channel form and those that initiate channel change. *Pickup and Warner* (1976) found that channel form depended on the ability of the event to erode channel banks, generally with a return period between 4 and 10 years. This idea was supported by *Pizzuto* (1994), who found that Powder River expanded and contracted in response to variations in discharge where the relatively infrequent occurrence of rapid channel expansion, was followed by slow channel recovery. He felt that a satisfactory model of fluvial processes should consider the cumulative effects of a wide variety of flows operating over many decades.

In the field, the observations on the relation between discharge and channel form has been mixed. From an analysis of gravel-bed rivers in Alberta, *Bray* (1975) found that the best correlation between discharge and channel geometry was the 2-yr flood. Like *Pizzuto* (1994), *McNamara et al.* (2008) found that channel morphology was maintained by large and infrequent summer flow events. *Bartholdy and Billi* (2002) found that moderate floods were associated with bend migration, while channel cutoffs were associated with major floods, those on a 10-yr to 20-yr recurrence interval. *Hooke* (2007) found that process thresholds for bank erosion, aggradation and degradation occurred on average several times a year.

Parker et al. (2003) used a flume to investigate the effects of flow variability and water diversion on mountain streams. They found that channels with a full hydrograph and no diversion of water tended to reduce the fines content in the bed surface observed at low flows and increase variability of bed elevation. Surface fines content progressively increased, the surface median grain size of the model gravel decreased, and the variability of bed elevation decreased as the degree of diversion became stronger (*Parker et al.*, 2003). This contradicts earlier work by *Parker et al.* (1982) wherein they found that variations in flow and differential entrainment of bed particles may not be essential to the formation of a bed surface in some gravel-bed rivers.

1.2.4 Summary

Much research has investigated how channels respond to changes in sediment supply and discharge. The majority of the sediment supply experiments have tended to focus only on the response of the bed surface to imposed changes in supply. The understanding of channel response at the bedform or reach scale has been done in the field, where the lack of experimental control limits the ability of the research to isolate the underlying source of the response. The majority of the earlier experimental work focused on the effects of low sediment supply on the bed surface, where recent work has investigated the fate of sediment pulses. However, neither has addressed channel response to either sustained changes in sediment supply or variable peaks, as occurs in natural rivers. Additionally, most of the experimental work has been conducted in flumes which, by design, limits response to changes in the surface grain size.

Experiments conducted with meandering channels seem more appropriate for larger floodplain systems, and not to mountain streams. In mountain streams, channels are generally straighter and exhibit an irregular meandering or more complex pattern. Channel planform is dictated more by boundary conditions, such as riparian forests, than by alluvial processes. The complexity in channel planform may be an additional factor in determining channel response and has not been sufficiently investigated to date.

From a review of the literature, it is evident that there is still a need to acquire more information on the response mechanisms available to complex mountain channels. The limited research done in these systems has either been in the field, where complex responses are difficult to interpret or in the laboratory where too much oversimplification to channel platform has been generally used. Additionally, as pointed out by *Madej* (2001), very little work has been done on how bedforms respond, and further on how grain, bedform and reach scale adjustments work together under changes in governing conditions. A fundamental study on mountain channels is required in order to better understand pathways of channel adjustment to changes in governing conditions. This project was designed to address some of these gaps.

1.3 Objectives

Forested mountain streams are continually subject to variable flows and sediment loads, and for the most part they remain relatively stable. For the most part, variability in the governing conditions can be accommodated within the channel boundaries. Only major disturbances, those that exceed the capacity of the channel to adjust, lead to channel relocation or widening. Consequently, the banks of the channels remain relatively static, or at least remain stable around some mean value over time. Most channel response scenarios rely on discrete step changes in one or more independent variable and ignore the history under which the pre-existing channel configuration was developed. This project will focus on the temporal and spatial patterns of channel response to changes in sediment supply and discharge. Specific objectives of the project were to:

- Investigate the effects of varying sediment supply and discharge on surface texture and characteristics of the transported sediment; and,
- Investigate the effects of varying sediment supply and discharge on channel storage and morphology, and sediment transport rates.
- Investigate sediment transport processes and pathways;

Sediment transport and morphological response of a semi-alluvial channel was investigated using a Froude scaled physical model. The model was designed using Fishtrap Creek as a field prototype. Long-term channel processes cannot be observed in the field and thus laboratory experiments offer an opportunity to explore long-term river behaviour.

Equilibrium in the laboratory setting is commonly defined as being reached when sediment output equates to sediment feed, at which point many experiments are either stopped or one of the inputs is changed. One of the drivers in these experiments ended up being the pursuit of what happens after equilibrium is reached. Although it was not one of the stated objectives of the research, it ended up being responsible for the long experiments.

1.4 Thesis Organization

The thesis is organized into three research chapters. Chapter 2 introduces the experimental design and methods. Chapter 3 investigates the degree to which the level of sediment mobility describes the sediment transport dynamics in a laterally confined stream and compares these results to experiments conducted in a laterally unconfined stream.

In Chapter 4 the spatial and temporal patterns of sediment transport are explored. Additionally, the transport-storage relation proposed by *Lisle and Church* (2002) is tested in an aggradational environment under conditions of constant flow and sediment supply. Lastly, the response of sediment storage within the channel to changes in sediment supply and flow is investigated.

In Chapter 5, a qualitative approach was undertaken to describe the observations of sediment transport and transport pathways made during the experiments. Out of the ten experiments conducted during this project, Exp. 6 was selected to simplify the discussion. The visual observations of sediment transport were used to infer flow and sediment transport behaviour in the experimental channel.

A concluding chapter summarizes the results contained herein.

Chapter 2

Experimental Design and Methods

2.1 Introduction

The research presented in this thesis is based on two sets of experiments using physical models to study the processes of sediment transport and bed stability in gravel bed streams. One set was conducted in a stream table with fixed banks having an irregular planform and a mobile channel bed including a wide range of grain sizes. These experiments are designed to represent a specific field prototype stream (Fishtrap Creek, British Columbia) that has been extensively studied. Another set of experiments was conducted in a stream table with mobile bed and banks having a similar range of grain sizes as the first set. For these experiments, no specific prototype stream was identified, and they are considered to represent the morphodynamics of some unspecified, general set of gravel bed rivers. The majority of the work herein is based on the fixed bank runs.

2.2 Fixed bank - Mobile Bed Experiments

For the purposes of these experiments a stream table was constructed that was 7 m long and 0.9 m wide. Previous experiments investigating the effects of varying sediment supply and/or discharge on channel morphology have used narrow flumes with smooth vertical walls (*Parker et al.*, 1982; *Iseya and Ikeda*, 1987; *Dietrich et al.*, 1989; *Wilcock and Southard*, 1989; *Kuhnle and Southard*, 1990; *Lisle et al.*, 1993; *Wilcock and McArdell*, 1993; *Hassan and Church*, 2000; *Hassan et al.*, 2006; *Nelson et al.*, 2009) or fully alluvial boundaries (*Friedkin*, 1945; *Schumm and Khan*, 1972; *Eaton and Church*, 2004; *Tal and Paola*, 2007; *Braudrick et al.*, 2009). For these experiments, flume design was based on actual bank alignments for a prototype stream, and therefore exhibited a more complex (i.e., realistic) channel alignment than is typical in these types of experiments. A floodplain was constructed within the stream table using Styrofoam, into which a channel with irregular banks was cut; the channel was filled with sediment to a depth of 5 cm (Figure 2.2).

2.2.1 Prototype Stream and Scaling Considerations

Experimental design for the fixed bank experiments was based on field data collected in Fishtrap Creek. Fishtrap Creek is an intermediate size forested gravel-bed stream which drains a 158 km^2 watershed located in the Interior Plateau region of British Columbia,

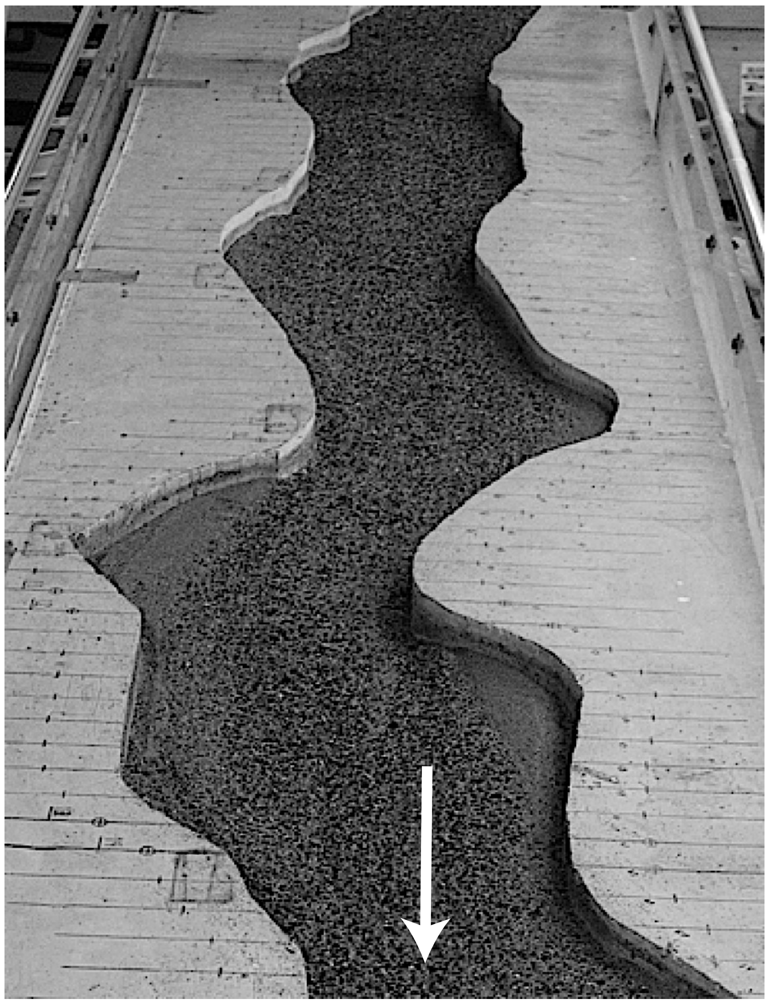

Figure 2.1: Apparatus used for the fixed bank experiments conducted at UBC , looking upstream. White arrow indicates flow direction.

Canada. Fishtrap Creek has been the focus of a number of studies investigating watershed response to an intense forest fire (for example, *Eaton et al.*, 2010a,b). The 2003 McLure forest fire was a high-intensity fire that burned more nearly 70% of the watershed, including a significant portion of the riparian zone of Fishtrap Creek. In 2004, 11 cross sections were established over a 130 m study reach; this was later expanded to 27 cross sections in 2006 (*Phillips*, 2007). In addition to channel cross sections, surface and subsurface sediment samples were collected and a reach survey was conducted which produced a detailed longitudinal profile and generalized planimetric map. The reach is located immediately upstream of a Water Survey of Canada (WSC) hydrometric station (08LB024), which has operated more or less continuously since 1971.

The basis of physical modelling is founded on the principles of similitude, which requires a sound understanding of the physical processes and recognition of a model's capacity to replicate those processes (*Ettema et al.*, 2000). Similitude is used to relate a processes that occurs in the prototype to the model, which is at a different scale. The power of similitude is that processes at different scales can be described using dimensionless parameters. The main advantages in physical model investigations are the direct control of specific variables and the possibility to observe and to measure the development of planimetric and elevational patterns (*Young and Warburton*, 1996).

Complete similitude between the model and the prototype requires geometric, kinematic and dynamic similarity. Geometric similarity requires that the linear proportions are kept between the model and the prototype and hence that they have the same shape, this is represented by:

$$\lambda_l = \frac{L_p}{L_m} \tag{2.1}$$

where λ_l represents the length ratio between the prototype (L_p) and the model (L_m). Kinematic similarity requires that ratios of time and motion are similar, for example the shape of the streamlines of the prototype are replicated by the model at any particular time. Dynamic similarity necessitates that the ratios corresponding forces in the model and the prototype are preserved.

The fixed bank model was designed using geometrically undistorted movable bed Froude scaling. A movable bed model must reproduce two phase flow (i.e. water and sediment) and can be described by the following seven characteristics parameters: water density (ρ), dynamic viscosity (μ), grain size (D), channel slope (S), hydraulic radius (R - defined as $R = A/P$, where A is the channel cross sectional area and P is the wetted perimeter), acceleration due to gravity (g), and sediment density (ρ_s) (*Yalin*, 1971). Some of the parameters can be combined to produced the shear velocity ($u_* = \sqrt{gdS}$), and the immersed specific weight of sediment ($\gamma_s = g(\rho_s - \rho)$), leaving a new set of parameter combinations $\rho, \mu, D, \rho_s, d, u_*, \gamma_s$, which produces four dimensionless parameters:

$$\Pi_1 = \frac{\rho D u_*}{\mu} \tag{2.2}$$

$$\Pi_2 = \frac{\rho u_*^2}{\gamma_s R}; \tag{2.3}$$

$$\Pi_3 = \frac{\rho_s}{\rho}; \tag{2.4}$$

$$\Pi_4 = \frac{R}{D}; \tag{2.5}$$

where the term Π_1 represents the grain Reynolds number (Re^*), which relates grain size to the thickness of the laminar sublayer, Π_2 is the dimensionless Shield number (θ), which is the ratio of the boundary shear stress to the submerged weight of the characteristic grain size, Π_3 and Π_4 represent relative density and roughness, respectively.

In undistorted Froude scaled models the time-scales associated with the transport of water and sediment are the same (unlike for distorted models), thus avoiding the complexities of the two fluids operating at different time-scales (*Yalin*, 1971; *Young and Warburton*, 1996). This scaling ensures that the dimensionless Shields number is the same in both model and prototype.

The experimental design also ensured that the boundaries of both model and prototype are hydraulically rough, since the critical Shields number is constant for hydraulically rough boundaries. This condition is maintained so long as the grain Reynolds number is greater than about 70 (*Yalin*, 1971), though some have argued for a lower limit (*Ashworth et al.*, 1994; *Peakall et al.*, 1996; *Shvidchenko and Kopaliani*, 1998; *Moreton et al.*, 2002). The grain Reynolds number is calculated as:

$$Re^* = \frac{D_{90s} u_*}{\nu} \tag{2.6}$$

where D_{90s} is the grain size at which 90% of the surface sediment is finer and ν is the kinematic viscosity of water. For these experiments, a length scaling ratio (λ_r) of 1/30 was selected, this yields $Re^* = 180$.

The following scaling relations relate the parameters of the model to those of the prototype:

1. the relative widths ($w_r = w_{model}/w_{prototype}$), depths ($d_r$), and grain sizes ($D_r$) are scaled linearly according to $w_r = d_r = D_r = \lambda_r$
2. the relative slope (S_r) is unity, such that $S_{model} = S_{prototype}$
3. the relative velocity (v_r) scales according to $v_r = \sqrt{\lambda_r}$
4. the relative time (t_r) scales according to $t_r = \sqrt{\lambda_r}$

5. the relative discharge (Q_r) scales according to $Q_r = \lambda_r^{5/2}$

The fixed bank model was constructed in a stream table with an overall slope of 0.016 m/m using a geometric scale ratio of 1:30. The design channel width (0.34 m) and depth (0.015 m) were determined by averaging the bankfull channel dimensions from 90 cross sections. See Table 2.1 for the prototype and model design parameters.

Table 2.1: Experimental design parameters in prototype and model

Value in Fishtrap Creek	Value in Model
Design Q (m^3/s) (*Return Period*)	(L/ s)
7.9 (*2.8-yr*)	1.6
9. (*6-yr*)	2.0
11.8 (*11-yr*)	2.4
W (m)	0.34
d (m)	0.015
S	0.016
D_{50feed} (mm)	1.14
D_{90feed} (mm)	3.28
Time (1 day)	4.38 hr (5 hrs used)

Streamflow: Streamflows at Fishtrap Creek are dominated by snowmelt generated events. Based on 40 years of record from the WSC gauge located immediately downstream of the study area, the estimated daily mean bankfull flood at the study site is 7.9 m^3/s having a return period of 2.8-yr, with a maximum mean daily flow of 14.9 m^3/s (1997) over the period of record. The streamflow return periods were determined using the Consolidate Frequency Analysis (CFA) program (*Pilon and Harvey*, 1993). The streamflow data were tested for independence, trend and randomness, and passed at the 5% significance level.

The duration of the average snowmelt event is ~1 month, with the peak of the hydrograph lasting, on average, one day. The estimated bankfull flow of 7.9 m^3/s translates to 1.6 L/s in the model. Larger magnitude flows of 2.0 L/s and 2.4 L/s were also used (see Table 2.1). The estimated prototype flood duration of one day translates to about 5 hrs in the model.

Grain Size Distributions: Field measurements made by *Phillips* (2007) and *Andrews* (2010) indicate that the median particle size of the subsurface (D_{50ss}) at Fishtrap Creek is about 36 mm and the D_{90ss} is about 91 mm (Figure 2.2). Furthermore, it was observed that there were differences between the bedload, surface (D_s) and subsurface (D_{ss}) grain size distributions. Surface grain size distribution data (*Phillips*, 2007; *Andrews*, 2010) indicates that the surface grain size distributions (D_{50s} = 69 mm and D_{90s} = 170 mm) were much coarser than the subsurface, which is not uncommon in mountain streams. The bed material load, although not directly sampled, was approximated by a bulk sample taken upstream of a hydrometric weir. This sample was much finer than both the surface samples and the other subsurface samples ($D_{50ss} = 15$ mm and $D_{90ss} = 61$ mm).

Pitlick et al. (2008) proposed that sediment in gravel-bed rivers consisted of two populations: one population which represents the subsurface and bedload material and another which represents the bed surface. Observations at Fishtrap Creek suggest that the bedload, subsurface and bed surface sediments are mostly from the same population, except for the larger grains. The larger clasts on the bed surface may be the result of processes exogenous to the modern channel or rarely move (*Church and Hassan*, 2002). The bedload and subsurface size distributions represent sediment transport via modern alluvial processes; this is also the case for most of the surface grain sizes. The larger clasts present on the surface appear less frequently in the subsurface and may be the result of either higher magnitude flow events, major disturbances or are of non-alluvial origin (for example, glaciofluvial deposits). Observationally, these larger clast sizes appear to represent a major stability component in Fishtrap Creek. During degradational periods the larger grains act as key members establishing stone clusters or can act as a degradational barrier when smaller size classes are selectively transported downstream.

The sediment used to create the bed in the model was collected from a sandur deposit; the bed material grain size distribution was sieved to fit a distribution that represented as closely as possible a 1:30 scale of the measured bed material grain size distribution in Fishtrap Creek (see Figure 2.2). The bed material grain size distribution for the experiments was truncated at 0.177 mm (equivalent to 5.3 mm in Fishtrap Creek) and 8.0 mm (equivalent to 240 mm in Fishtrap Creek). The bed material grain size distribution was the same for Exp. 1 to Exp. 7; for Exo. 8 the feed grain size had a distribution equal to the sediment output trapped during a previous run. The main difference between the two distributions is in the truncation of the tails (Figure 2.2).

Morphologic Characteristics: The average bed slope for the study reach is 0.02 m/m overall, and about 0.016 m/m in sections without significant volumes of large wood. According to *Montgomery and Buffington* (1997) these slopes are within those expected for plane-bed morphology (0.015 to 0.030), but greater than that expected for pool-riffle morphology (<0.015). However, these slopes are consistent with forced pool-riffle morphology, which can extend the gradient range of pool-riffle channels from 0.02 to 0.035 (*Montgomery et al.*, 1995). Since wood was not included in our fixed bank model, we set the channel gradient for the model to the value observed in the field for relatively wood-free sections of the stream.

Eaton and Giles (2009) suggested that the lateral stability in gravel bed streams like Fishtrap Creek is strongly conditioned by the nature of the riparian vegetation. The ability of such streams to migrate laterally across their floodplains appears to be directly linked to the disturbance regime of the forests adjacent to it, with migration events limited to those periods of time during which the root strength of the riparian vegetation has been compromised by, for example, wildfire. *Eaton and Church* (2009) speculate that, between disturbance events, Fishtrap Creek remains laterally confined within a fixed planform dictated

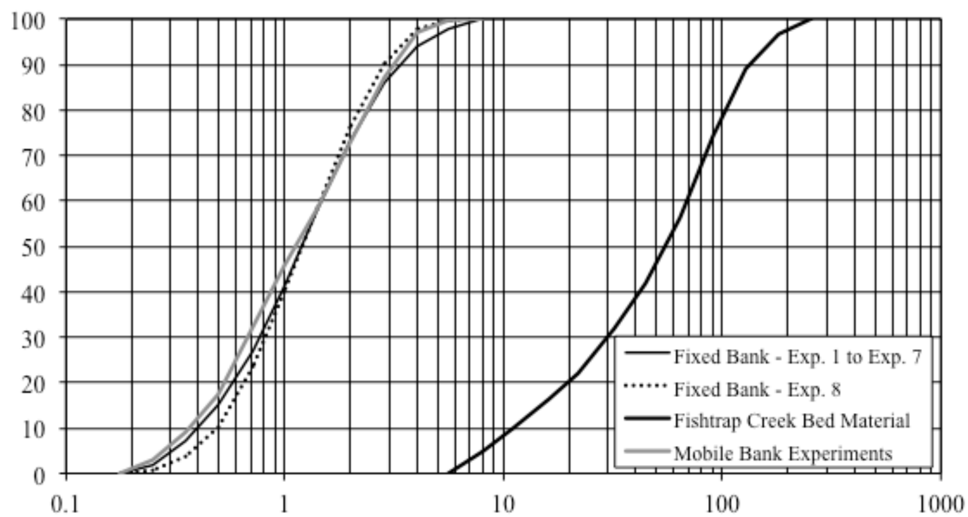

Figure 2.2: Prototype and model bed material grain size distributions.

by the riparian forest and that the throughput of water and sediment is accommodated by morphological adjustments within the active channel, not by lateral migration of the channel; as a result, the use of a fixed bank physical model is appropriate when studying the long-term morphodynamics of this kind of river system.

2.2.2 Flume Instrumentation and Measurements

The experiments employed a sediment feed system, only water was recirculated. Sediment was introduced at the upstream end of the stream table using a rotating sediment feeder (Figure 2.3). Prior to entering the channel, pre-mixed sediment was loaded into the feeder (Figure 2.3a). Sediment then exited the rotating sediment feeder into a PVC pipe which then exited onto the channel (Figure 2.3b). The volume of sediment exiting the feeder was checked every 5 hr to ensure that the feed rate remained constant. Water was pumped into a head pond then spilled over a broad crested weir before entering the channel.

Discharge was measured using an Omega FP-1521 digital flow transmitter, which is essentially an in-line impeller flow meter. Measurements of the flow meter, determined as the percentage of the actual value, are accurate to plus or minus 5%. Average flow velocities were measured using a tipping bucket that injected a 10 mL slug of a salt-water solution into the upstream end of the flume. The slug was introduced into the middle of the channel at the upstream end of the flume to ensure full mixing of the tracer by the time it reached the probe 5.5 m downstream (Figure 2.4a). Estimation of average velocity was calculated using the spatial harmonic mean velocity as described in *Waldon* (2004). *Waldon* (2004) found that the harmonic mean provides an unbiased measure of mean velocity compared to the peak of the pulse which over estimates the velocity and the centroid which underestimates the mean velocity.

All sediment leaving the table was initially collected at the outlet every 15 minutes in 1 L plastic sample jars. Trap efficiency problems led to a modification of the outlet; a Helley-Smith sample bag was attached to the outlet and a 0.0125 mm sieve placed underneath the sample bag to ensure all sediment transported out of system was captured. Collected sediment was dried and weighed at 15 minute interval. Hourly sediment samples were then combined from the 15 minute samples and split, the resulting sample was sieved to $1/2$ Φ intervals. The sediment was then re-mixed to the distribution of the initial feed mixture and put back into the sediment feeder.

Every hour during the experiment, observations of channel morphological development and sediment transport pathways were made and sketched onto maps. In addition, water surface elevations and depths on both sides of the channel were measured at 10 equally spaced cross sections using a ruler, and were used to map the water surface position during each experimental run. An overhead camera monitored a 2 m section of the channel and took images at 3 frames per second (fps). These images were post-processed after the experiment was completed to produce a video in which sediment movement could be more easily observed. This information provided additional verification to the information a)

b)

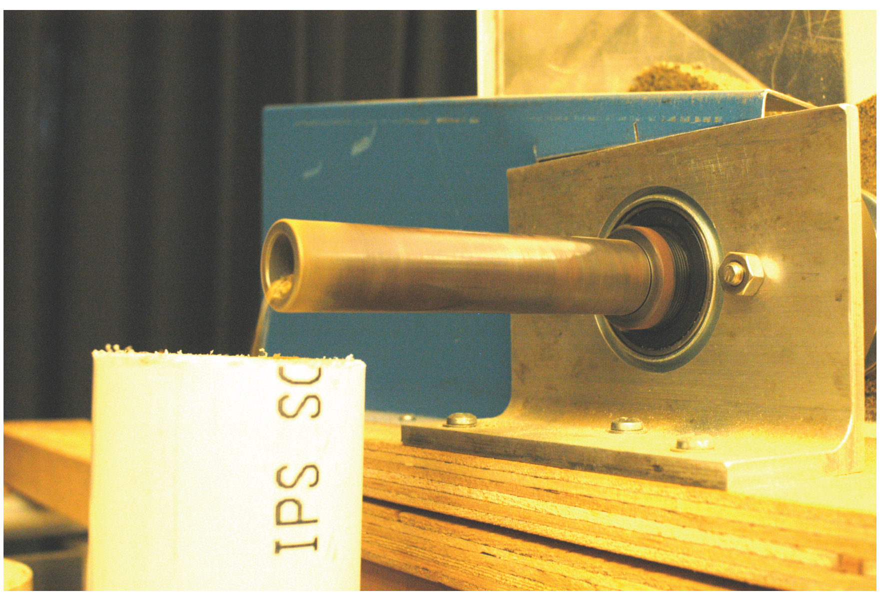

Figure 2.3: Photo of a) sediment exiting the feeder, and b) sediment feeder with sediment.

a)

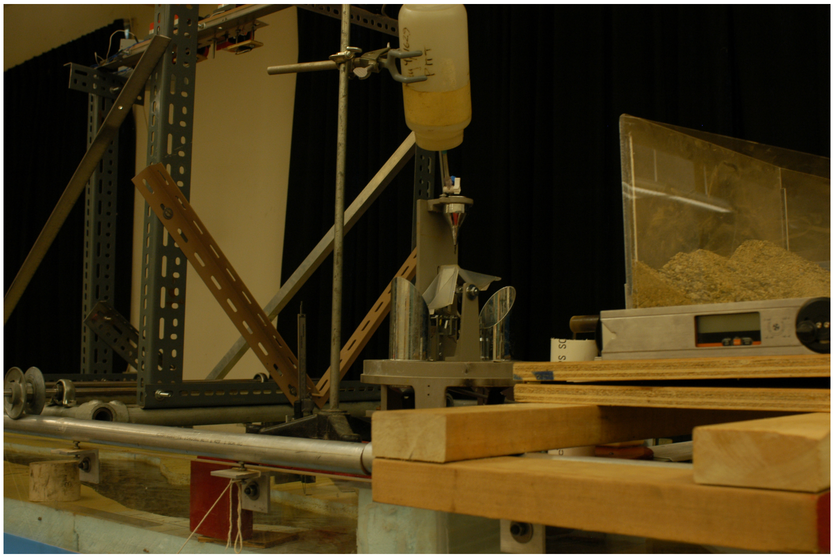

b)

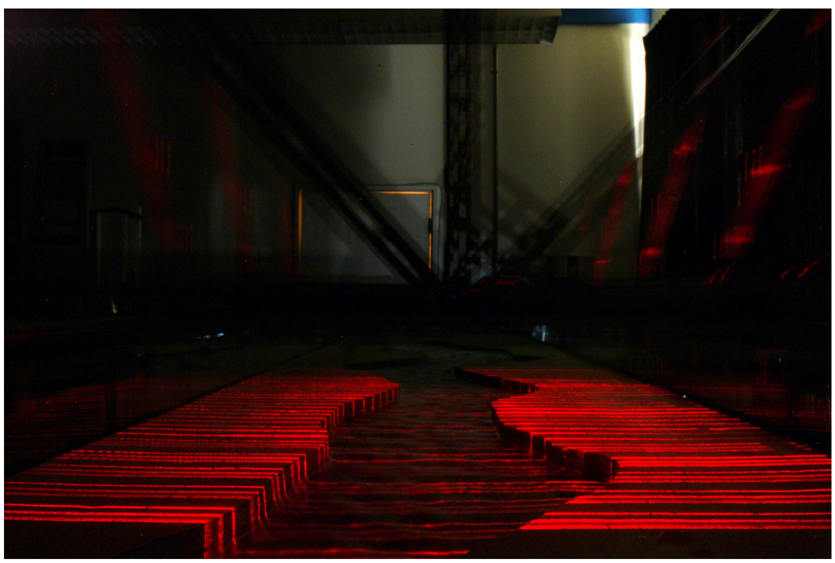

Figure 2.4: Photos of a) converted tipping bucket rain gauge used to introduce salt mixture into the stream, and b) time delayed image of laser cart during a measurement of the channel.

recorded on the hand drawn maps.

Every 5 hours the experiment was halted to collect surface sediment samples and survey the bed of the channel. However, for Exp. 1 surface sediment samples were collected every hour. Nine surface sediment samples were taken at the same locations in the flume every 5 hours. Samples were collected using a square plexiglass plate, side length of 3.7 cm and surface area of 13.7 cm^2, covered with a layer of wet clay, ≈1 cm thick (*Diplas and Fripp*, 1992). The plate was pressed firmly against the bed and dipped into water to release any sediment adhering to the sample due to surface tension effects. A series of pilot studies determined that, while the presence of the plunger produced local erosion and deposition, these effects were generally short-lived. The minimum sampling area was calculated using the maximum particle size of the surface material, 0.8 cm, and equations from *Diplas and Fripp* (1992) and *Fripp and Diplas* (1993). The minimum sampling area was determine to be 64 cm^2. To ensure an adequate sample size between six and nine samples were taken during each sampling period (*Diplas and Fripp*, 1992; *Fripp and Diplas*, 1993). The clay-sediment mixture was rinsed onto a 0.125 mm sieve to remove the clay, the remaining sediment was dried, weighed, and sieved at $1/2$ Φ intervals.

To survey the channel bed, five red line lasers (3.5V ≈ 4.5 mW 16 mm) were mounted on an instrument cart at 10 cm intervals approximately 0.8 m from the bed surface. A Prosilica EC 1280 (1280 x 1040 pixels) firewire video camera was used to photograph each laser line from an oblique angle, to obtain cross sectional topographic data with a 1 mm resolution. This system produced a survey that had cross sections spaced at 1 cm intervals over a 4.50 m length in the middle of the stream table. Capture and processing of the data was achieved using a combination of Labview and Matlab programs. DEMs were generated from the original data using triangular based linear interpolation to 2 mm^2 grid cells. These grids were then imported into SAGA GIS and the grid difference module was used to document changes in channel morphology between surveys. Channel slope was determined by fitting a regression through the mean elevation of each of the 450 cross sections. An example of a scan in progress is provided in Figure 2.4b.

Samples of surface grain size were collected before, during and after each experiment using a square plexiglass plate, side length of 3.7 cm and surface area of 13.7 cm^2, covered with a layer of wet clay, ≈1 cm thick (*Diplas and Fripp*, 1992). Samples were taken every hour. The plate was pressed firmly against the bed and dipped into water to release any sediment adhering to the sample due to surface tension effects. A series of pilot studies determined that, while the presence of the plunger produced local erosion and deposition, these effects were generally short-lived. The minimum sampling area was calculated using the maximum particle size of the surface material, 0.8 cm, and equations from *Diplas and Fripp* (1992) and *Fripp and Diplas* (1993). The minimum sampling area was determine to be 64 cm^2. To ensure an adequate sample size between six and nine samples were taken during each sampling period (*Diplas and Fripp*, 1992; *Fripp and Diplas*, 1993). The clay-sediment mixture was rinsed onto a 0.125 mm sieve to remove the clay, the remaining sediment was dried, weighed, and sieved at $1/2$ Φ intervals.

2.2.3 Experimental Protocols

Ten experimental runs were conducted using varying rates of discharge and sediment supply (see Table 2.2). Experimental runs either began from a screeded bed, having a uniform sediment depth and surface grain size distribution, or on a bed inherited from the previous experiment, referred to as a conditioned bed. Experiments that began with a screeded bed are indicated by bold numbers in Table 2.2. Prior to the start of those experiments with a screeded bed, flows were run at about half the estimated bankfull flow (0.8 L/s) for 2 hours in order to wet up the bed and let an initial bed surface develop. Although sediment transport was observed in the channel during this initial phase, no sediment exited the stream table. As discussed in more detail above, after every 5 hours during an experimental run, flows were turned off and various measurements were made: at the beginning of the next run, flows were ramped up incrementally over 15 minutes in order to prevent major morphologic changes from occurring. While minor adjustments did occur during the shut down and start up period, they were restricted primarily to pool heads and riffle tails. The only deviation from this experimental protocol occurred during Exp. 10, which was run in 2 hr increments between bed surveys.

The return period of the equivalent prototype discharge in the experiment is provided in Table 2.2. The table also provides the sediment feed rate (Q_f) for each experiment and the average sediment output over the duration of the experiment (Q_b). The D_{50} of the bed surface (D_{50s}) and the transported sediment recorded at the outlet (D_{50t}) are given.

Equilibrium conditions during the experiments were defined as equality in sediment input and output, which is consistent with previous experimental work (for example, *Dietrich et al.*, 1989; *Lisle et al.*, 1993; *Eaton and Church*, 2004, 2009; *Venditti et al.*, 2010).

Table 2.2: Experimental conditions

Exp.	Q	T_r[a]	Q_f	Time	Bed Slope	Depth	τ_b[b]	Q_b	D_{50s}[c]	D_{50t}[d]	D_{50s}/D_{50t}
	L\s	yrs	kg\hr	min	$\times 10^2$	cm	Pa	kg\hr	mm	mm	observed
Feed											
1	1.6	2	3.24	5700	1.53±0.062	1.47±0.080	2.21±0.16	2.72±0.54	2.59	1.15	2.28
2	1.6	2	1.65	2400	1.65±0.032	1.50±0.076	2.42±0.16	1.37±0.24	3.03	1.12	2.72
3	1.6	2	1.65	2400	1.51±0.042	1.58±0.051	2.34±0.11	0.76±0.19	2.37	1.04	2.28
4	2.0	4	1.98	2400	1.52±0.093	1.60±0.067	2.39±0.18	1.54±0.32	2.89	1.16	2.51
5	2.4	11	2.47	1800	1.62±0.038	1.85±0.025	2.93±0.08	2.16±0.54	3.29	1.06	3.10
6	2.0	4	1.80	2400	1.62±0.112	1.72±0.045	2.73±0.24	1.23±0.42	2.64	1.03	2.59
7	2.4	11	1.80	1800	1.61±0.060	1.81±0.041	2.84±0.15	1.74±0.68	3.13	1.13	2.79
8	2.4	11	1.80	1500	1.66±0.052	1.79±0.020	2.91±0.08	1.86±0.11	3.22	1.14	2.84
No feed											
9	2.4	11	-	900	1.62±0.009	1.99±0.104	3.16±0.17	0.21±0.27	3.12	1.11	3.09
10-1	2.6	18	-	120	1.61	2.18	3.45	0.09	3.27	1.64	2.00
10-2	2.8	30	-	120	1.60	2.60	4.08	0.14	3.81	1.40	2.72
10-3	3.0	55	-	120	1.60	2.43	3.82	0.36	3.60	1.55	2.33
10-4	3.2	95	-	120	1.50	2.52	3.70	0.66	3.61	1.55	2.33
10-5	3.4	150	-	120	1.46	3.19	4.58	0.72	3.17	1.12	2.61

[a] T_r equals return period of equivalent prototype discharge, estimated using Extreme Value Gumbel distribution.
[b] τ_b calculated as $\rho g d S$.
[c] D_{50s} is the median particle size of the bed surface.
[d] D_{50t} is the median particle size of the transported bed material collected at the channel outlet.

2.3 Mobile bank - Mobile Bed Experiments

The details of the mobile bed experiments have been previously discussed in *Eaton and Church* (2004), so only a brief summary of the methods are presented here. The mobile bank experiments were conducted in a 20 m long tilting stream table set at a slope of 0.01 m/m (see Figure 2.5). The channel was allowed to freely migrate across a 3 m wide, 12 cm deep floodplain composed of material with a grain size distribution identical to the bed and the sediment feed. Each experiment began with a straight rectangular channel cut into the floodplain. The physical model was a generic, 1:32 scale representation of a moderately steep (1%), meandering gravel bed river with a D_{50} of about 22 mm and a bankfull discharge of $\approx$ 17 m^3/s. A commercially available sand mixture (see Figure 2.2) was used to create the floodplain approximately 12 cm deep on the stream table with $D_{50} \approx 1$ mm. This material was collected from a naturally sorted beach deposit, and was not modified during excavation on-site, nor in the laboratory.

As in the fixed bank experiments, the model grain size was truncated at 0.177 mm. Water flowed onto the centre of the stream table at the upstream end through a tray oriented at 25° relative to the stream table centreline, so as to generate an initial bend. A sediment feed unit introduced sediment to the system that had the same grain size distribution as the floodplain sediment. All sediment leaving the stream table at the downstream end was captured in a sediment trap. Trap efficiency was nearly 100% for most size classes, but dropped for the smallest size classes that were carried out of the trap by turbulent eddies.

Measurements of the water surface elevation and of the bed topography were made using a point gauge. Surveyed cross sections were located at each apex and cross-over to characterize the channel bed topography. All results are based on measurements from the middle half of the stream table, away from any potential inlet and outlet effects (total study length of $\approx$10 m).

Samples of the bed and bank surface texture were collected following each experiment using a flexible rubber plate covered with a layer of wet clay. Samples were also taken of the bed armour, approximately located at the thalweg, for each cross section.

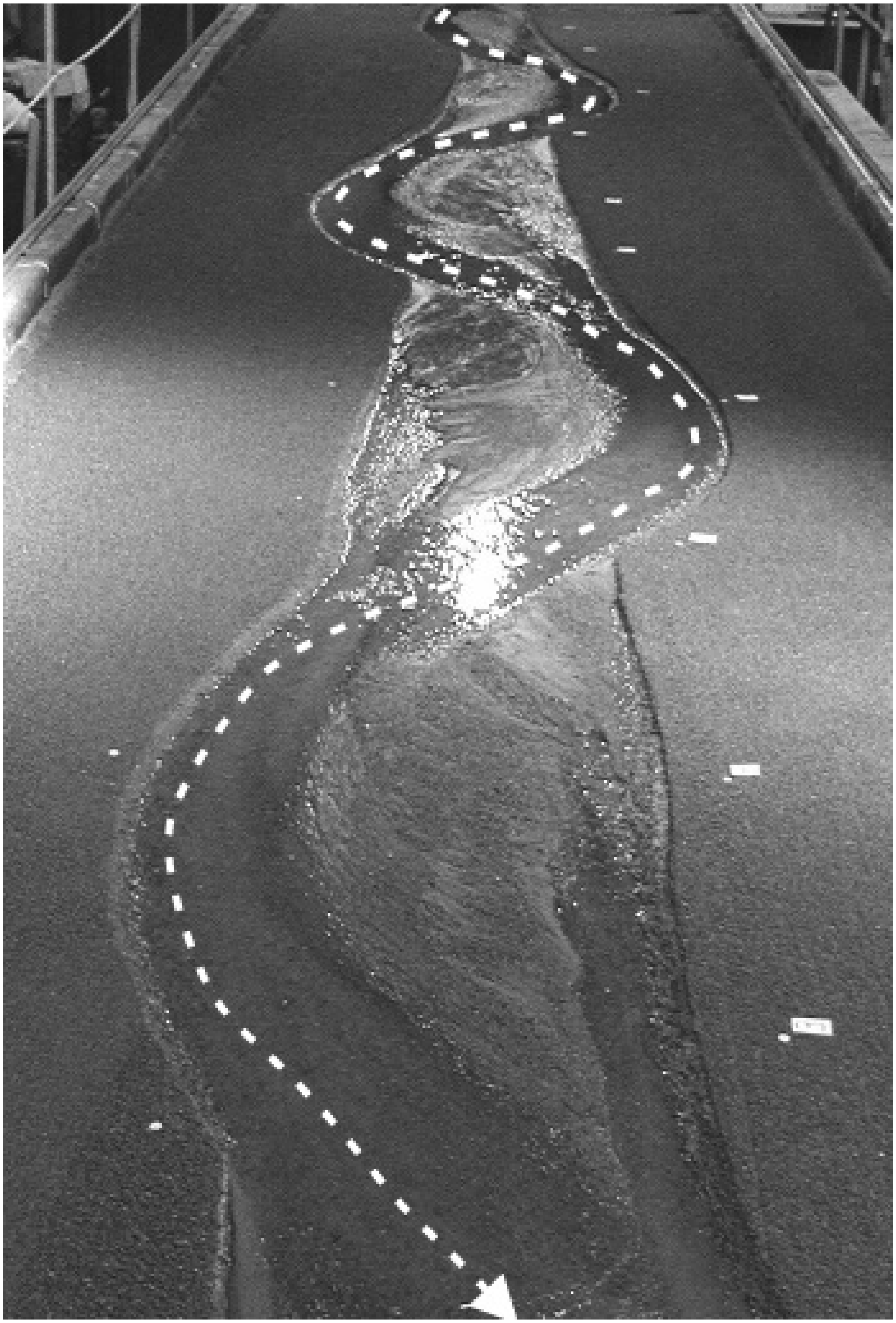

Figure 2.5: Photo looking upstream at the mobile bank model.

Chapter 3

Sediment Mobility and Channel Stability: Implications from Froude-scaled Experiments

3.1 Introduction

The morphology of gravel-bed rivers is primarily a consequence of the erosion, transport and deposition of bed material. Bed material found in mountain gravel-bed rivers may originate from either endogenous or exogenous sources and processes, and consequently the grain size distribution of the material may span orders of magnitude. The ability of the channel to erode and transport the range of sizes found within the channel determines, in a large part, its stability.

Field studies have observed bed material transport to occur in either two or three distinct phases. *Jackson and Beschta* (1982) (see also *Emmett*, 1976; *Andrews*, 1983) proposed two phases of bedload transport in pool-riffle morphologies: Phase I involves the transport of fine material during low to moderate flows over a static bed, this material is usually recruited from pools, channel margins and behind in-stream obstructions; Phase II occurs during flows high enough to entrain sediment in riffles, and involves the transport of most grain sizes found in the bed material, and is associated with local mobilization of the armour layer.

Ashworth and Ferguson (1989) redefined the two phases of *Jackson and Beschta* (1982) based on observations of sediment transport in gravel-bed rivers into three phases. Phase I involves movement of fine material over a static bed during low flow periods. Phase II occurs during moderate flows when local bed material is entrained and transported. The existence of this phase suggests that at some flows entrainment is size dependent, in that smaller grains are more likely to be entrained under these flow conditions than larger grains. Phase III occurs during high flow events and produces conditions similar to the classical notion of full mobility. *Warburton* (1992) extended the model of *Ashworth and Ferguson* (1989) to step-pool streams; during his Phase 2 flows were high enough to break up of the gravel portion of the bed. During Phase 3, flows were high enough to result in the destruction of boulder structures and step-pool sequences (*Warburton*, 1992).

Wilcock and McArdell (1993, 1997) introduced the concept of partial mobility in contrast to the classical notion of full mobility. *Church and Hassan* (2002) and *Hassan et al.* (2005) modified the existing model to include the concepts of partial (Phase II) and full mobility (Phase III) to describe the three sediment transport phases. Partial transport occurs when only a given size range of surface grains are mobilized, and the remainder are immobile (*Wilcock and McArdell*, 1993). *Haschenburger and Wilcock* (2003) later modified this definition of partial mobility to describe conditions in which only portions of the bed surface are mobile, irrespective of grain size, and other portions remain immobile. Earlier, in his three-phase model, *Carling* (1988) attributed the partial mobilization of "smaller framework gravels" to Phase II sediment transport which is associated with flows greater than 60% of bankfull; during this phase only a minority of the coarser grains are entrained. Selective transport occurs when the all of the sizes present on the bed surface are present in the transported bed material, but the transported load is finer (*Parker et al.*, 2007b).

A final condition that is related to bed mobility is equal mobility. The hypothesis of equal mobility was initially proposed by *Parker et al.* (1982) and *Parker and Klingeman* (1982) and suggests that in order for a graded stream to move the coarse half of its mean annual load at the same rate as the finer portion, the grain size distribution of the surface layer must adjust so that the coarse portion of the surface sediment is overexposed and is therefore more likely to be entrained compared to the finer portion. The result is that the armouring and over exposure of coarse grains ensures that both portions move through the system at the same rate. *Parker and Toro-Escobar* (2002) referred to this as the 'weak form' of the equal mobility hypothesis; the 'strong form' additionally requires that the grain size distribution of the bed material load is equivalent to that of the subsurface when averaged over multiple flood events. The 'strong' form of the hypothesis can be seen as a time averaged phenomenon relating the development of the armour layer to particle mobility.

In experiments using scaled models of mountain streams *Parker and Toro-Escobar* (2002) found evidence for both forms of the hypothesis. *Lisle* (1995) compared the long term average grain size distributions of bed material load to the subsurface grain size distributions from data available for 14 reaches of 13 gravel-bed rivers. The data he presented showed that 8 of the 14 supported the strong form of the hypothesis; however, in 6 of the 14 reaches analyzed the load was finer than the substrate. He observed that these streams were commonly steep channels with coarse surfaces that presumably limited the annual amount of scour and fill. This lack of scour and fill may have limited the exchange between the surface and subsurface layers during floods, thus invalidating the strong form of the hypothesis (*Parker and Toro-Escobar*, 2002). Others have also found that transported load tends to be systematically finer that the bed material (for example *Church and Hassan*, 2002; *Gomi and Sidle*, 2003; *Ryan et al.*, 2005; *Wathen et al.*, 1995; *Whiting et al.*, 1999; *Pitlick et al.*, 2008; *Thompson and Croke*, 2008).

Pitlick et al. (2008) proposed that sediment in gravel-bed rivers consist of two populations: one population represents the subsurface and bedload material and another which represents the bed surface. Observations at Fishtrap Creek suggest that the bedload, subsurface and bed surface sediments are mostly from the same population, except of the larger grains. The larger coasts on the bed surface may be the results of processes exogenous to the modern channel or rarely move (*Church and Hassan*, 2002). The bedload and subsurface size distributions represent sediment transport via modern alluvial processes. This is also the case for most of the surface grain sizes. The larger clasts present on the surface appear less frequently in the subsurface and may be the result of either higher magnitude flow events, major disturbances or are of non-alluvial origin (for example, glaciofluvial deposits). Observationally, these larger coasts sizes appear to represent a major stability component in the system. During degradation periods the larger grains act as key members establishing stone clusters or can act as a degradation barrier when smaller size classes are selectively transported downstream.

In addition to the stability in the channel due to the presence of larger grain coasts, as previously mentioned, *Eaton and Giles* (2009) suggested that the lateral stability of Fishtrap Creek is related to the riparian forest. This lateral stability in the channel is directly linked to the disturbance regime of the forests adjacent to it. The recurrence interval of riparian disturbance, which in the interior region of British Columbia is mainly forest fires, occurs approximately every 100 years (*Eaton and Church*, 2009). This suggests that for a majority of the time Fishtrap Creek remains laterally stable with a fixed planform dictated by the riparian forest and that the throughput of water and sediment is accommodated by morphological adjustments within the active channel.

The objectives of this chapter are to:

1. design a Froude scaled physical model using Fishtrap Creek as a prototype;

2. test the degree to which the level of sediment mobility describes the sediment transport dynamics in a laterally confined stream for flood flows that typically occur over the period between disturbances (in Fishtrap Creek this period is approximately 100 years); and,

3. compare these results with a previous study in which the channel banks were as erodible as the bed.

3.2 Results

3.2.1 Sediment Transport Rates

Summary data for the observed sediment transport rates, calculated at 15 minute intervals, for all of the experiments are presented in Table 3.1. Exp. 1 displayed the highest average transport rate, which would be expected as it was also conducted with the highest sediment feed rate, the lowest transport rates were associated with the degradation experiments (Exp. 9 and Exp. 10) and Exp. 3. To account for the role of sediment feed rate in sediment transport rates, the mean transport rate for each experiment was divided by the respective sediment feed rate (presented as the standardized mean in Table 3.1). On average, Exp. 7 and Exp. 8 operated near equilibrium conditions; Exp. 3 appears to be the outlier.

Plots of sediment transport rates are shown in Figure 3.1 along with the respective sediment feed rates, where applicable. Included on each plot is the centred moving average, with a width of 180 min. The moving average line provides a clear indication of trend in transport rates over time, as well as when the experiment is in equilibrium with the sediment feed rates. It can be seen that for most experiments sediment transport rates were lower than the feed rates, indicating aggradation. Exp. 9 and Exp. 10 were the exception as they were degradational experiments. Exp. 8 appears to be in equilibrium for nearly the entire run time (Figure 3.1h), while Exp. 1 (3.1a), Exp. 2 (3.1b) and Exp. 7 (3.1g) experience periods of equilibrium.

Table 3.1: Summary statistics related to sediment transport rates

Experiment	1	2	3	4	5	6	7	8	9	10
Duration [a]	5700	2400	2400	2400	1800	2400	1800	1500	900	600
Average [b]	1.34	0.72	0.37	0.76	1.06	0.61	0.86	0.91	0.10	0.48
Standardized Mean [c]	0.84	0.89	0.46	0.78	0.87	0.69	0.97	1.02	-	-
Max [b]	3.03	1.81	1.03	3.56	4.22	3.84	5.85	1.85	1.27	2.02
Min [b]	0.18	0.13	0.01	0.16	0.29	0.12	0.21	0.42	0.00	0.07
SD [b,d]	0.48	0.29	0.18	0.56	0.60	0.46	0.63	0.27	0.20	0.43
Aggradation [e]	8.92	3.03	14.11	7.32	4.06	9.44	0.89	-0.97	-3.55	-16.44

a. Duration of experiment in minutes.
b. Sediment transport rates in g/min-cm.
c. Standardized mean was calculated for each experiment as the average sediment transport rate divided by the sediment feed rate.
d. Standard deviation.
e. Average aggradation rate in g/min.

The sediment output data can also be presented as cumulative differences between sediment feed rates and sediment transport rates (Figure 3.2). Inspection of these plots reveals how significant the aggradation was for most of the experiments. Average aggradation rates for each experiment are provided in Table 3.1.

Average transport rates for the first 2010 minutes in Exp. 1 were 1.00 g/min-cm which is 30% less than the sediment feed rate (Figure 3.1a), an average sediment output rate of 1.39 g/min-cm was maintained for the duration of the experiment. From the figure, Exp. 1 appears to approach equilibrium following 2010 minutes; however, it was obvious that bed elevations were increasing at various locations. From Figure 3.2a it is evident that Exp. 1 experienced persistent, but minor aggradation. The overall aggradation rate was 11.89 g/min, however two breakpoints can be seen in the plot which indicates three different periods of aggradation, separated by periods of relative equilibrium in sediment flux. The first period lasted 1950 minutes and had an average aggradation rate of 21.07

g/min. The second period, with a an average rate of 11.66 g/min, lasted between 2130 and 2985 minutes. The final period began after 3735 minutes and lasted for the remainder of the experiment, during which an average aggradation rate of 9.43 g/min was observed.

Exp. 2 (which continued on the bed from Exp. 1) had the same design discharge, but the sediment feed rate was reduced by 56% (see Figure 3.2b), producing a feed rate that was well below the volume of sediment transport rate consistently observed during Exp. 1. However, the average sediment output rate for the experiment was 0.67 g/min-cm, which is still below the reduced feed rate of 0.80 g/min-cm. Inspection of Figure 3.2b shows persistent aggradation during Exp. 2 (average rate of 4.76 g/min). The experiment was halted once flows began to over-top channel banks.

During Exp. 3 flow was the same as Exp. 1 and 2 and the sediment feed rate was the same as Exp. 2. The conditions were kept the same to explore the role which aggradation played during Exp. 1 on sediment transport rates observed during Exp. 2, or more specifically the role of the increase in channel slope (i.e. stream power). The average sediment output rate for Exp. 3 was 0.35 g/min-cm, which is 43% of the sediment feed rate. This led to persistent aggradation, which is evident in Figure 3.2c. The average rate of aggradation during Exp. 3 was 14.79 g/min, compared to only 4.76 g/min during Exp. 2. The average aggradation rate during the first 2400 minutes of Exp. 1 was 18.47 g/min. Sediment output rates during the first 2400 minutes of Exp. 1 were 1.06 g/min-cm, which is three times greater than Exp. 3.

Following the results of the first three experiments, discharge was increased to simulate the 6-yr return period event in the prototype. The sediment feed rate for Exp. 4 was determined by keeping the sediment concentration the same as it was during Exp. 2 and 3.

After an initial period of degradation, related to erosion of the unarmoured bed surface, the sediment output for Exp. 4 remained below the feed rate for the duration of the experiment (Figure 3.1d). Sediment output was greater than the sediment feed rate only 20 times over the course of the experiment, with only two periods as long as 1 hour which occurred at 1575 minutes and 2070 minutes. Persistent aggradation is evident in Figure 3.2d, with the overall aggradation rate of 9.58 g/min following the first 60 minutes of degradation. A distinct breakpoint can be seen in the plot around 1575 minutes when the average aggradation rate changes from 11.89 g/min to 6.26 g/min for the remainder of the experiment.

In Exp. 5 flows were increased to 2.4 L/s to simulate approximately the 11-yr return interval flood. The feed rate was also increased to keep sediment concentration the same as it had been during Exp. 4. The transport rate remained elevated above the input rate for 165 minutes during the first 225 minutes (Figure 3.1e). Sediment output rate exceeded the feed rate 34 times during the course of Exp. 5, 14 times more than had during Exp. 4. Following the initial period of incision, however, aggradation returned to an overall rate of 0.55 g/min, which is much lower than the previous experiments. Additionally, the rate is not consistent after 225 minutes, with breakpoints in the plot being associated with periods

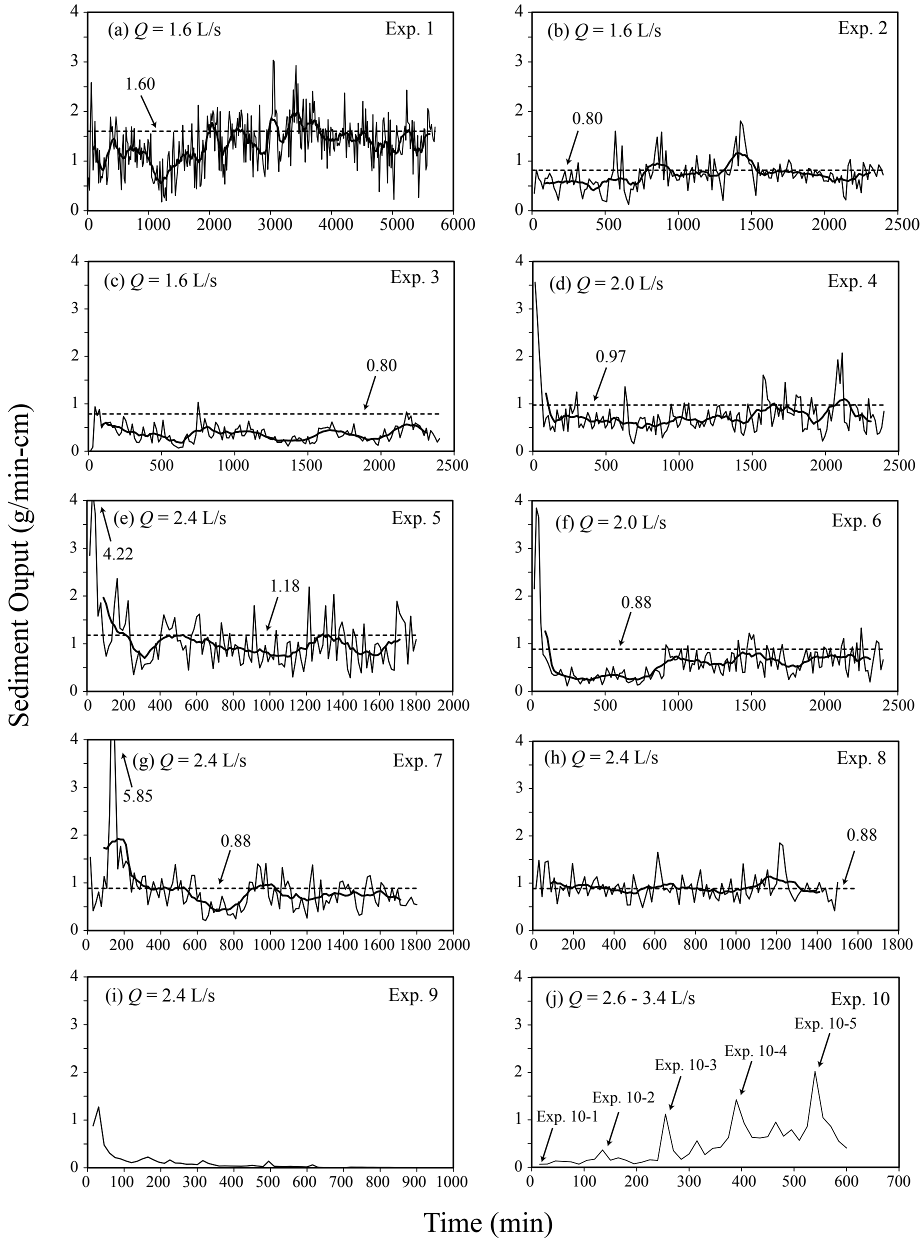

Figure 3.1: Experimental results of sediment output plotted against time. Data represents standardized 15-min average transport rates (g/min-cm). The thicker black line for each experiment represents a 180 min centred moving average. For each experiment, the experiment number is shown in the top right corner. For Exp. 10, the individual 2 hour experiments are also identified. The sediment feed rate (horizontal dashed line) is shown for reference purposes (except for Exp. 9 and Exp. 10 where there was no sediment feed).

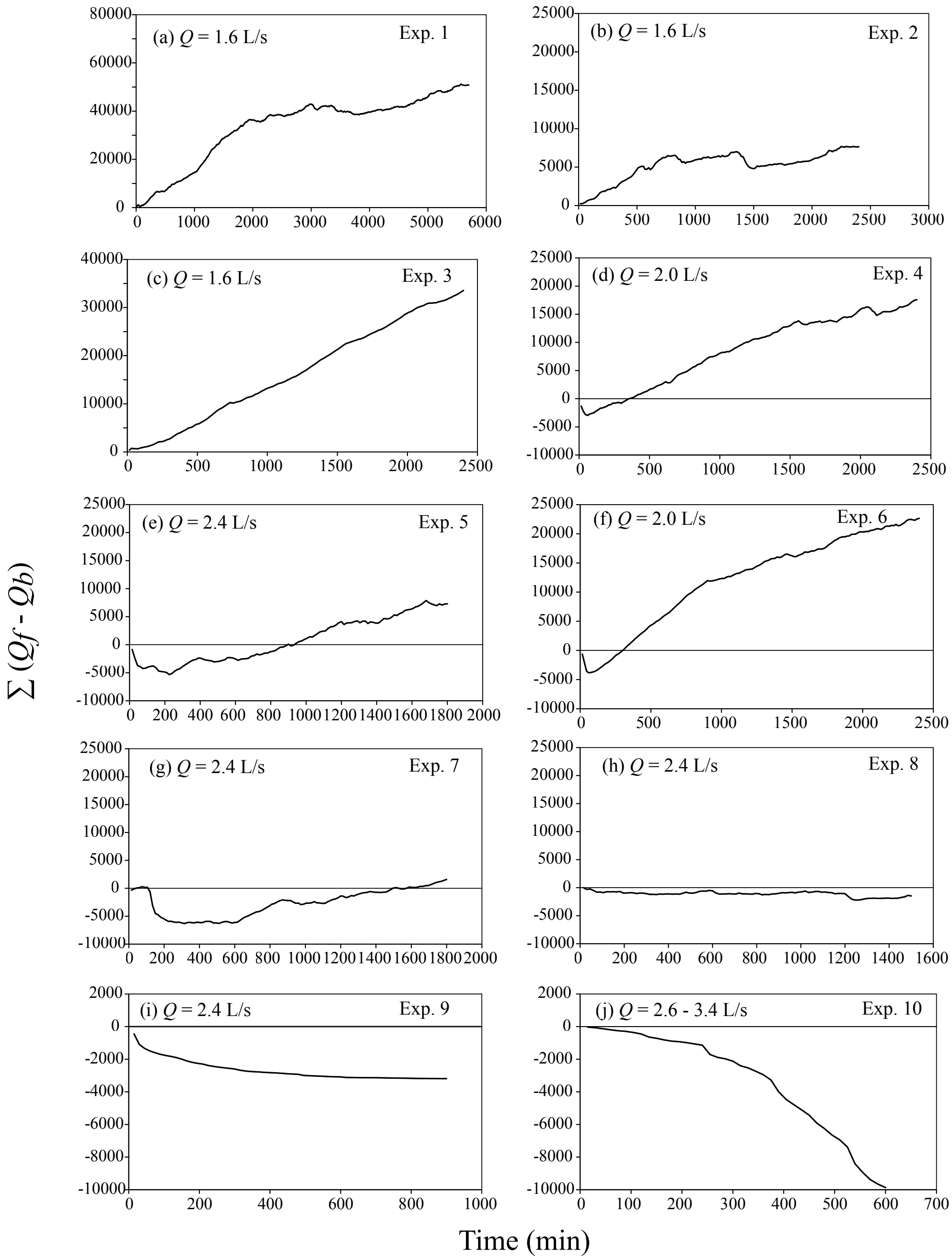

Figure 3.2: Cumulative sediment flux plotted against time. Data represents the cumulative difference between sediment input (Q_f) and sediment output (Q_b) measured in (g). For each experiment, the experiment number is shown in the top right corner.

where sediment output rates exceed the sediment feed rate. Similar to Exp. 4, following these breakpoint periods average aggradational rates appear to shift, which may indicate minor morphological adjustments enabling the increased transport of sediment.

The results from Exp. 6 and 7 are shown in Figures 3.1f and 3.1g. This set of experiments was relatively similar to Exp. 4 and Exp. 5. except that the sediment feed rate was reduced by about 10% compared to Exp. 4 and was held constant for the discharge increase in Exp. 7. The result for Exp. 6 was fairly similar to Exp. 4, which exhibited scour of the un-armoured bed at the start followed by an extended period where sediment output was below the sediment feed rate. However, for Exp. 6 the period following the high sediment output rates was followed by an extended period of very low sediment output rates, average of 0.31 g/min-cm (Figure 3.2f). During this period aggradation in the flume was concentrated over the areas scoured during the initial 60 minutes of the experiment. For the remainder of the experiment the average sediment output rate was 0.67 g/min/cm. When looking at the cumulative plot for Exp. 6 (Figure 3.2f), it appears similar to the Exp. 4 plot, except the breakpoint occurs much earlier (915 minutes). For the duration of the experiment, after the first 75 minutes, during which sediment output exceeded sediment input, the channel aggraded at an average rate of 0.73 g/min. However when the average aggradation rate is divided into pre and post 915 minutes, the average rates become 1.25 g/min and 0.48 g/min, respectively.

After the first 15 minutes of the experiment, Exp. 7 experienced a period of aggradation that lasted for an hour and then sediment output rates exceeded feed rates beginning after 75 minutes (Figure 3.1g). The large spike in the rate of sediment output at 135 minutes resulted from a large degradational event which connected two pools on either side of the channel. This resulted in a high volume of residual scour, the scoured channel exposed a large area of un-armoured bed sediment. The average sediment output rate for the remainder of the experiment after 240 minutes was 0.74 g/min-cm. Following the large scour event an extended period of relative equilibrium occurred from 195 minutes until 615 minutes, during this period slight degradation of the channel occurred at a rate of 0.05 g/min (Figure 3.2g). Over the next 255 minutes a period of rapid aggradation occurred, with average aggradation rates of 15.65 g/min. Following a brief period of equilibrium, aggradation returned with an average rate of 3.95 g/min for the remainder of the experiment.

The grain size distribution (GSD) of the sediment feed for Exp. 8 was changed from the previous experiments. Instead of the initial bed mixture, the sediment output from Exp. 6 was used to ensure that the feed would be fully mobile (as it was mobile at the lower flow discharge used in Exp. 6). The result seen in Figure 3.1h shows that equilibrium in the sediment flux was attained rapidly and maintained for the duration of the experiment. The average sediment output rate for the experiment was 0.91 g/min-cm, slightly greater than the sediment feed rate. Inspection of Figure 3.2h also illustrates this, and in fact slight degradation is evident during the extent of the run.

For Exp. 9 no sediment was fed and the flow rate was kept the same as Exp. 8. The peak in sediment output rates occurred during the first 30 minutes and quickly declined after that. After 600 minutes, sediment output was less than 1 % of the beginning value (Figure 3.1i). The peaks evident in Figure 3.1i reflect the 5 hour experimental interval, every restart of the experiment produced a pulse of sediment. As the volume of material output from this experiment was so minimal it appears as a relatively large effect. Most of the sediment moved was related to the entrainment of sediment that settled while flows were down-ramped from the previous run. In Figure 3.2i the degradational nature of this run is clearly evident, the trend fits a logarithmic decay function.

Exp. 10 was designed to explore the effects of increased discharge on channel response and consisted of five 120 minute experiments with no sediment feed. The experiments were conducted on bed inherited from Exp. 9. Figure 3.1j shows the sediment outputs rates over time. Sediment output rates increased with each experiment, however, the percentage increase in output rates declined following Exp. 10-3.

3.2.2 Sediment Mobility - Fixed Bank Experiments

Following *Church and Hassan* (2002), the relative mobility of individual size classes is presented as the ratio P_i/f_i, where P_i is the proportion of the transported load in the ith size class, and f_i is the size distribution of the bulk sediment mix. As sediment transport is typically a stochastic phenomenon it was felt that box-plots better display the characteristics exhibited by the fractional transport ratios. Unity in the plots represents equal mobility of transport for that size class with respect to its proportion in the bulk sediment mix, or that the transport ratio for that size class is independent of the particle size and the transport rate of the fraction depends on its proportion in the feed (*Church and Hassan*, 2002; *Wilcock and McArdell*, 1993).

For most of the feed experiments presented below the grain size distribution of the bulk sediment mix and the sediment feed are the same. The exceptions are Exp. 8, for which a modified sediment feed grain size was used, and Exp. 9 and Exp. 10, which had no sediment feed.

In Figures 3.3a, 3.3b and 3.3c the smallest three grain sizes (the region greyed out in the figure) were under-represented in the sediment output due to trapping inefficiency of the smallest grains in transport (as discussed above, this continued for Exp. 4 and Exp. 5). The region of equal mobility, grains $\geq$ 0.500 mm and $<$2.83 mm, is similar for Figures 3.3a and 3.3b, even with the reduction in sediment feed. The region of partial mobility, $\geq$ 2.83 mm, is similar for both experiments (Figures 3.3a and 3.3b). The mobility of the three larger grain size classes within the partial mobility region for Exp. 2 is greater than Exp. 1, especially for grains $\geq$ 4.00 mm.

From Figure 3.3c, it is clear that the range of grains sizes in the region of equal mobility is smaller in Exp. 3, grains $\geq$ 0.500 mm and $<$2.00 mm, than in the previous two experiments. It is interesting to note, however, the classes experiencing equal mobility are much more mobile than in the previous experiments. A more marked decline and lower

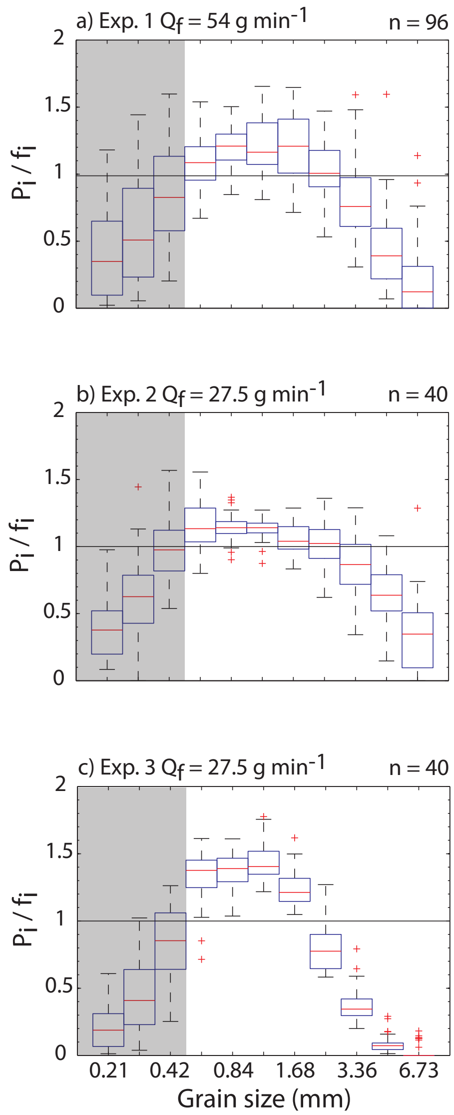

Figure 3.3: Fractional transport ratio diagrams of mobile size classes from a) Exp. 1, b) Exp. 2, and c) Exp. 3. Box-plots show P_i/f_i vs particle size, the size shown in mm is the arithmetic mean between the retaining and passing sieve sizes (sieves in $1/2$ Φ units). The box has lines at the lower quartile, median, and upper quartile of the data. Whiskers extend from each end of the box to the adjacent values in the data. Grey boxes in the figures indicate partial values due to trap inefficiencies (for Exp. 1 - Exp. 5). Additionally, the number of individual observations in each experiment is included.

values in fractional transport ratios for grains $\geq$ 2.00 mm is seen on the right hand side of 3.3c when compared to either Figure 3.3a or 3.3b.

The regions of equal mobility in Figures 3.4a (Exp. 4) and 3.4b (Exp. 5) are very similar to those during Exp. 1 and Exp. 2. (see Figure 3.3). The result is surprising given the higher discharge used in these experiments. The increased discharge in Exp. 5 only resulted in a slight increase in the ratios in the region of partial mobility for grains $\geq$ 2.00 mm and <2.83 mm compared to Exp. 4.

For Exp. 6 and Exp. 7 reconfiguration of the sediment trap lead to confidence in the measured output for the lower grain size classes, thus the greyed out region is no longer needed in the figures (Figure 3.5). The feed rate (Q_f = 30 g min^{-1}) used in these experiments was the same for Exp. 6, Exp. 7 and Exp. 8. The same bulk sediment mixture was used for the feed in Exp. 6 and Exp. 7, and a modified feed mix was employed for Exp. 8. No sediment was fed during Exp. 9 and Exp. 10. Discharge in Exp. 6 (2.0 L s^{-1}) was 20 % lower than in Exp. 7 through to Exp. 9 (2.4 L/s inclusive), discharge increased steadily at 0.2 L/s increments during the five runs in Exp. 10.

With improved trap efficiency, the region of equal mobility extends from grains $\geq$ 0.177 mm to grains <2.00 mm in Figure 3.5a and <4.00 mm in Figure 3.5b. Although the smaller size classes, $\leq$ 0.354, appear to be partially mobile during a majority of the time. The results suggest that for greater than 50% of the measurements, the finer material is being retained by the bed. It is possible that this material is being trapped behind the coarser grains that are only partially mobile and are accumulating on the bed surface. The figures show the increased mobility of grains under higher flows, but still equal mobility for all grain sizes was not witnessed. Comparatively, Exp. 4 and Exp. 6 differ negligibly yet the fractional transport ratios are greater for grains $\geq$ 2.83 mm appears. Sediment feed rate was 27% lower in Exp. 7 than Exp. 5, yet the mobility of the grains appear to be relatively similar.

For Exp. 8 the sediment feed was modified compared to the mix used in Exp. 6 and Exp. 7, the mobility plots for Exp. 8 are shown in Figure 3.6a. In order to maintain consistency in the presentation of results between experiments the GSD of the initial feed mixture was used to scale the output from Exp. 8. The figure illustrates that there is a clear under-representation of the smaller size classes in the output, this is partly due to differences in the GSD of the sediment feed, but it is also due to a reduced proportion of these grains remaining on the surface. The region of equal mobility is similar to that shown in Figure 3.5b, although it can arguably be extended to include grains <4.00 mm, as this size class is close to unity. The grains sizes in the partial transport regime, those $\geq$ 4.00 mm (Figure 3.6a), appear to be more mobile than those in Figure 3.5b. Interestingly, the variability in the observations has reduced between Exp. 7 and Exp. 8, as represented by width of the boxes. The results suggest that using the modified feed can increase the mobility grains, although only moderately.

Figure 3.7 shows the fractional transport ratios from Exp. 8 using the GSD of the feed instead of that of the original bulk sediment mix. When viewed from this reference point

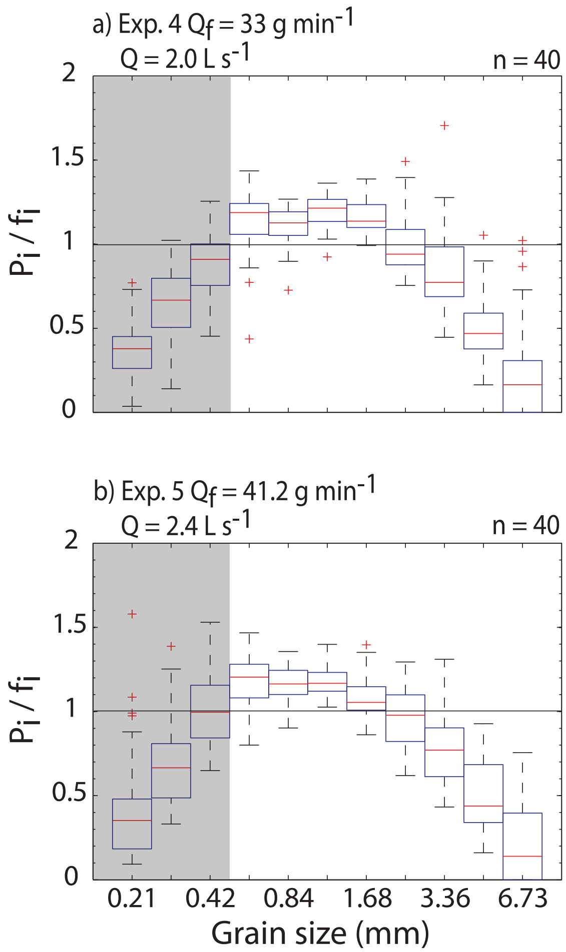

Figure 3.4: Fractional transport ratio diagrams of mobile size classes from a) Exp. 4 and b) Exp. 5. See Figure 3.3 for definitions.

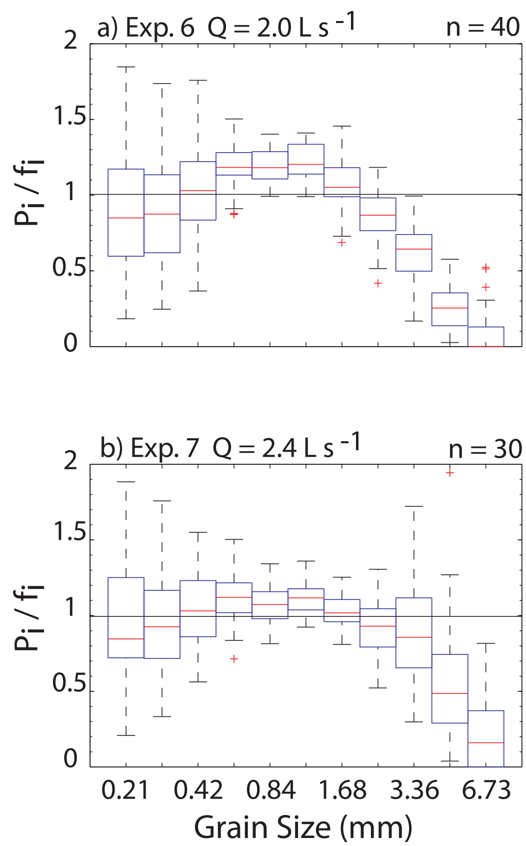

Figure 3.5: Fractional transport ratio diagrams of mobile size classes from a) Exp. 6 and b) Exp. 7. The two experiments have the same feed rate ($Q_s = 30$ g min^{-1}) but discharge was increased in Exp. 7, see Figure 3.3 for definitions.

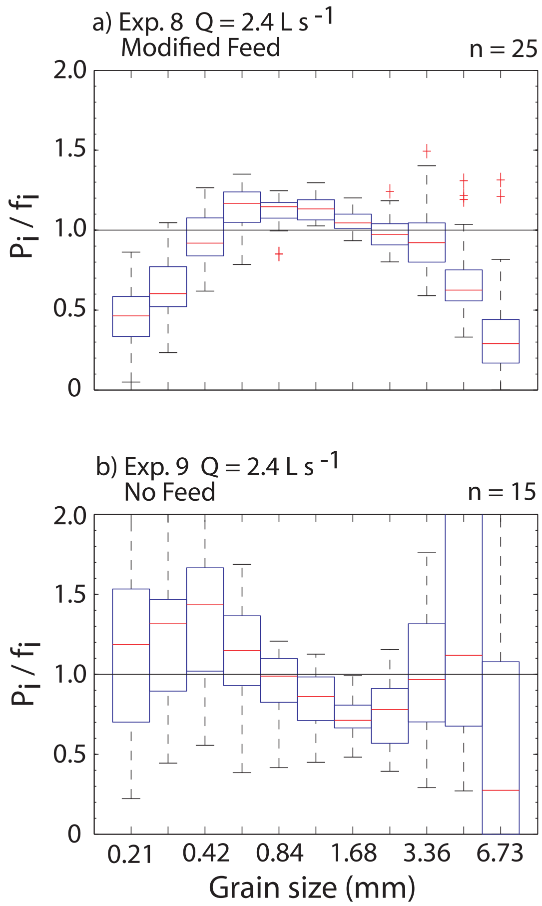

Figure 3.6: Fractional transport ratio diagrams of mobile size classes from a) Exp. 8 and b) Exp. 9. Exp. 8 was conducted with the same feed rate as Exp. 6 and Exp. 7 but employed a modified feed. Exp. 9 used no feed. See Figure 3.3 for definitions.

it suggests that full mobility occurred for all grain sizes of the sediment feed. Grains $<.707$ mm were overrepresented in the sediment output when referenced to the feed, suggesting that these sizes were entrained from the bed during the run. However, this effect was also influenced by increased bed scour. The over representation of grains ≥ 2.83 mm, indicates that these grains were being transported in a greater proportion than in the feed, and were therefore also being entrained from the bed. This may also reflect increased bed scour, but it is also attributable to increased entrainment from the bed surface.

Exp. 9 was a no feed, degradational experiment. Figure 3.6b shows that the fractional transport ratios are near full mobility for all size classes. For grains <0.707 mm in most of the samples these size classes are over represented in the sediment output. This is likely the result of entrainment of grains from the subsurface layer following pool scour events during the run and partial breaching of the armour layer. Grain sizes ≥ 0.707 mm and <1.00 mm are near unity for half of the samples. Grains ≥ 1.00 mm and <2.83 mm are only partially mobile for most of the time. A region of partial transport is evident for grains >5.6 mm, although equal mobility occurs greater than 25% of the time. It should be noted that mobility of the larger grains >4.00 mm increased over the duration of the experiment.

The partial transport rates for Exp. 10 are shown in Figure 3.8. It is clear from all of the experiments that during the first 60 min of each run all size classes were partially to fully mobile. Many of the experiments experienced a higher proportion of the smaller and larger size classes being transported. By the second hour most of the experiments tended toward equal mobility of the grains (Figure 3.8). The exception being seen in Figure 3.8c, which reflects the formation of a large pool near the downstream end of the channel. The scour associated with pool development exposed the subsurface material, which has the same GSD as feed, to entrainment. Given the proximity of the pool to the outlet, all eroded material went directly to the trap. These experiments clearly reflect armour breaching during the first hour of the experiment, but also reflect a relatively rapid recovery in the armour layer during the second hour.

3.2.3 Sediment Mobility - Mobile Bank Experiments

In Figure 3.9 the fractional transport ratios are again plotted as a function of particle size for the mobile bank experiments. The experiments are divided into stable and unstable channels (Figure 3.9). The data for the stable channels comprise 22 samples from 12 different experiments. The unstable data consist of 9 samples from 7 different experiments. It should be noted that stable and unstable channels may have existed during the same experimental run. For the stable channel the pathway to stability was mainly accomplished through slope adjustments, with negligible surface coarsening (*Eaton and Church*, 2004). The unstable channels exhibited accelerated bank erosion, slope reduction and rapid aggradation, that would have eventually led to braiding if the experiments were not stopped.

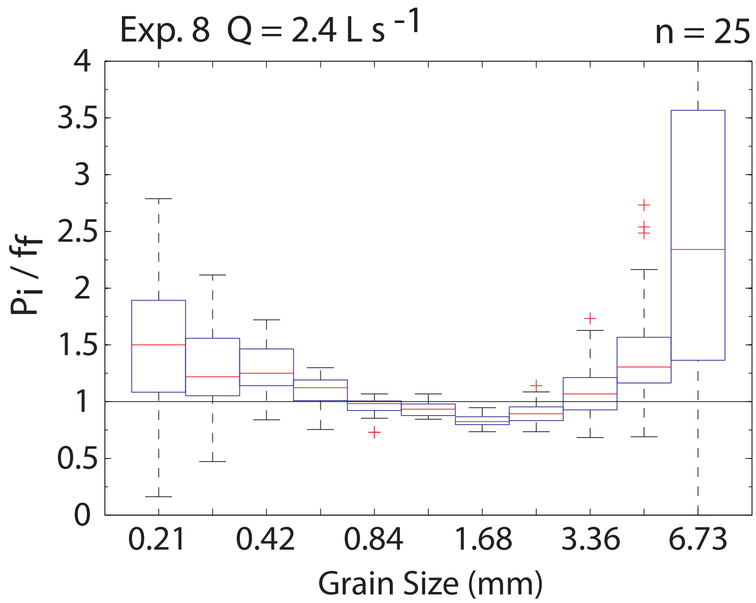

Figure 3.7: Modified fractional transport ratio diagrams of mobile size classes from fixed bank Exp. 8. This figure slightly modifies the fractional transport ratio (P_i/f_i) to (P_i/f_f) by employing the feed grain size distribution (f_f) rather than the subsurface as in previous plots. See Figure 3.3 for definitions.

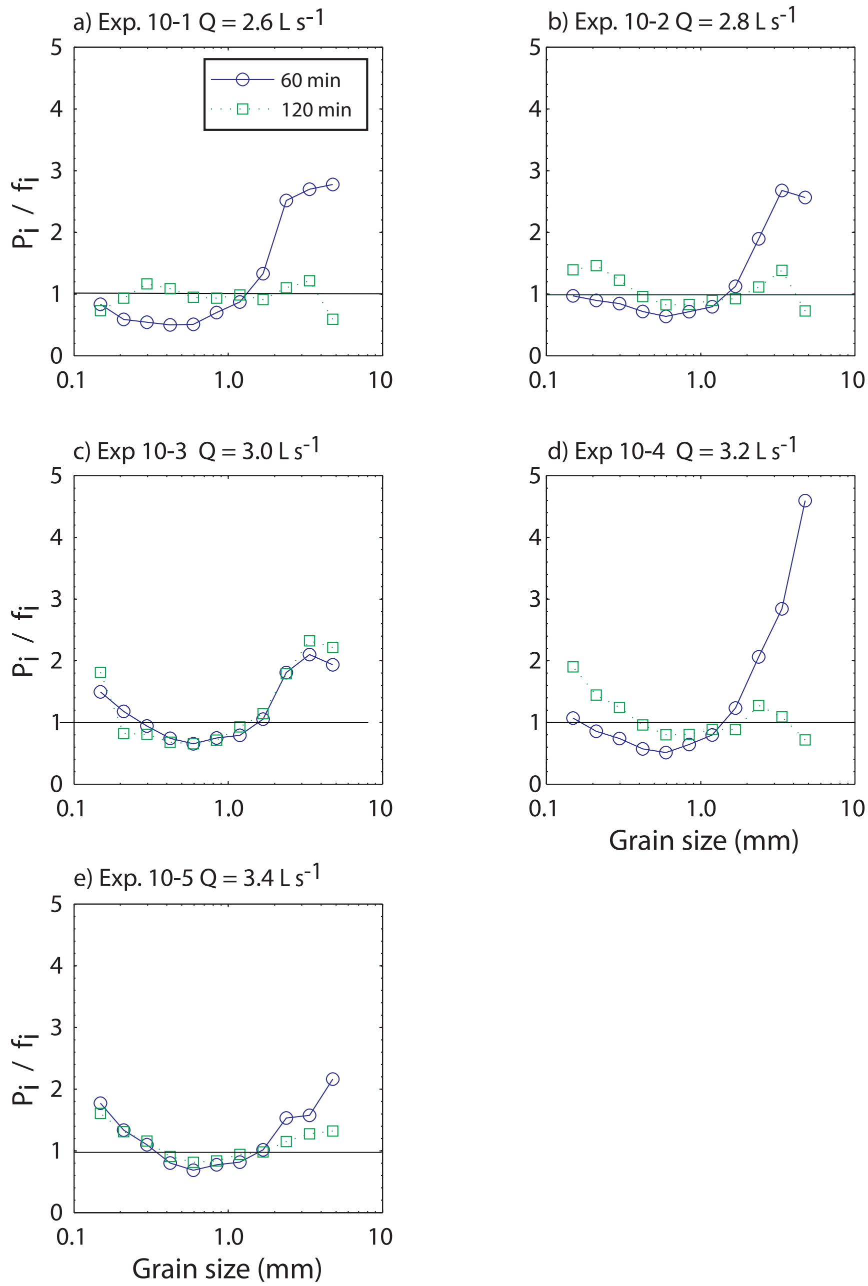

Figure 3.8: Fractional transport ratio diagrams from Exp. 10 with no sediment feed and increasing discharge: a) Exp. 10-1, b) Exp. 10-2, c) Exp. 10-3, d) Exp. 10-4, e) Exp. 10-5. All experiments were run for 120 min. For these experiments the fractional transport ratios are presented in terms of P_i/f_i. See Figure 3.3 for definitions.

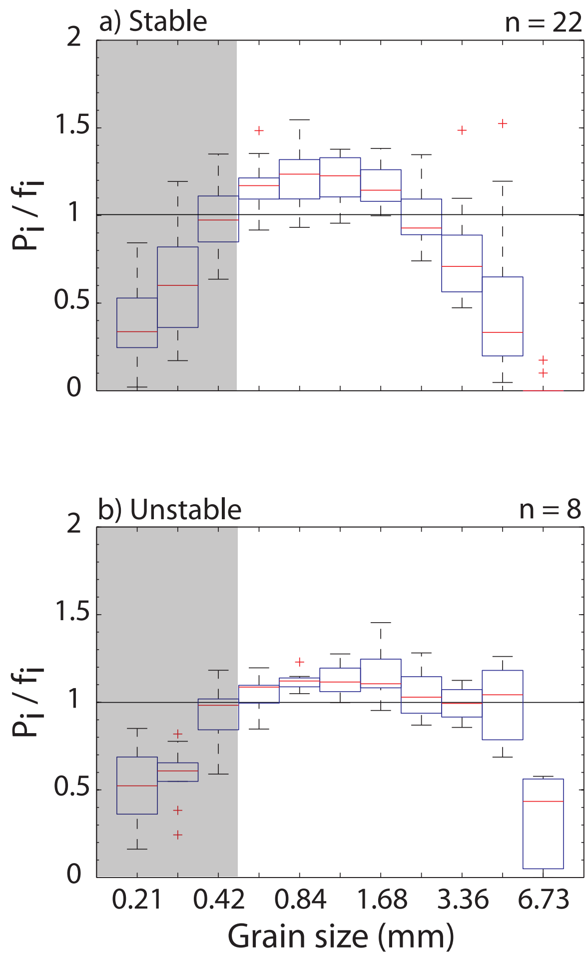

Figure 3.9: Fractional transport ratio diagrams of mobile size classes from the mobile bank experiments for a) stable and b) unstable periods. See Figure 3.3 for definitions.

Three regions of transport can be identified in the plots from the mobile bank experiments (Figure 3.9). For both Figures 3.9a and 3.9b size fractions <0.500 mm are under represented in the output with respect to the bulk mix. This result is due to trap efficiencies (discussed above), thus no conclusions can be reached about the behaviour of these size classes, although it is assumed that they would plot near unity.

Grain sizes $\geq$ 0.500 mm and <2.00 mm in the stable samples are equally mobile for a majority of the observations (Figure 3.9a). For the unstable periods grains sizes $\geq$ 0.500 mm and <5.60 mm exhibit equal mobility, median ratio values were either equal to or greater than unity (Figure 3.9b). A value of unity indicates equal mobility of these grain sizes or that these sizes are transported at proportions similar to their presence in the sediment mix. The median values for grain sizes between 0.500 mm and 2.00 mm appear to be higher in the stable experiments compared to the unstable experiments, indicating a relatively higher mobility for these size classes during stable periods.

The right side of Figure 3.9a shows a steady decline in the fractional transport ratio of larger size classes, $\geq$ 2.00 mm, following the sizes that exhibit equal mobility. For the largest size class, >5.6 mm, for most experiments no grains were observed at the outlet (Figure 3.9a). It should be noted that this does not negate the potential for movement within the channel, just that it was not recorded at the outlet.

This steady decline in the transport ratios indicates the decreasing mobility of grains with reference to their presence in the bed, a condition referred to as partial transport. In Figure 3.9b, however, the region of equal mobility is much greater than observed during stable periods, and extends up to grain sizes <5.6 mm. A sharp drop in the mobility for grains $\geq$ 5.6 mm is seen, however, in comparison to the stable channels its mobility in the unstable channels is much greater.

3.3 Discussion

In general, the experiments highlight the usefulness of prototype scaling as it can give insight into the frequency and magnitude of channel response and time-scales of channel evolution. The combination of a field prototype and Froude scaled physical models allows one with a discharge record to use emergent channel features and be able to contextualize results found in the lab to those in the field. The scaling of time and sediment transport has proved difficult to numerically model due to gaps in our understanding of how to account for evolving beds. Much historic information has been gleaned from previous field based studies, physical models offer another geomorphic tool that can be used alongside field based studies to develop improved understanding of geomorphic processes (for example, *Yalin*, 1971; *Davies and Lee*, 1988; *Warburton and Davies*, 1994; *Hassan and Church*, 2000; *Eaton and Church*, 2004; *Gran et al.*, 2006; *Madej et al.*, 2009; *Pryor et al.*, 2011). The use of realistic physical models is standard practise outside of academia to inform hydraulic design and to understand potential impacts that an proposed or existing infrastructure may produce. Their use may shed more insight into river behaviour than the standard flume set-up, upon which much of our understanding of river processes has been built.

The experiments demonstrated that slight size selective transport can occur at a range of transport rates and discharges, and that it is governed by the particle size of the feed, and not the feed rate. The decline in P_i/f_i ratios for the larger grain size classes has been observed in both field (*Powell et al.*, 2001; *Church and Hassan*, 2002; *Thompson and Croke*, 2008) and flume (*Wilcock and Southard*, 1989; *Wilcock and McArdell*, 1993, 1997; *Hassan and Church*, 2000; *Hassan et al.*, 2006) experiments. The mobility of the larger size classes present on the bed surface is an important determinant of channel stability. Exp. 10 illustrated that once the coarser size classes approached equal mobility the channel became unstable. The results from the mobile bank experiments also illustrated that unstable channels are represented by more mobile coarse fractions than were stable channels. This suggests that determining at what discharge the D_{90s} or D_{95s} of the bed surface becomes mobile can determine at what flow magnitude the channel may potentially become unstable.

An additional factor in the stability of the fixed bank experiments is the morphology of the channel. A link between the stability of bars, for example, is likely tied to the stability of the larger grains on the bed. An additive effect is suggested to exist between bed surface armouring and channel bedforms, which has a net positive increase on the stability of both and likely the channel overall.

The degree of size selective transport was found to vary with the applied discharge and with the grain size distribution of the sediment feed. The experiments demonstrated that beds aggraded at a slow rate due to a persistent (but slight) selective deposition/transport of bed material. The rate of the aggradation would typically go unnoticed in most field environments. The timescales at which the rates of aggradation observed in these experiment would occur in the field is nearly 100 years, and is on the same scale as the disturbance regime. In cases where the channel is not laterally constrained, slow aggradation rates coupled with surface coarsening would induce lateral channel movement, as was evident in the New Zealand experiments. The experiments also demonstrated that the channel does not aggrade when the sediment was slightly finer, Exp. 8.

Church and Hassan (2005) wondered whether in channels that exhibit partial and selective transport if the coarse grain sizes would continue to accumulate. These experiments suggests that they do, and that this accumulation results in slow, persistent channel aggradation. Similar persistent aggradation has been observed in the experiments of *Pryor et al.* (2011), *Recking et al.* (2009) and *Braudrick et al.* (2009), although they avoided long-term aggradation by reducing the proportion of coarse feed. Although, this rate of aggradation has yet to be observed in the field, the rates of aggradation observed here suggest that it would be difficult to identify with annual surveys as it is within the measurement error of most channel surveys. *Church and Hassan* (2005), also suggested two mechanisms by which this phenomenon could be avoided in natural channels:

1. large floods that are of sufficient magnitude to mobilize the large material and there-

fore establish a long term equilibrium between sediment supply and output. This suggests that equal mobility is a long term phenomenon, and would not be observed at shorter, more dynamic, time scales.

2. abrasion that reduces the size of larger clasts and enables the transport of this material out of the reach.

In these experiments, even under flow conditions with magnitudes greater than the 10-yr flood, aggradation was still observed. This suggests that in these types of channels, flows with magnitudes above the 10-yr flood event are required to mobilize the larger clasts in the channel or that weathering in situ is required to maintain conservation of mass. These results also may explain the discrepancy of some of the channels studied by *Lisle* (1995), that appeared to deviate from equal mobility. The bedload data was not sampled from a flow large enough, that equal mobility would be expected to occur.

Church and Hassan (2005) attributed the attrition of grains to weathering processes during storage within the channel (for example, *Jones and Humphrey*, 1997) as opposed to abrasion during transport (for example, *Sklar et al.*, 2006). An additional mechanism of weathering is suggested here. This mechanism is related to the lateral activity of the channel. Disturbance of the riparian zone, such as from forest fires in the case of Fishtrap Creek, can result in temporary periods of increased lateral activity. A direct result of lateral activity can be channel avulsions, which results in the abandonment of the former channel into a new channel that is cut into the floodplain. This process can result in two outcomes:

1. the sediment in the abandoned channel is exposed to increased weathering activity, physical and biological, and particularly freeze-thaw weathering.

2. the sediment in the new floodplain channel has been sufficiently weathered during its sequestration to the floodplain environment, that grain sizes have decreased enough to now be transported by lower magnitude flow events.

Over time it is anticipated that the former floodplain sediment will be transported downstream and replaced by sediment from upstream sources as the channel moves about its floodplain, and the cycle will repeat. Even moderate channel erosion into the floodplain material can lead to a decreased sediment size. As Exp. 8 has shown, even a moderate increase in the proportion of the more mobile fractions in the feed, can increase the mobility of the larger classes.

The aggradation observed here produced a coarse surface, which suppressed pool-riffle development and led to a plane-bed like morphology. This pathway to plane-bed channels differs from that proposed by *Montgomery and Buffington* (1997), as plane-bed channels are degradational in nature. As observed during these experiments, and by the author in various field settings, plane-bed channels can develop in forested streams even during periods of net aggradation. Plane-bed morphologies can also temporarily exist in reaches the have received landslide deposits that bury the existing morphology in material not readily erodible by normal flows. This morphology may also be characteristic of channels that are unable to erode their banks (due to, for example, riparian forests) which would prevent the exchange of sediment between the channel and the floodplain. For channels with erodible banks, the lower mobility of the coarser size fractions has a less rapid effect on the bed surface texture since sediment is constantly being exchanged between the channel and floodplain, and may be counter-balanced by weathering-related changes in the sediment size distribution that can occur in the interval between deposition and re-entrainment. In these cases, the channel does not aggrade due to coarse sediment deposition. Furthermore, when the largest grains do become fully mobile, the bank erosion rate accelerates, channel sinuosity increases, thereby decreasing the reach-average energy gradient and ultimately the bed material transport capacity. This feedback intensifies the morphodynamic instability and ultimately is likely to result in a change in channel morphology from a single-thread channel to a braided one.

3.4 Conclusions

The experiments were used to investigate sediment mobility during various sediment feed and flow regimes. In general, the largest size fractions were under-represented in transport. This under representation led to channel aggradation. However, when sediment fed into the system was equivalent to sediment that was output from the system, no aggradation was observed. In fact, the introduction of this feed actually increased the mobility of some of the larger previously less mobile size classes.

Aggradation due to partial mobility of selective transport can potentially be avoided in channels by increased lateral activity. Lateral activity can result in the re-activation of weathered channel sediment in the floodplain in exchange for the coarser sediment responsible for the aggradation. The observed aggradation produced plane-bed like morphologies, which creates another pathway for the creation of this channel type.

Full mobility only appears to be characteristic of unstable/degrading systems in gravel-bed rivers. Partial mobility in these experiments led to aggradation, not a capacity limitation but competence limitation in the ability to move the largest grain sizes. These experiments indicate that stability in mountain channels may hinge on the mobility of the largest grain size class less than the D_{90} in our experiments. Mobility of this size class may be an indication of current or future channel instability.

Chapter 4

Spatial and Temporal Patterns in Sediment Transport and Storage

4.1 Introduction

A proper accounting of sediment transport in gravel-bed rivers is important for fluvial geomorphology, channel assessments, river engineering, sediment budgeting, landscape evolution models, fisheries habitat assessments, and river rehabilitation projects. The sampling of sediment transport data is both financially and temporally cumbersome, and is usually only feasible under selected circumstances (for example, *Wilcock*, 2001a). Thus most estimates of sediment transport are made using a variety of transport equations. These equations generally contain a combination of theoretical and empirical components, that are mostly based on averages of local hydraulic and sedimentological variables. When applied to gravel-bed rivers these equations tend to either under- or over-estimate the observed values by an order of magnitude or more (*Carson and Griffiths*, 1987; *Gomez and Church*, 1989; *Lenzi et al.*, 1999; *Bravo-Espinosa et al.*, 2003; *Barry et al.*, 2004; *Pitlick et al.*, 2008; *Recking*, 2010; *Nitsche et al.*, 2011).

Measurements of sediment transport rates in field and laboratory environments have been observed to fluctuate both spatially and temporally even under steady state conditions (*Hoey*, 1992; *Kuhnle*, 1996). The causative mechanisms behind this variability have been attributed to flow regime (*Nordin*, 1985; *Lisle*, 1989; *Nash*, 1994), sediment regime (*Dietrich et al.*, 1989; *Hoey and Sutherland*, 1991; *Lisle et al.*, 1993; *Gintz et al.*, 1996; *Benda and Dunne*, 1997b; *Gomi and Sidle*, 2003; *Venditti et al.*, 2010), the passage of bed forms (*Reid et al.*, 1985; *Iseya and Ikeda*, 1987; *Lisle et al.*, 2000; *Recking et al.*, 2009; *Nelson et al.*, 2009), and the evolution of bed topography and bed structures (*Laronne and Carson*, 1976; *Komar*, 1987; *Kuhnle and Southard*, 1988; *Church et al.*, 1998; *Papanicolaou and Schuyler*, 2003; *Nelson et al.*, 2010). In essence, the variability in transport rates has been linked to the variability in sediment supply and storage.

To overcome the limitations of the current transport theory, *Lisle and Church* (2002) proposed to shift the focus away from hydraulic related parameters and to focus on sediment supply and storage instead. In order to achieve this, they focused on transport capacity, which they see as being a mediator between sediment supply, transport and storage. *Lisle and Church* (2002) proposed that transport capacity is not a fixed quantity, as is frequently assumed, but varies according to the volume of sediment stored within each sediment reservoir and the bed state. They defined a sediment reservoir as homogeneous reach of the channel and its associated floodplain that has the potential to store sediment and can be accessed by the channel under the current hydroclimatic regime. Using data from field and flume studies they asserted that the transport capacity of each sediment reservoir was a unique positive function of the volume of sediment stored within that reservoir; storage volume influences sediment mobility and availability though surface texture, channel gradient and availability of sediment stored in the floodplain. They proposed two phases in the transport-storage relation for degrading experimental channels: Phase I, comparable to transport-limited conditions, is associated with conditions of high sediment supply and transport rates, non-selective transport and weak armouring; Phase II, comparable to supply-limited conditions, is characterized by selective transport, bed armouring and transport rates that decrease as sediment storage decreases. *Lisle and Church* (2002) recognized that their understanding of the transport-storage was limited as only degrading systems were investigated.

Flume experiments by *Pryor et al.* (2011) were conducted in order to investigate the transport-storage relation over periods of both aggradation and degradation. They reported that full aggradation-degradation cycles exhibited counter-clockwise hysteresis or a cyclic pattern in the transport-storage relation, and thus a unique relation between sediment transport and sediment storage was not observed. Similar observations were made by *Madej et al.* (2009) in their flume experiments and by *Hassan et al.* (2007) using long-term field data. Together these newer results concluded that the hysteresis occurred during disequilibrium conditions and that the cycles are a result of an external perturbation, such as a change in sediment supply or flow characteristics. However, this hysteretic effect may in fact be an inherent response in sediment transport rates to the evolution of the bed surface and within channel morphological adjustments to changes in sediment supply. It is possible that a non-linear relationship between transport rates and sediment storage may be more the norm than not.

In light of these recent results, *Lisle* (2012) re-visited the earlier model and modified it to include two general scenarios: Scenario 1 - a state of dynamic equilibrium between transport capacity and sediment storage, a common relation at a given stage of sediment storage in the channel is the same whether the channel is aggrading or degrading; Scenario 2 - a state of transient equilibrium, where increased transport rates are experienced during degrading conditions and depressed transport rates occur during aggrading conditions for a given sediment stage. *Lisle* (2012) concluded that the conditions represented by Scenario 2 were caused by short-term variations in supply. The results of experiments conducted by *Pryor et al.* (2011) and *Madej et al.* (2009) support Scenario 2.

All of the experiments under which the transport-storage relations have been developed and/or tested have been conducted using variable sediment input rates to induce channel degradation of short-term periods of either aggradation or degradation. It may be argued that the variability of sediment input may artificially inhibit Scenario 1 from occurring. Most of the previous experiments cited above, only observed Scenario 1 during degradational phases of the experiment. The experiments presented here are a further attempt to elucidate the relation between transport capacity and sediment storage. As with the previous experiments, intermediate size forested gravel-bed rivers were the targeted prototype for experimental design.

Intermediate size forested gravel-bed rivers are subject to variable flows and sediment loads, yet they remain relatively stable, at least in the lateral sense. For the most part, variability in the governing conditions is accommodated within the channel boundaries. Only major disturbances, those that exceed the capacity of the channel to adjust, lead to channel relocation or widening. Consequently, the banks of the channels remain relatively static or are stable around some mean value over time. Channel planform in these environments appears to be dictated more by boundary conditions, such as riparian forests and non-alluvial boundaries, than by alluvial processes. Most experiments to date have been conducted in straight relatively narrow flumes with no consideration to the channel planform. The experimental channel used here, was designed based on the planform geometry of a mountain gravel-bed river to explore the effects of irregular channel walls and to generate results comparable to the field.

The objectives of this chapter are to:

1. explore spatial and temporal patterns of sediment transport;
2. investigate the transport-storage relation under steady state forcing conditions; and,
3. investigate the response of the channel in terms of sediment storage in changes in sediment supply and flow conditions.

4.2 Results

Results are presented for the following topics: sediment transport rates, sediment transport-storage relations, patterns of channel adjustments, and the sediment texture of bed surface and transported material. In order to explore each topic area, the experiments are organized according to themes. The first theme explores the effects of the initial conditions of the channel, with initial conditions beginning on a screeded bed and discharge and feed rates being similar (Exp. 4 versus Exp. 6) or different initial conditions with similar discharge and feed rate (Exp. 2 versus Exp. 3). Secondly, the effects of stream discharge with constant sediment feed rate and texture (Exp. 6 versus Exp. 7) is explored. For the second theme, the sediment feed rates are varied while the stream discharge and sediment feed texture are held constant (Exp. 1 versus Exp. 2 and Exp. 3, Exp. 4 versus Exp. 6, and Exp. 5 versus Exp. 7). Lastly, the effects of a change in the sediment feed texture while holding flow discharge and sediment feed rate constant is explored (Exp. 8 versus Exp. 7).

Summary data of the experimental conditions and results are presented in Table 4.1.

Table 4.1: Summary data of the experimental conditions and results. For some of the values that are averages the standard deviation has been included in brackets.

Exp.[a]	Time (min)	Discharge (L/s)	Sediment Feed Rate (g/s)	Average[b] Velocity (m/s)	Average[c] Slope (m/m)	Average[d] Depth (cm)	Average[e] τ_b (Pa)	D_{50s} (mm)	Cycle Number	Maximum Storage Difference (g)	Length of Cycle (min)	Number of Cycles
1	5700	1.6	0.91	0.32	0.0153	1.47 (0.08)	2.21 (0.15)	2.58 (0.35)	1	648.9	105	1
									2	225.3	60	1
									3	886.1	285	3
									4	733.6	195	1
									5	4336.7	1680	11
									6	666.0	195	1
									7	750.1	165	1
2	2400	1.6	0.45	0.31	0.0164	1.50 (0.08)	2.44 (0.08)	3.03 (0.19)	1	453.7	135	2
									2	1044.5	510	5
									3	2226.0	840	3
3	2400	1.6	0.45	0.30	0.0152	1.58 (0.05)	2.31 (0.12)	2.37 (0.31)	No cycles	-	-	-
4	2400	2.0	0.55	0.37	0.0152	1.60 (0.07)	2.35 (0.13)	2.89 (0.20)	1	677.2	225	2
									2	1486.1	270	1
5	1800	2.4	0.67	0.38	0.0158	1.85 (0.03)	2.90 (0.09)	3.29 (0.14)	1	1541.6	195	1
									2	762.2	240	2
									3	648.8	225	1
									4	897.2	105	1
6	2400	2.0	0.50	0.35	0.0163	1.72 (0.05)	2.71 (0.27)	2.64 (0.22)	1	426.5	135	1
7	1800	2.4	0.50	0.39	0.0161	1.81 (0.04)	2.86 (0.17)	3.13 (0.31)	1	623.8	105	1
									2	6616.7	1470	1
									3	436.1	375	5
									4	846.1	315	2
									5	288.4	60	1
									6	177.7	105	1
8	1500	2.4	0.50	0.40	0.0168	1.79 (0.02)	2.92 (0.07)	3.22 (0.13)	1	794.0	1125	14
									2	67.2	105	3
9	900	2.4	0	0.37	0.0162	1.99 (0.10)	3.24 (0.26)	3.12 (0.55)	No cycles	-	-	-

[a] Experiments with bold numbers indicate experiment started on hand screeded bed, and non bolded numbers identify experiments conducted on bed inherited from preceding experiment.
[b] Average velocity determined using the mean of hourly velocity averages, standard deviation is included.
[c] Following *Eaton and Church* (2009), average slope determined using a linear regression of the mean bed elevation at each cross section and the down valley distance of each cross section.
[d] Average depths were determined using continuity.
[e] Average shear stress (τ_b) was calculated using $\tau_b = \rho g d S$

4.2.1 Sediment Transport Rates

For all of the experiments in which the sediment feed grain size distribution was the same as the bed material grain size distribution, the sediment output was consistently lower than the sediment input, regardless of the actual supply rate or the imposed stream discharge (Figure 4.1). This effect has been quantified by calculating a bed material transport efficiency term, T_{eff}, for which:

$$T_{eff} = \frac{Q_b}{Q_f} \tag{4.1}$$

The value of T_{eff} varies significantly between experiments with the same inputs and initial conditions. For example, Exp. 4 and Exp. 6 had identical flows and nearly identical sediment feeds, and both began from the same featureless initial bed state. However, due to differences in the channel morphology, evident in the different reach-average flow velocities, the transport efficiencies were about 20% higher for Exp. 4 (see Table 4.2). Differences in channel response during the initial phase of each experiment were also observed, Exp. 6 experienced more scour than Exp. 4 which lead to a much longer period where transport rates were much lower than the feed rates (Figures 4.1d and 4.1f), up to 900 minutes for Exp. 6. Histograms of T_{eff}, calculated for each 15 minute sampling period (Figure 4.2c), show that values of T_{eff} fluctuated greatly during both experiments, with most observations ranging 0.50 to 1.1. The histograms show data from the experiments starting at 120 min. in order to remove the high transport rates at the onset of the experiments. A two-sample Kolmogorov-Smirnov (K-S) goodness-of-fit test (p = 0.05) was used to determine if the transport efficiencies from the two experiments were drawn from the same underlying continuous distribution. The result of the test was that these two distributions are significantly different from each other. It is interesting to note, that when comparing T_{eff} values after 900 minutes the distributions were no longer statistically different.

Table 4.2: Transport efficiency for experiments with similar stream discharge and sediment feed.

Experiment	Q	Q_f	$\overline{Q_b/Q_f}$	95% Confidence Range
4	2.0	0.55	0.74	0.69 – 0.79
6	2.0	0.50	0.62	0.57 – 0.67
2	1.6	0.45	0.89	0.83 – 0.95
3	1.6	0.45	0.46	0.42 – 0.49

Similarly, Exp. 2 and 3 had identical flows and sediment feed rates, the difference was the initial conditions at the beginning of the experiment. Exp. 2 was initiated using the final bed morphology created during Exp. 1, while Exp. 3 was initiated on a featureless

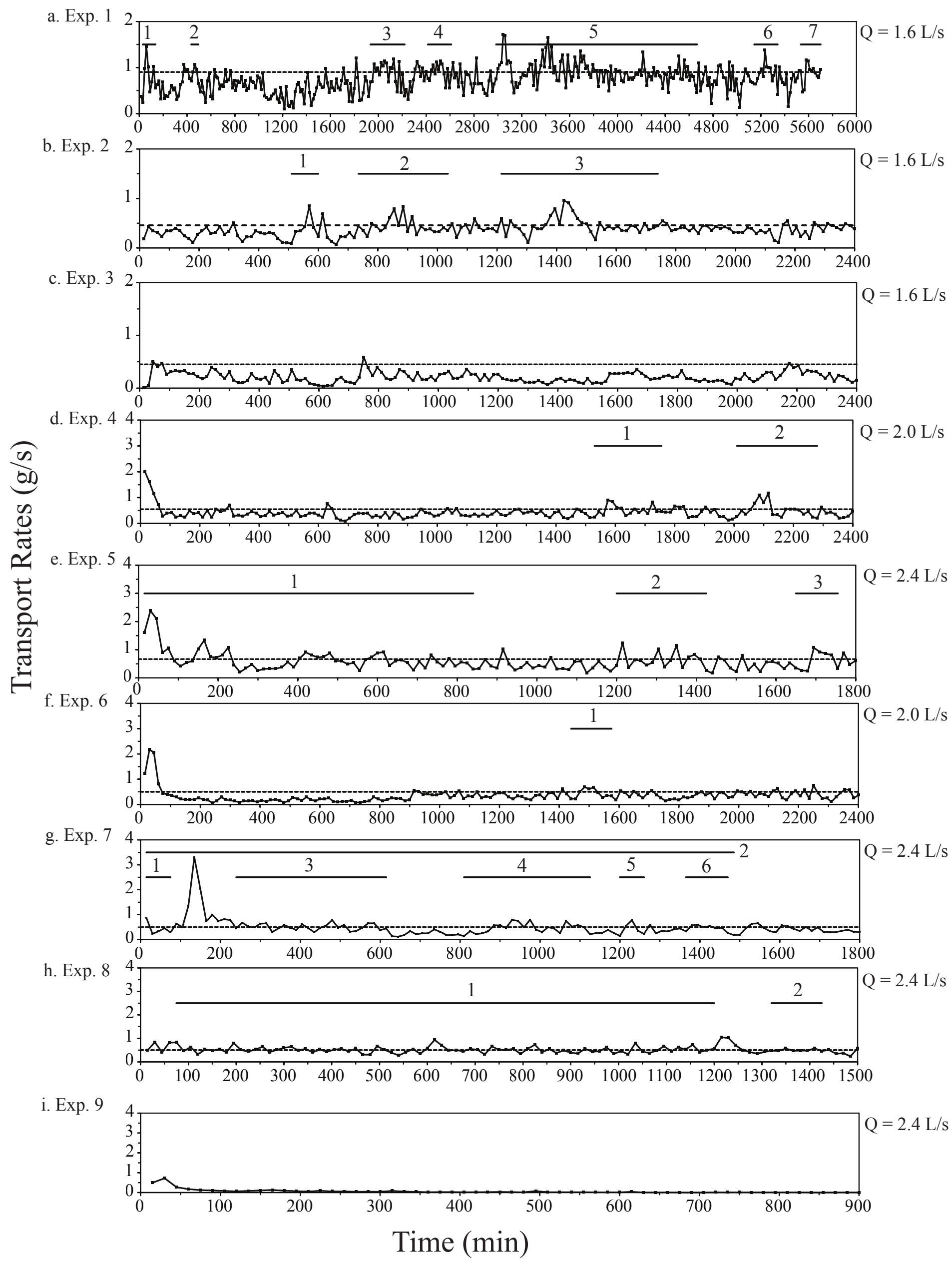

Figure 4.1: Variations in sediment transport rates with respect to time. The sediment feed rates are indicated by the dotted lines. For most of the experiments there are additional lines and numbers indicating the occurrence, duration, and number of cycles in the sediment transport-storage relations (refer to Table 4.1 for more details).

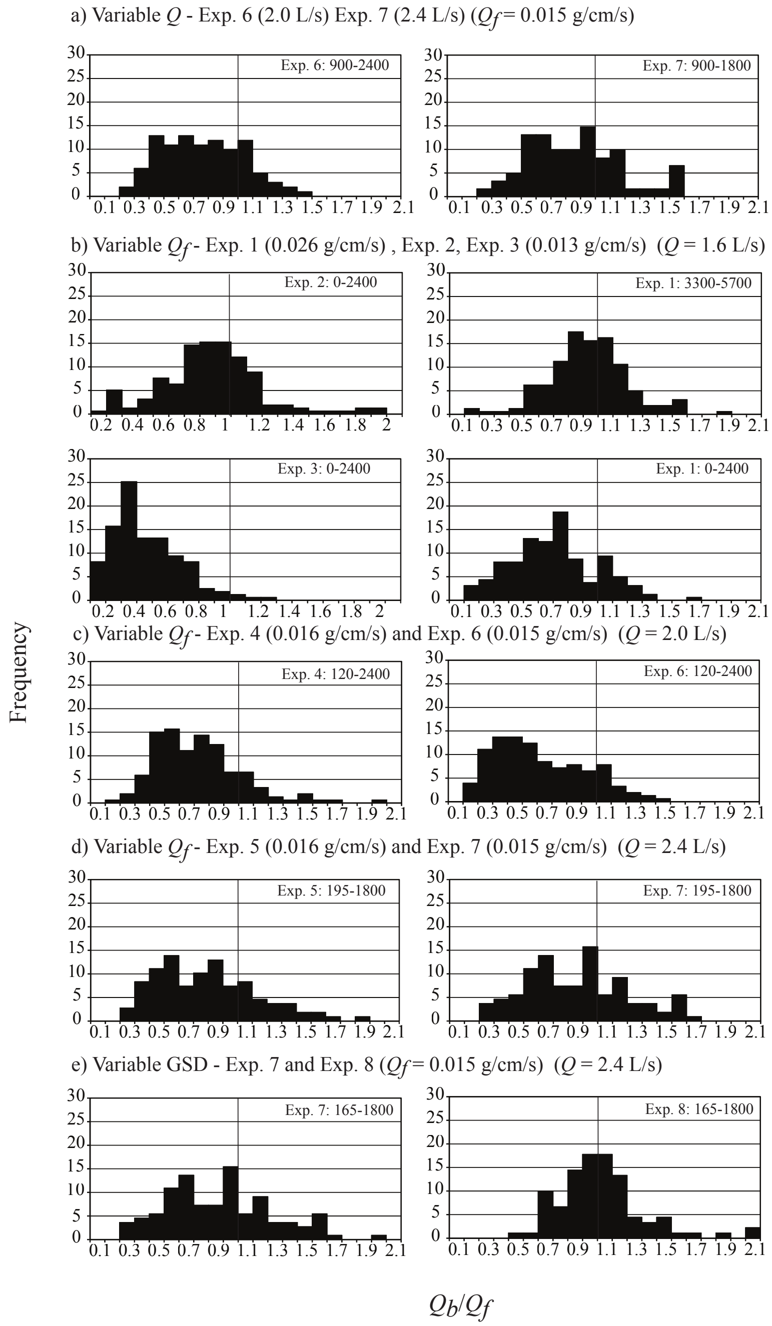

Figure 4.2: Histograms of sediment transport rates (Q_b) normalized by the sediment feed rate (Q_f). For each theme histograms are shown for data truncated to exclude the initial start-up spikes in transport rates. Q represents stream discharge. Solid vertical lines represents $Q_b/Q_f = 1$ for reference.

initial bed. This resulted in much lower T_{eff} values for Exp. 3. Only on a few occasions did sediment transport rates (Q_b) exceed feed rates (Q_f) during Exp. 3, this occurrence was more frequent during Exp. 2 (Figure 4.1b and 4.1c). The histograms of T_{eff} for Exp. 2 and 3 are both visually and statistically different (based on a K-S test): while T_{eff} varies between 0.8 and 1.2 during most of Exp. 2, it almost never exceeds 0.8 during Exp. 3 (Figure 4.2b). The cause of this significant discrepancy is attributed to differences in the historical contingency of the two experiments. Exp. 2 was conducted on the bed developed during Exp.1, except Q_f was two times greater. Compared with the initial conditions of Exp. 3 (a flat screeded bed), Exp. 2 began on a bed with a higher slope, thus higher stream power, and well developed morphology, in which sediment transport pathways and hydraulic efficiencies had already been established. These two initial conditions resulted in only minor morphological and textural adjustments during Exp. 2 to accommodate the reduction in Q_f. Further evidence of differences in transport efficiency due to initial conditions, is seen by comparing the histograms of Exp. 1 which illustrate how different T_{eff} is when comparing the two temporal periods plotted in Figure 4.2b.

When experiments with similar discharges (but different sediment feed rates) are compared, no clear effect of sediment feed rate on the transport efficiency emerges (see Table 4.3). Two experiments were conducted at the equivalent of bankfull flow: in Exp. 1 (Q_f = 0.91 g/s), the system was able to transport 0.76 g/s with a T_{eff} = 0.83; however, when Q_f was reduced nearly 50% for Exp. 2, T_{eff} increased to 0.89, the increase was not statistically significant. When only the data between 3300 and 5700 minutes for Exp. 1 are examined the T_{eff} becomes 0.93, suggesting that feed difference and resultant morphological changes resulted in a slightly improved T_{eff} during the later part of Exp. 1, as discussed above. Furthermore, the distributions of 15 minute estimates of T_{eff} for both experiments are not statistically different (see Figure 4.2b, Exp. 1 from 3300 to 5700 min). Exp. 1 and Exp. 2 had different initial conditions, thus the conclusions reached in this comparison cannot be entirely attributed to sediment feed rates alone. However, Exp. 1 and Exp. 3 had similar initial conditions and discharges, and differed only in the volumetric rate of sediment feed. In Exp. 3 (Q_f = 0.45 g/s), the system was able to transport 0.21 g/s with a T_{eff} = 0.46; thus, a 50% reduction in the sediment feed rate resulted in nearly a 55% reduction in transport efficiency, the decrease was statistically significant. The distributions of 15 minute estimates of T_{eff} for both experiments are not statistically different (see Figure 4.2b, Exp. 1 from 0 to 2400 min).

For flows near the 10-yr recurrence interval (i.e. Exp. 5 and 7 in Table 4.3), a similar pattern results: a decline in feed rate produced an increase in T_{eff} that is not statistically significant. As for the first pair, the histograms of T_{eff} estimates for Exp. 5 and 7 (Figure 4.2d) are visually similar (and a K-S test shows that they are not statistically different). The start-up conditions between Exp. 5 and Exp. 7 also appear to be a little different, the initial scour period during Exp. 7 was delayed by 100 minutes when compared to Exp. 5 (Figure 4.1e and 4.1g), possibly due to differences in armouring at the end of Exp. 4 and Exp. 6. At the end of Exp. 4, 17 600 g had accumulated in the channel, compared to 22

650 g for Exp. 6, which resulted in a higher slope at the end of Exp. 6 (0.0178) compared to Exp. 4 (0.0158).

Table 4.3: Transport efficiency for experiments with similar stream discharge

Experiment	Q	Q_f	$\overline{Q_b/Q_f}$	95% Confidence Range
1	1.6	0.91	0.84	0.81 – 0.87
2	1.6	0.45	0.89	0.83 – 0.95
3	1.6	0.45	0.46	0.42 – 0.49
5	2.4	0.67	0.78	0.72 – 0.84
7	2.4	0.50	0.88	0.81 – 0.94

Only one set of experiments had similar sediment feed rates but different discharges, the average T_{eff} shows that higher values are associated with higher stream discharge (Table 4.4). The histograms of T_{eff} seem to show that T_{eff} becomes more variable as Q increases, since the spread of the histograms increases and the relative size of the peaks decreases (Figure 4.2a); but there are not enough replicate experiments to decide the matter. Additionally, the experiments had different initial conditions.

Table 4.4: Transport efficiency for experiments with similar sediment feed

Experiment	Q	Q_f	$\overline{Q_b/Q_f}$	95% Confidence Range
6	2.0	0.50	0.62	0.57 – 0.67
7	2.4	0.50	0.88	0.81 – 0.94

Table 4.5: Transport efficiency for experiments with similar stream discharge and sediment feed rates, but differing grain size distribution of the feed.

Experiment	Q	Q_f	$\overline{Q_b/Q_f}$	95% Confidence Range
7	2.4	0.50	0.88	0.81 – 0.94
8	2.4	0.50	1.03	0.97 – 1.09

One set of experiments had similar discharge and sediment feed rates but different grain size distribution of the feed, the average T_{eff} shows that higher values are associated with feed of Exp. 8 (Table 4.4). The histograms of T_{eff} seem to show that distribution of T_{eff} becomes more narrow in Exp. 8, since the spread of the histograms decreases in Exp. 8

and is wider in Exp. 7 (Figure 4.2e); not enough replicate experiments were conducted to extrapolate to a general case.

4.2.2 Sediment Transport-Storage Relations

To further explore the interactions among flow, sediment feed, and channel morphology we analyzed sediment transport-storage relations. Sediment transport-storage relations were developed for our experiments using transport rates and cumulative storage volume; the sediment feed rate is also provided for each experiment in Figure 4.3. Changes in storage volume were calculated from differences between the sediment feed rate and sediment output.

Hysteresis loops in the transport-storage relations were observed in a number of experiments (Figure 4.3). These loops or cycles, appear to be the result of periods where transport rates out of the reach are below the rates into the reach, which then leads to an increase in the volume of sediment stored in the channel. This aggradational period is followed by a period of higher transport rates and bed degradation and a return to the previous lower transport regime completes the loop. Following the terminology of *Smith* (2004), *Pryor et al.* (2011) and *Hassan et al.* (2007) the hysteresis loops will be referred to as aggradation-degradation cycles. *Hassan et al.* (2007) further differentiated between major and minor cycles of aggradation and degradation using a volumetric threshold. In these experiments major cycles were cycles that lasted longer than 1000 minutes or had a maximum storage difference within the cycle $\geq$ 1000 g. In addition to a volumetric threshold, a temporal threshold was added to identify a cycle that had was clearly important, however sediment availability may have limited large sediment movement and thus the volumetric threshold was not met. Throughout the experiments, many cycles contained multiple smaller cycles within them, making it difficult to identify where one cycle began and another ended. For reporting purposes the values presented in Table 4.1 represent total values of the entire cycle (which may or may not have been classified as being major), if multiple cycles occurred and were able to be differentiated the total number of cycles was also noted.

The transport-storage relations of Exp. 6 and 7 (Figure 4.3f and 4.3g respectively), the experiments had the same feed rate, illustrate the effects of varying discharge on the relation. A comparison of the two figures reveals a clear difference between the number and scale of the transport-storage cycles. High transport rates at the beginning of Exp. 6 reflect channel degradation; a partial loop occurred in the relation at the start of Exp. 6. The initial degradation at the start of the experiment was followed by an aggradational period, which is reflected by the relatively constant transport rate (Figure 4.3g); this is similar to Phase 1 of *Lisle and Church* (2002). The transport-storage relation appears to become less stable as the transport rate approached the feed rate, starting at around 12 000 g of storage. The variability in the transport-storage relation persisted for the remainder of the experiment. The only complete aggradation-degradation cycle in Exp. 6 occurred

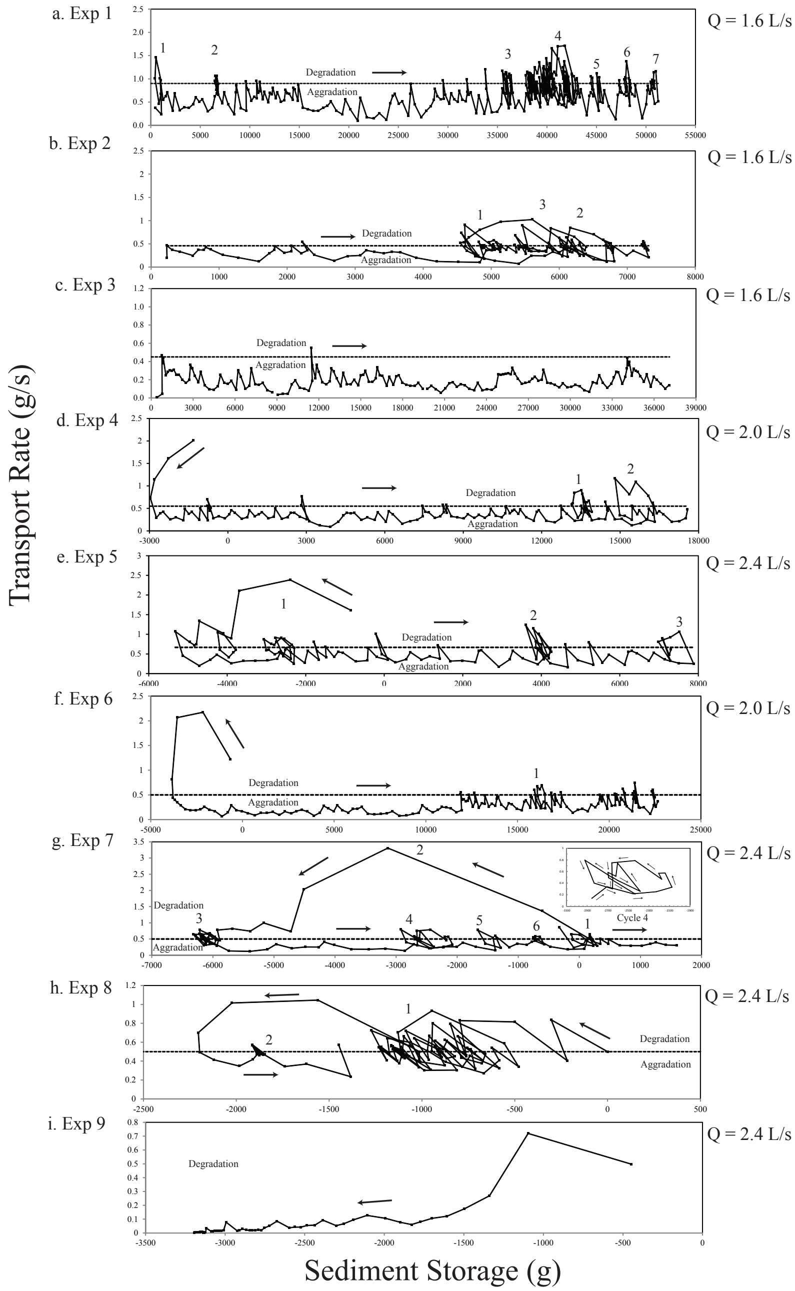

Figure 4.3: Transport-storage relations between transport rate and sediment storage. Feed rates are indicated by the dotted lines. Arrows show the temporal direction of the relations. The numbers refer to cycle number during a given experiment, refer to Table 4.1 for more information. A more detailed look at cycle 4 of Exp. 7 is provided as an inset.

around 16 000 g (Cycle 1, Figure 4.3f).

Contrary to Exp. 6, multiple aggradation-degradation cycles are evident in the transport-storage relation of Exp. 7 (Figure 4.3g). Six cycles in total were identified, one major and five minor. Cycle 2, the largest, lasted 1 470 minutes and represented a maximum storage change of 6615 g during the cycle. The remaining five minor cycles all occurred within the first cycle and ranged in duration from 60 to 375 minutes (Table 4.1). The main difference between Exp. 6 and Exp.7 is the net transport through the channel, Exp. 7 had a higher T_{eff}, which is likely the result of the higher discharge and the historical contingency. By this we mean that Exp. 7 needed to make only minor modifications to the pre-existing morphology in order to attain equilibrium in sediment transport rates and had begun on an initial channel slope which was greater than the initial slope of Exp. 6.

Figures 4.3a, 4.3b, and 4.3c show the transport-storage relations for Exp. 1, 2, and 3. In Exp. 1, seven separate cycles were identified; of these only one cycle (Cycle 5) was classified as being major (Figure 4.3a). Cycle 5, which consisted of eleven minor cycles, lasted for 1680 minutes and had a maximum storage difference of 4337 g, the seven other cycles lasted between 60 minutes and 285 minutes and displaced 225 to 886 g of sediment (Table 4.1). The interesting feature of Figure 4.3a is the long period of aggradation (1440 minutes) during which no cycle occurred. For Exp. 2, three cycles were identified (Figure 4.3b). Two of these cycles were classified as being major because maximum storage differences during each cycle was greater than 1000 g. The differences were 1045 g and 2226 g for Cycle 2 and 3, respectively. Exp. 3 exhibited no cycles at all (Figure 4.3c). This suggests that there must have been a transport capacity limitation. Comparing Exp. 3 to Exp. 1 one can postulate that it was not until the channel stored at least 35 000 g of material that the transport rate equalled the feed rate. Channel aggradation led to increased channel slope and filled the available sediment reservoirs, which in turn increased transport capacity. This would also explain the result in Exp. 2 as a greater slope and channel storage already existed.

The transport-storage relations for Exp. 4 and 6 are shown in Figure 4.3d and 4.3f, the two experiments had the same flows and relatively similar feed rates. The transport-storage relation for Exp. 4 mainly reflects the aggradational nature of this experiment; transport rates remained relatively constant or flat as channel storage increased. Only two cycles can be observed in Figure 4.3d, Cycle 2 is a major cycle as it was the result of a nearly 1500 g storage difference. Exp. 6 (Figure 4.3f) was mainly aggradational. The relations for both experiments look very similar and the first cycle occurred at a relatively similar time and volume of sediment storage (15 000 g).

Figure 4.3i, 4.3g and 4.3e show the transport-storage relations for Exp. 9, 7, and 5. The no-feed experiment (Exp. 9) shows an exponential relationship between transport rate and volume of sediment storage with declining transport rates associated with the depletion of stored sediment available for transport due to armouring and winnowing, similar to Phase II of *Lisle and Church* (2002) (Figure 4.3i). As discussed above, the relationship between the transport rate and storage for Exp. 7 is complex, with a constant transport rate associated with aggradational periods, and hysteresis during periods of quasi equilibrium (Figure 4.3g). Exp. 5 shows a similar relationship between transport and storage as Exp. 7, except that periods of equilibrium occurred less frequently and for shorter duration.

Exp. 5 exhibited three aggradation-degradation cycles (Figure 4.3e). Cycle 1 lasted 825 minutes, and was the largest cycle in terms of volume of material (4595 g). Flume observations showed that the degradational phase of this cycle was related to the additional scouring of a large pool located at the downstream end of the flume. On the other hand, the aggradational phase of the cycle was dominated by the growth of a bar located downstream of the same pool. The remaining two cycles were related to deposition and erosion within a pool and bar. The range of sediment input for these three experiments offers additional insight into the transport-storage relation. Exp. 9 had no cycles which suggested that the channel was not in equilibrium and that upstream sediment supply is needed for the cycles to occur, as internal supply is not sufficient These results indicate that the channel may have achieved brief periods of temporary dynamic equilibrium during Exp. 5, as indicated by the cycles, whereas Exp. 7 exhibited longer periods of dynamic equilibrium.

The transport-storage relation for Exp. 8 shows a system in equilibrium (Figure 4.3f). Two cycles of aggradation-degradation were identified. Cycle 1 began after 75 minutes and lasted 1125 minutes and 790 g were displaced, nearly fourteen cycles occurred within cycle 1. Cycle 1 is obviously the largest cycle during Exp. 8 but it is relatively small compared to the large cycle in Exp. 7. The transport-storage relation for Exp. 8 suggests relatively little change in channel morphology occurred during Exp. 8 compared to Exp. 7.

In general, the experiments indicate that cycles occurred when transport rates were similar to the feed rates. The cycles tended represent periods of elevated transport rates, which lead to a decrease in the sediment stored in the channel, followed by lowered transport rates, during which sediment stores were replenished. Cycles exhibited a very complex relation between transport and storage, and not just simple hysteresis. Cycle 4 of Exp. 7 (inset of Figure 4.3f) clearly indicates that multiple transport rates can be associated with a single storage value.

4.2.3 Patterns of Channel Adjustments

In this section patterns of channel morphological adjustments which occurred during the experiments are examined. Observations of channel adjustments were made hourly with hand sketched maps and every 5 hours using the DEMs generated from the laser scans of the bed. Figure 4.4 shows hillshaded DEMs from the experiments and includes selected DEMs from all of the experiments. This section will be organized in a different manner than the previous sections. In the previous section it was shown that historical contingencies play an important role in morphological development. Thus, in order to chronologically show the patterns of channel adjustment, the experiments will be presented in the order that they occurred.

Exp. 1 and Exp. 2 were run sequentially on the same bed, the experiments investigated the changes in sediment feed rate. Exp. 1 was the longest running experiment and had the highest sediment feed rate (0.91 g/s), stream discharge was the same ($Q = 1.6$ L/s) for Exp. 2 but the feed was significantly lower (0.45 g/s) . The hillshaded DEMs (Figure 4.4) provide context for the channel conditions at the start of each of the two experiments. Exp. 1 began on a bed exposed to 2 hours of conditioning flows only, sediment lobes are evident in the DEM as is the uniformity of the bed at this stage. Exp. 2 started on the bed left by Exp. 1 (Exp. 1 5700 min in Figure 4.4), pools and riffles are clearly evident in the DEM. The difference DEMs illustrate the patterns of channel adjustment at selected intervals during each of the experiments (Figure 4.5). The first 300 minutes in Exp. 1 resulted in scouring of pools and aggradational areas associated with bar development. The location of pools are relatively well distributed throughout the length of the channel. For the majority of the experiment aggradational areas were dominant. Degradation during the experiment was mainly the result of the removal of material associated with collapsed bar faces and pool scour. Exp. 2 had behaved similarly to the final 900 minutes of Exp. 1. The pattern of channel adjustments during Exp. 2 appear to follow the template inherited from Exp. 1. It is likely that the reduction of sediment supply was not entirely completed during the duration of the experiment (the experiment was halted as flows overtoppped the banks). Inspection of the final hillshade DEMs show that the adjustments during Exp. 2 were relatively minor when the two DEMs from Exp. 1 are compared (Figure 4.4).

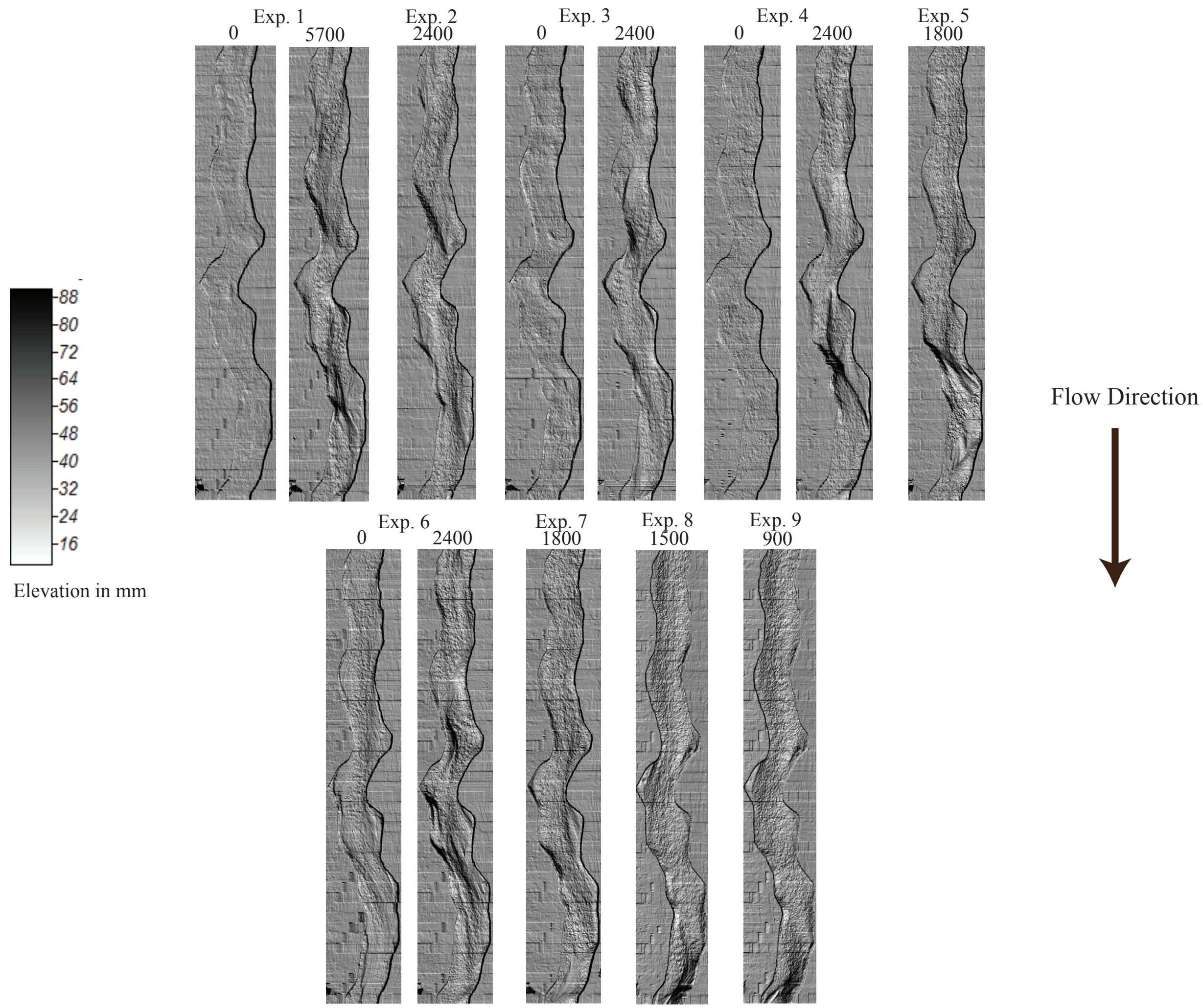

Figure 4.4: Hillshaded DEMs for selected time periods for all experiments. DEMs for the initial, screeded bed after 2 hours conditioning, and final DEM of each experiment are shown. In addition to the experiment number, the experimental time in minutes for each DEM is included. The scale of the plots represents relative elevation in mm, an arbitrary datum was used.

Exp. 3 was conducted using similar governing conditions as Exp. 2 except that it was started on a new bed (Figure 4.4). The difference DEMs for Exp. 3 are provided in Figure 4.5. During the first 300 minutes channel scour associated with the development of pools was the primary adjustment mechanism. Following this initial period of activity, aggradational processes dominated. The final DEM in Figure 4.4 for Exp. 3 (2400 minutes) shows that the channel pattern established during the first 300 minutes remained throughout the experiment, with minor adjustment.

The next set of comparative experiments are Exp. 4 and Exp. 5. Exp. 4 (Q = 2.0 L/s and Q_f = 0.55 g/s) began on a new bed and had lower stream discharge and sediment feed rates than Exp. 5 (Q = 2.4 L/s and Q_f = 0.68 g/s). The experiments, however, had similar sediment concentrations.The hillshaded DEMs show a similar configuration (i.e.,the location of pools and riffles) as the earlier experiments (Figure 4.4). The downstream pool is substantially larger in Exp. 4 and Exp. 5 than in the previous, lower flow, experiments. Additionally, the upper portion of the channel, exhibits a more plane-bed morphology than was seen in the previous experiments. The first 300 minutes of Exp. 4 was predominantly degradational, as the flow incised into the previously undisturbed bed and a pool-riffle morphology developed (Figure 4.5). After this period, patterns of channel adjustment in Exp. 4 were focused around these areas up until the last five hours, when a pool located along the left bank half way down the channel began to fill in. This appears to be the result of the extension of plane-bed morphology downstream.

As with Exp. 4, the first 300 minutes of Exp. 5 shows degradation and scour of pools inherited from Exp. 4 (Figure 4.5). For the remainder of the experiment, most of the activity occurred in the lower portion of the flume. The hillshaded DEM shows how the plane-bed morphology extended further downstream during Exp. 5 than it had by the end of Exp. 4.

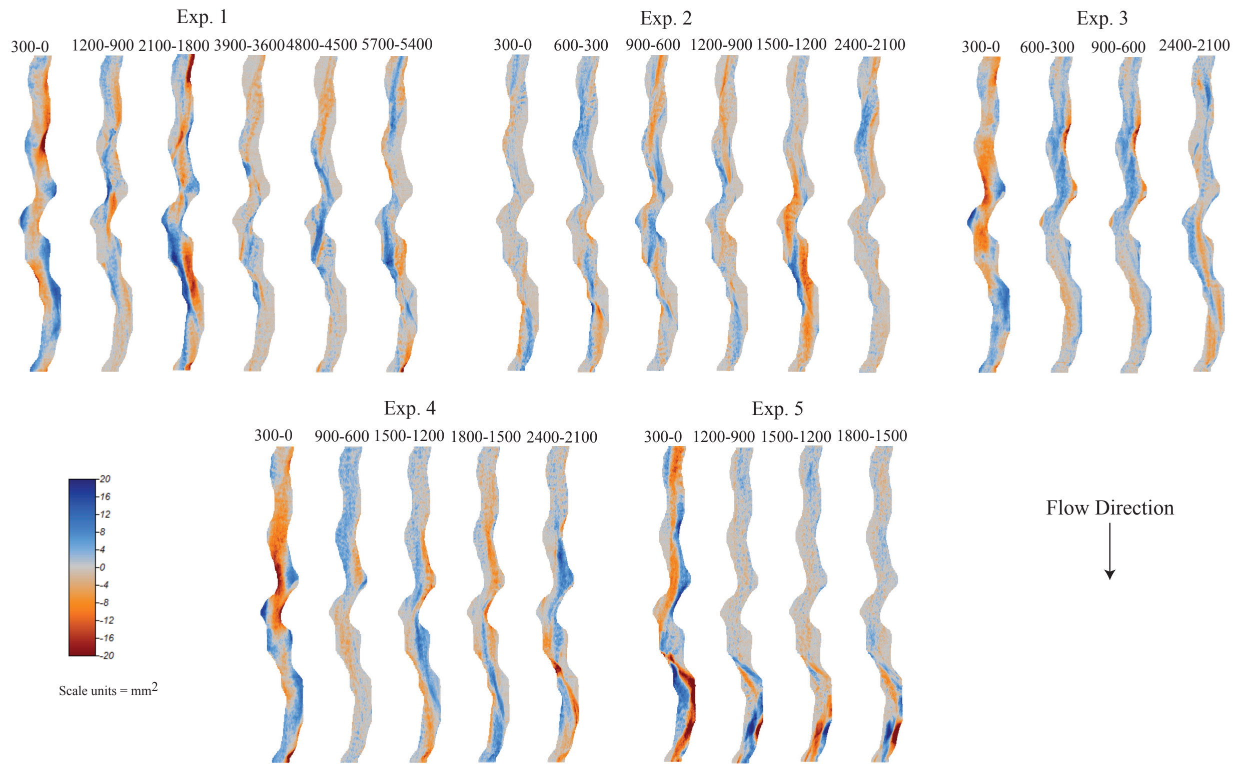

Figure 4.5: Changes in channel storage illustrated through DEM difference maps for Exp. 1 to Exp. 5. Scale units are in mm^2, and negative values represent degradation (orange-red) and positive values aggradation (blue). Each individual map represents the difference between a DEM generated following one 5 hour run subtracted by a DEM generated from the previous 5 hour run. For example, in Exp. 2 the difference between the DEMs generated after 300 min and at 0 min is labeled 300-0. Flow direction is common for both experiments.

The comparison between Exp. 6 and 7 examines differences in discharge, which increased from 2.0 L/s in Exp. 6 to 2.4 L/s in Exp. 7, sediment feed rates were held constant ($Q_f = 0.50$ g/s). Additionally, Exp. 7 began on a bed which had been conditioned during Exp. 6. Within the first 15 minutes of Exp. 6, the formation of incipient bars began to occur as downstream migrating tongues of finer sediment were prevented from further downstream movement possibly due to interactions with channel banks (some of which are evident in Figure 4.4). After 300 minutes, three pools are evident in the DEM (represent by the orange-red colour in Figure 4.6), the upper part of the channel exhibited plane-bed like morphology and the lower half resembled pool-riffle morphology. Over the next 1 500 minutes the channel evolved by increasing lateral variability, pools and bars became more prominent and as such became a more dominant influence on flow patterns and patterns of sediment transport. Pool locations for the duration of the experiment appeared to remain in place although their pool dimensions (length, width and depth) varied overtime. An important observation was that the alignment of most pools varied as well, with the pool inlet and outlet angles varying over time. The orientation of the inlet and outlet were initially determined by the channel banks and over time the orientation evolved in response to pools that developed upstream and downstream (see Exp. 6 2400 min Figure 4.4).

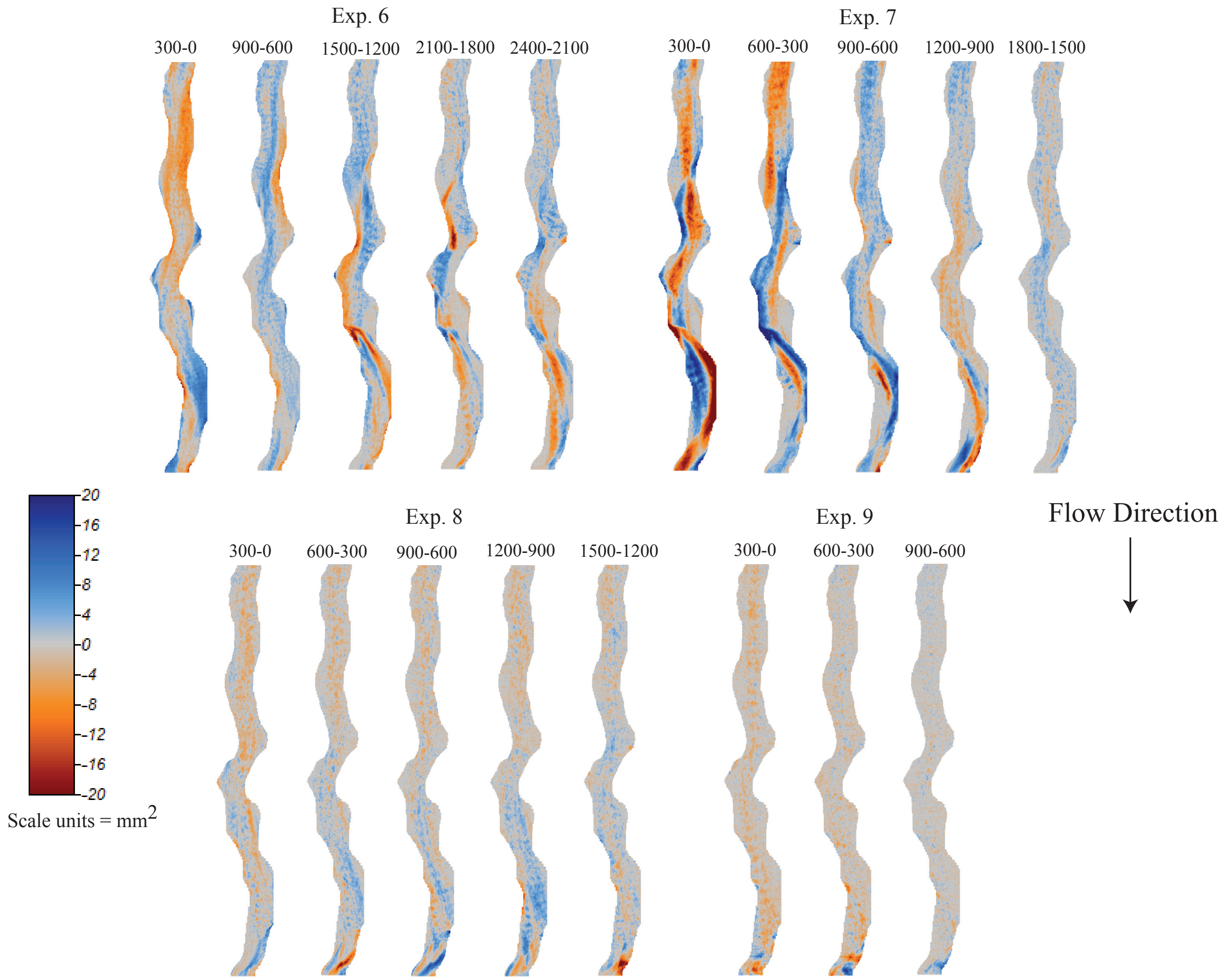

Figure 4.6: Changes in channel storage illustrated through DEM difference maps for Exp. 6 to Exp. 9. Scale units are in mm^2, and negative values represent degradation (orange-red) and positive values aggradation (blue). Each individual map represents the difference between a DEM generated following one 5 hour run subtracted by a DEM generated from the previous 5 hour run. Flow direction is common for both experiments.

The higher stream discharge in Exp. 7 capitalized on the pre-existing flow pathways established during Exp. 6 and the resultant scour along these routes is evident in the Exp. 7 300-0 difference map (Figure 4.6). Surface structures and armouring were observed in the upper section of the flume. The lower section exhibited pool-riffle morphology and responded immediately to the higher flows with deepening of the pools and degradation and aggradation on some of the bars. The first 300 minutes showed the greatest change as the bed and morphology adjusted to the increased flows. Morphological change dramatically slowed after the first 5 hours as evident in the 600-300 difference map in Figure 4.6, and the channel appeared to quickly accommodate the higher flows. After 600 minutes the upstream end of the flume degraded, and the downstream end aggraded as pools were in-filled and the complexity diminished. After 900 minutes, and for the remainder of the experiment, relatively little morphological changes occurred. During Exp. 7 most of the adjustments were surface coarsening and the extension of plane-bed morphology downstream the channel, although a large pool remained at the lower end of the observation area (Figure 4.4).

Exp. 8 started on the bed inherited from Exp. 7; discharge and feed rates were the same, but the size distribution of the feed was different. The difference maps in Figure 4.6 for Exp. 8 are a much lighter shade than the previous two experiments, which indicates that there was less scour and fill during this experiment. Very small differences are evident at the end of Exp. 8 as compared to the DEM end of Exp. 7 (Figure 4.4).

This trend of limited morphological activity continued for Exp. 9, a no feed experiment which continued on the bed from Exp. 8. During the first 300 minutes of Exp. 8, little change is evident in the difference maps (Figure 4.6). Even by the end of Exp. 9 relatively little change is evident in the hillshade DEMs (Figure 4.4).

4.2.4 Sediment Texture of the Transported Material and Bed Surface

Temporal patterns in bed surface texture and sediment output to changes in sediment supply, flow conditions and within channel storage, are shown in plots of the D_{50} and D_{90} of both the bed surface and the bedload material as trapped at the outlet (Figure 4.7). For comparison, D_{50f} and D_{90f} of the sediment feed mixture is included. For Exp. 1 both the bed surface and outlet are presented at 60 minutes intervals, for the remainder of the experiments the bed surface samples are presented at 300 minute intervals and sediment output at 60 minute intervals. A summary of the average values for each experiment is provided in Table 4.6, also included is the average armour ratio calculated using the D_{50} and D_{90}.

In each experiment the transported D_{90t} is relatively similar to the surface D_{50s}, except for Exp. 9 (Figure 4.7). Exp. 9 was a degradation experiment and had no sediment feed, it was also conducted on a bed that had a well developed armour layer and exhibited fairly entrenched plane-bed morphology. Deviations between the D_{50s} of the surface and the transported D_{90t} likely reflect armour breaching conditions and thus mobilization of larger

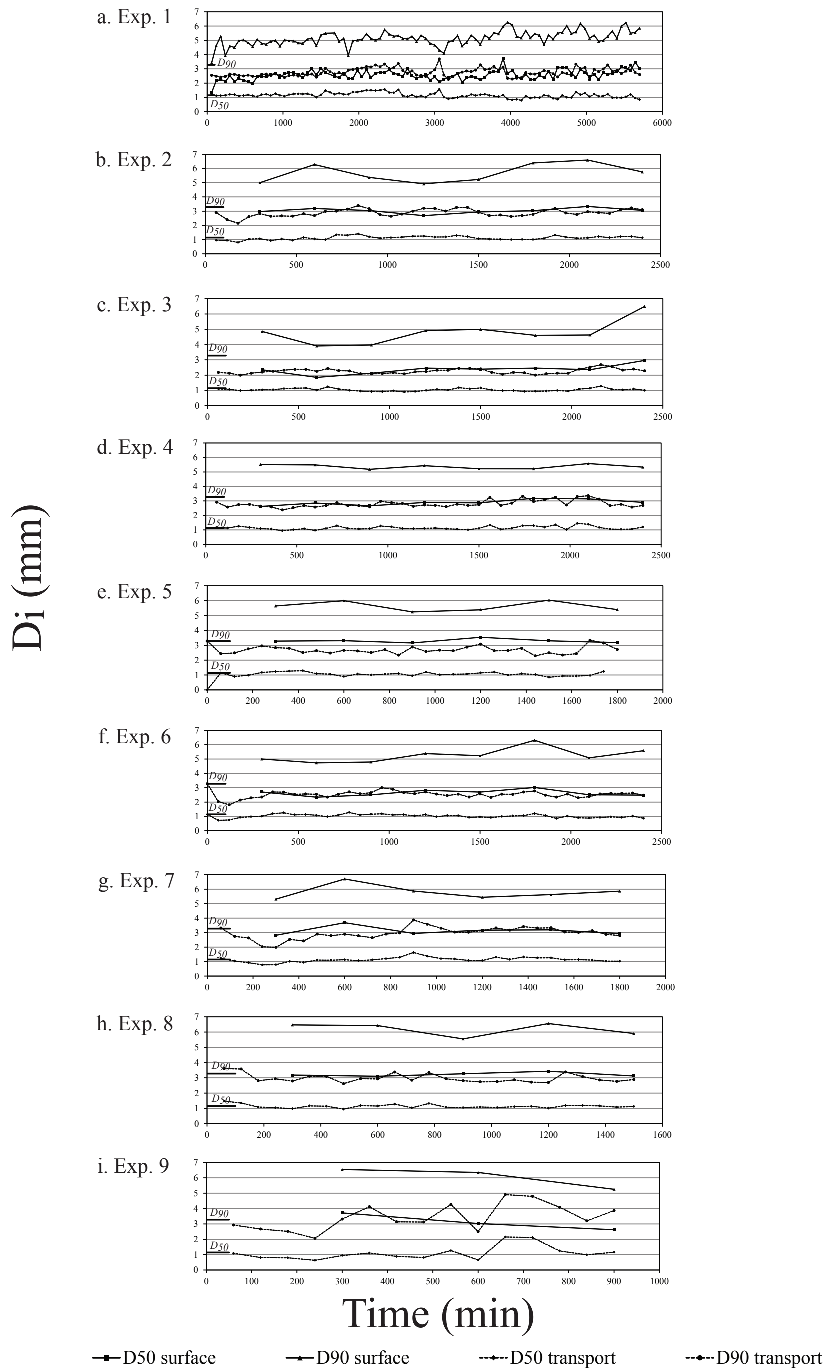

Figure 4.7: Particle sizes (D_{50} and D_{90}) of bed surface and bed material measured at the outlet for all experiments.

grain sizes. Further the D_{50t} of the transported sediment in Exp. 9 was not different from the D_{50f} of the feed, neither was there a difference in the relative values of the D_{90}.

Table 4.6: The $\overline{D_{50t}}$ and $\overline{D_{90t}}$ of transported and $\overline{D_{50s}}$ and $\overline{D_{90s}}$ surface sediment are presented. The D_{50f} is 1.14 mm and D_{90f} is 3.28 mm for the sediment feed. The average armour ratio ($\overline{AR}$) using the D_{50} and D_{90} are also provided.

Experiment	$\overline{D_{50t}}$	$\overline{D_{90t}}$	$\overline{D_{50s}}$	$\overline{D_{90s}}$	$\overline{AR}$ D_{50}	$\overline{AR}$ D_{90}
1	1.15	2.76	2.58	5.16	2.26	1.53
2	1.12	2.89	3.03	5.69	2.65	1.73
3	1.04	2.25	2.37	4.80	2.07	1.46
4	1.14	2.80	2.89	5.37	2.53	1.64
5	1.06	2.67	3.29	5.62	2.88	1.71
6	1.03	2.52	2.64	5.27	2.30	1.61
7	1.13	2.96	3.13	5.81	2.73	1.77
8	1.14	2.98	3.22	6.18	2.81	1.88
9	1.11	3.43	3.12	6.05	2.73	1.84

Generally, the results suggest that the response of the bed may not be as dependent upon sediment supply and discharge, but on the range of sediment sizes supplied to the channel. The D_{50t} for all of the experiments did not differ greatly from that of the initial sediment feed, the larger range in values observed in the D_{90t} suggest that this may be a better metric for evaluating channel responses. The armour ratios observed in these experiments is well within the range of those observed in the field, suggesting that this process was replicated for these experiments.

4.3 Discussion

The nine experiments presented above were designed to explore the spatial and temporal patterns of sediment transport. In addition, channel response to changes in sediment supply and flow was observed through changes in sediment storage. The experiments were grouped into themes based on differences in either discharge, sediment supply or sediment feed grain size. The first theme explored the effects of the initial conditions of the channel, with initial conditions beginning on a screeded bed and discharge and feed rates being similar (Exp. 4 versus Exp. 6) or different initial conditions with similar discharge and feed rate (Exp. 2 versus Exp. 3). Secondly, the effects of stream discharge with constant sediment feed rate and texture (Exp. 6 versus Exp. 7) is explored. For the second theme, the sediment feed rates were varied while the stream discharge and sediment feed texture were held constant (Exp. 1 versus Exp. 2 and Exp. 3, Exp. 4 versus Exp. 6, and Exp. 5

versus Exp. 7). Lastly, the effects of a change in the sediment feed texture while holding flow discharge and sediment feed rate constant was explored (Exp. 8 versus Exp. 7).

4.3.1 Sediment Transport Patterns

Sediment transport for all nine experiments exhibited both spatial and temporal variability within each experiment even under conditions of constant sediment feed and flow discharge. The experiments were designed to investigate the effects of formative flows and time on sediment transport patterns. The design provided a unique opportunity to observe and measure long-term patterns in sediment transport.

Differences in sediment transport patterns emerged when the experiments within a specific theme were compared. Exp. 6 and Exp. 7 explored the effects of increased discharge and found that a 20% increase in discharge resulted in a 35% increase in sediment transport rates, after the initial scour period was excluded. The elevated transport rates in Exp. 7 were associated with channel scour in pools and along the channel thalweg. The increase in sediment transport rates is more reflective of the increase in sediment availability, than to the changes in transport capacity due to the flow increase. Channel scour resulted in increased transport rates due to: 1) increased availability of sediment for transport and, 2) increased efficiencies in the bed shear stress distribution due to increased lateral variability (*Ferguson*, 2003; *Francalanci et al.*, 2012). After the initial scour period, minor adjustments in the size distribution of the surface material associated with individual bedforms and surface structuring, transport rates declined. The surface grain size adjustments effectively acted to stabilize the new morphological configuration, allowing an efficient yet stable morphology to develop.

Previous experiments have indicated the importance of adjustments of surface texture in regards to sediment transport (for example, *Dietrich et al.*, 1989; *Buffington and Montgomery*, 1999b), with little or no mention of morphological adjustments. The process appears to be more complex in channels with a more complex planform when compared to straight flumes. The experiments were conducted using formative flows (i.e. bankfull and above), in pursuit of understanding the morphological development of this type of channel. What was observed under these flow and transport conditions, was that morphological adjustment was the primary response mechanism, after the surface layer was breached, and textural changes were secondary. Typically, the higher transport events which dominated transport rates were associated with channel unit changes, rather than textural changes. Channel unit adjustment was manifested by pool/bar development as well as the development of surface structuring in the straighter upstream section of the flume. After the initial morphological adjustment period had slowed down, the adjustment never stopped occurring as pool and bar dimensions generally evolved throughout the experiments; surface material size adjustments were a secondary mechanism and appeared to adjust in response to altered flow velocities associated with newly formed morphology (for example, topographic steering *Nelson* (1988)).

The importance of morphological adjustment can be seen by examining the spatial differences between Exp. 6 and Exp. 7 (Figure 4.6). The location of scour and fill is slightly different between the two experiments, and the magnitude of the changes appears greater in the plots. The deeper scour in Exp. 7 is associated with channel banks, especially at the downstream end of the channel and along the left bank. This bank-channel coupling was not as pronounced during Exp. 6. Thus, during high flows it appears that the flow can be temporarily attracted to non-erodible banks, which results in deep scour holes. It is interesting to note that a similar scour feature was observed in Fishtrap Creek, when the creek encountered a bedrock outcrop along its left bank. We have also observed this behaviour in the field in many channels where the flow gets keyed into some non-erodible bank feature and an associated deep scour hole develops. These experiments suggest that this behaviour is at least initially associated with some high magnitude flow event, greater than 10 years in this experimental case. This may suggest that above some magnitude flow event within-channel transport processes are unable to accommodate the associated flow energy and that the boundary conditions (such as hardened banks) are attractors because they can dissipate the additional energy.

The DEM difference maps can be used to highlight the spatial and temporal variability of in-channel sediment reservoirs (Figures 4.5 and 4.6). For example, inspection of the difference DEMs of Exp. 2 (Figure 4.5) reveals a variable pattern of channel aggradation and degradation both laterally and longitudinally during the course of the experiment. Patterns of bar building (blue areas) and pool scouring (orange-red areas) vary in both magnitude and space. Similar differences can be seen in the Exp. 5 maps, especially when comparing the the top 1/4 and lower 1/4 of the channel. The behaviour suggests that in-channel sediment reservoirs are closely linked to individual morphologically units, and that this may be a more important driver of in-channel adjustments to changes in sediment supply than reach scale information. This may also be the scale at which transport-capacity is determined.

An additional observation can be made regarding discharge magnitude and channel morphology. Examination of the hill shade DEMs from Exp. 1 to Exp. 3 in Figure 4.4, reveals the development of a pool-riffle morphology throughout the entire experimental channel. A pool can be clearly identified in the Exp. 3 2400 minute DEM. When discharge is increased (for example, Exp. 5 1800 minute DEM in Figure 4.4) the upper, straighter section of the channel exhibits plane-bed morphology. I believe that this change represents the more dominant role that channel alignment and planform have in channel morphological development as flood stage increases. This suggests that during higher magnitude flood events, channel morphology is increasingly dependent upon hydraulic forcing due to the boundary conditions and bank alignment than either armouring or morphologic units.

The effects of changes in sediment supply were examined by comparing the results from Exp. 1, Exp. 2 and Exp. 3 and Exp. 5 and Exp. 7. The sediment feed rate in Exp. 2 and Exp. 3 was half of that in Exp. 1, this resulted in a 46% reduction in transport rates in Exp. 2 and a 72% reduction rates during Exp. 3. When transport efficiency was used as the metric a different picture emerges, Exp. 2 had the highest transport efficiency (0.84), followed by Exp. 1 (0.78) and Exp. 3 (0.44). As Exp. 2 inherited the bed from Exp. 1, it is likely that the gain in sediment transport efficiency is related to increased channel slope. Transport efficiency during the last 1500 minutes of Exp. 1 is 0.81, which is more similar to Exp. 2. This similarity is likely the result of two morphologic changes in the channel of Exp. 1, the first is increased channel slope, but the second is increased transport efficiency due to the establishment of sediment pathways, the result of morphologic forcing. The results for Exp. 3, however, cannot be attributed to slope alone. The start conditions for Exp. 1 and Exp. 3 were similar, so the experiments should have produced relatively similar results. When the first 2400 minutes of Exp. 1 are examined transport rates are 0.60 g/s with an efficiency of 0.65 which is still more than double the results observed for Exp. 3.

The feed rate for Exp. 5 was 34% higher than Exp. 7, but the discharge for these experiments was 20% higher than Exp. 4 and Exp. 6, the beds upon which Exp. 5 and Exp. 7 were conducted. The result was that the overall transport rate for Exp. 5 was only 16% higher than Exp. 7, this increased to 24% when the initial scour event was removed from both experiments. Interestingly, the transport efficiency was actually reduced by 11%, from 0.84 in Exp. 7 to 0.75 in Exp. 5. These results indicate the importance of historical contingencies in sediment transport patterns. Differences in the initial conditions can produce unique transport pathways that can result in different transport efficiencies and unique morphological characteristics that can be promoted under differing governing conditions. This validates the complexity in responses observed when trying to understand changes in the governing conditions and channel characteristics. It does suggest that a better understanding of conditions prior to the disturbance may help in improving our understanding of channel response pathways.

The role of changes in the grain size of sediment feed did not produce dramatic changes in the morphology of the channel. The result may have been different if the experiments were both started on screened beds. Comparing Exp. 7 and Exp. 8 the results indicate that sediment transport equilibrium was reached relatively rapidly during Exp. 8, using the alluvium of Exp. 6. As to be expected Exp. 8 resulted in relatively minor changes in channel morphology, with the majority of channel adjustment occurred in the lower tenth of the flume.

4.3.2 Transport-Storage Relations

The primary outcome of *Lisle and Church* (2002) was the identification that transport capacity is not a static value. In their paper they supported this outcome using both experimental and field evidence from degrading channels and found that a unique, positive relation existed between sediment transport rates and storage. Later experiments conducted by *Madej et al.* (2009) and *Pryor et al.* (2011) looked at this transport-storage relation over episodes of degradation and aggradation, and found that in some instances cycles in the relation occurred. Therefore a unique relation between transport and storage could not be supported given their experimental conditions.

Lisle (2012) amended the initial model and proposed two general scenarios: Scenario 1 represents a dynamic equilibrium between transport capacity and sediment storage; and, Scenario 2 both the channel response and transport capacity vary as sediment storage changes due to a transient disequilibrium related to changes in the rate of sediment supply. The conditions observed here display both scenarios. Under Scenario 1 transport rates appear to represent a dynamic equilibrium during the aggradational phase, similar to those reported in *Madej et al.* (2009) and *Pryor et al.* (2011). Scenario 2 conditions were also observed here, under constant sediment feed rates and flows, which contradicts the hypothesis that the cycles are due to changes in the rate of sediment supply. From our experiments we suggest that the cycles tend to occur when rates of sediment output are similar to sediment input rates. This could also occur, as evident in the results of *Madej et al.* (2009) and *Pryor et al.* (2011), when episodes of the degradation and aggradation occur such that the new sediment output rates are similar to the new sediment feed rates. During this cross-over period between the two episodes, sediment output can temporarily equal sediment input and a hysteretic event could occur.

I propose that the probability of hysteresis occurring in the transport-storage relation is directly related to the difference between sediment feed and sediment output. As the transport rate nears the feed rate the probability of cycles occurring increases; this is represented graphically in Figure 4.8.

An additional feature of these hysteretic events emerged from our experiments; that is the temporal legacy of these cycles. As the experiments were Froude scaled the length of these cycles can be converted from experimental time to time in the prototype. This conversion results in a cycle duration time of over 2 years for a small cycle in Exp. 1 (60 minutes in model) to over 50 years for a larger cycle in Exp. 7 (1470 minutes). These cycles can occur over periods that are generally much greater than common periods of field investigation, and therefore the evidence of such cycles is likely not frequently observed. Examining annual cross-sectional data from a long-term dataset in Carnation Creek, *Hassan et al.* (2007) found cycles greater than 10 years in duration in reaches where in-channel storage is predominantly associated with large woody debris. The potential duration of cycles in the transport-storage relation further reaffirms the importance of considering variability of transport capacity in landscape evolution models. More importantly, if assuming a static value, depending on where in the cycle the current channel is, may have a strong effect on values measured in the field and then applied to a model.

Hassan et al. (2007) concluded that the cycles depended more on the rate of sediment supplied to the channel, bedform dynamics and the supply of LWD than on hydraulic forcing. The LWD component aside, these experiments tend to partially support this conclusion, with the addendum that conditions must exist such that the rate of sediment supplied to the reach is nearly equal to the rate exiting the reach.

Partial cycles in the transport-storage relation were observed at the beginning of Exp.

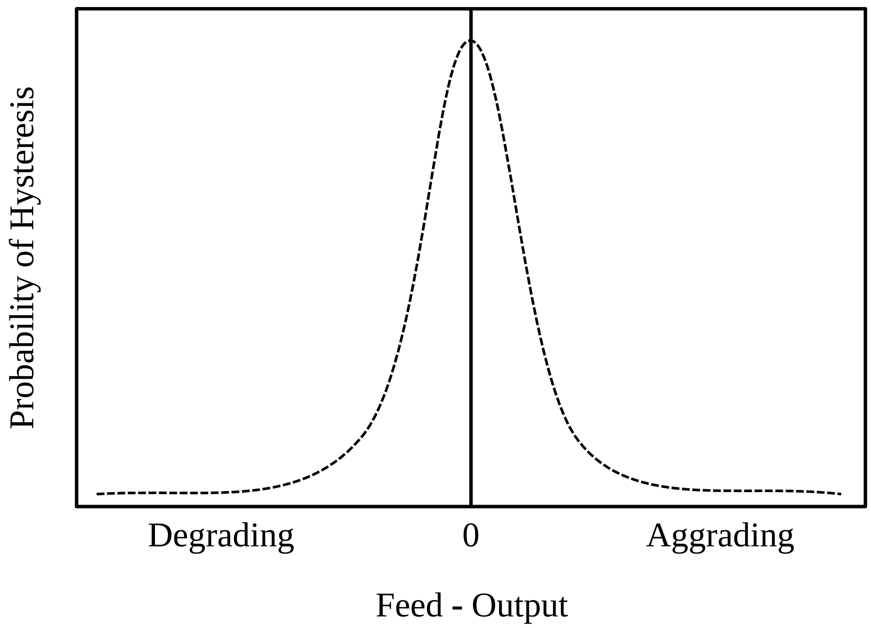

Figure 4.8: Conceptual model of the probability of hysteresis occurring in the transport-storage-feed relation. The plot shows the probability of hysteresis occurring vs the feed-output (F-O); when F-O > 0 the system is aggrading, when F-O < 0 the system is degrading.

4, Exp. 5 and Exp. 6 (see Figure 4.3d, 4.3e, 4.3f), the appearance of these cycles is in response to the initial degradation followed by form resistance and channel armouring. The initial flows in these experiments, whether they began on a conditioned bed or not, resulted in scour of the bed as the armour has either not been formed (Exp. 4 and Exp. 6) or was formed under lower discharge conditions (Exp. 5). Once the armour layer has adjusted to the new flows, bed scour lessens and the channel begins to aggrade, however, this results in transport rates much lower than the initial transport rates. This difference in transport rates between the armoured and un-armoured bed, resulted in the partial cycles evident during these three experiments.

Only Exp. 9 and Exp. 3 did not experience cycles in the transport-storage relation. In both experiments it appears to be due to sediment feed rates. In Exp. 9 there was no sediment feed and the channel remained degradational throughout the experiment. The relatively high transport rates at the beginning of the experiment represent an abundant supply of in-channel sediment was initially available for transport, as this sediment was removed, transport rates declined. Exp. 3 had sediment feed, but transport rates never approached feed rates (see Figure 4.1c). In both experiments equilibrium was not reached, this is in contrast to the conclusions reached by *Pryor et al.* (2011), who determined that the cycles they had a observed were a disequilibrium phenomena. In these experiments disequilibrium appeared to have negated the occurrence of cycles.

Full cycles in the transport-storage relation were observed for all of the remaining experiments. Close inspection of Figure 4.1 reveals that all of the cycles occur when the channel is in a state of dynamic equilibrium, or where transport rates fluctuated around the feed rate. During minor cycles the additional sediment is easily accommodated by available storage reservoirs within the channel causing minor alterations in transport capacity. *Hassan et al.* (2007) associated small-scale aggradation-degradation cycles to the growth and shifting of lateral bars, similarly the minor cycles observed during these experiments were associated with minor morphologic adjustments. These adjustments included the expansion and contraction of bars, as well as the scouring and deposition in pools. Whereas most of the adjustments for *Hassan et al.* (2007) were hypothesized to be associated with wood accumulations. Coarsening and structuring of the surface layer also played a part in the development of minor cycles observed. Although the direct mechanism is more related to minor morphologic adjustments, the state of the surface layer obviously determines the availability of sediment to be eroded.

Major cycles seem to reflect an initial perturbation, usually degradational, followed by recovery. For example, in Exp. 7 the perturbation was the initial period of degradation at the beginning of the experiment. For *Pryor et al.* (2011) complete cycles of aggradation-degradation were related to external perturbations introduced by the experimenters in the form of changes in the sediment feed rate, similar results and outcomes were observed by *Madej et al.* (2009). These experiments clearly illustrate that no external perturbation to the channel is required, and that these major cycles can be induced endogenously under steady state forcing conditions.

The cycles seem to represent a period of internal morphologic adjustment to the forcing conditions. In the experiments of *Madej et al.* (2009) and *Pryor et al.* (2011) this morphological adjustment was manifested by changes to channel pattern from a single-threaded channel to braided, and back to single-thread. However, in these experiments where the channel was laterally constrained this did not occur, instead storage reservoirs within the channel stored and released sediment in response. The releases represent perturbations in the system, and are hypothesized to represent limitation in storage capacity. Although adjustments to the texture of the bed surface are more frequently discussed, it is apparent from these experiments that the bedform level of response if the more dominant and important. It is these features that give the most elasticity of the channel to exogenous perturbations, the surface armour offers a limited response to changes in sediment supply but channel bars offer a much greater mechanism to accommodate changes in supply and can internally regulate these changes by the storage and release of sediment in response to the supply of sediment relative to channel flows.

Lisle and Church (2002) suggested that experiments in which only the sediment feed rate is varied over-represent the adjustment of armouring to variations in sediment supply. This stems from *Wilcock* (2001b) who wrote that in order to replicate a realistic armouring response in a flume, varying sediment size, feed rate as well as flow is difficult. Added to Wilcock's statement is that realistic armouring also required realistic planform. Channel armouring is not only dependent upon sediment size, feed rate and flow, but on morphologic variability which creates complex hydraulic environments.

4.4 Conclusions

The experiments conducted herein focused on channel forming conditions, so higher flows were employed. The results of these conditions showed that sediment transport rates varied both spatially and temporally. This variability was found to be more dependent upon changes in the morphology of the channel, rather than adjustments in the surface grain size distribution. The primary self-adjusting mechanism in the experimental channel was to adjust channel form. Adjustments to bed surface texture, tended to be a short-term response and the development of patches appeared to develop more in response to the channel topography rather than vice-versa.

Sediment transport efficiency of the experimental channel was strongly influenced by morphology and historical contingencies. Although, no replicate tests were conducted higher transport efficiency occurred when discharge was greater or the grain size distribution of the feed was finer, all other governing conditions remaining equal.

The transport-storage relation was investigated under constant forcing conditions. It was found that sediment transport capacity was not constant and did change as the volume stored in the channel changed. As others have observed, hysteresis cycles were observed to occur in a number of experiments. Unlike previous studies, the cycles observed here tended to occur when transport rates were approximately equal to the feed rates (i.e., when the channel was near equilibrium). Cycles of aggradation-degradation were observed without changes in either sediment supply or flow discharge. It was concluded that the transport-storage relation does not offer a unique relation between transport rates and sediment storage, thus limiting its usefulness in the development of an improved sediment transport model.

The results suggest that the idea of sediment reservoirs is more complex than envisioned and that these reservoirs are transitional and multiple reservoirs may exist within homogeneous reaches and they may all have different time signatures in terms of their response. This difference is dependent upon flows, sediment supply, and local adjustment to the topography, which in addition to the previous parameters is dependent upon boundary conditions (such as bank stability, bank form and alignment (important in most forested landscapes). The importance of the capacity of these reservoirs is shown in these results; however the capacity evolves with the morphology of the channel, so a simple relationship could not be identified.

Further attention to the role of topographic evolution within channels and their associated effect on sediment transport rates is suggested. It is believed that the topographic signature of the channel plays a dominant role not only in hydraulic, and the distribution of shear stresses, but on the development of in-channel surface patches and sediment reservoirs.

Chapter 5

Sediment Transport at the Pool-Riffle Scale: Observations from a Physical Model

In this chapter a less formal style has been taken. During the course of the experiments a number of phenomena were observed that were not anticipated at the experimental design stage. Consequently appropriate data were not collected. Some of the qualitative observations that were made include hand drawn maps and videos created from digital photography of the channel. This allowed me to make inferences in a manner similar to that proposed by *Drake et al.* (1988) in their study of bedload transport at Duck Creek. Similarly, I use these data to elucidate the processes of sediment movement and sorting in the experimental channel.

The general topic of this chapter is the movement of sediment through the experimental channel. Specifically, how sediment moves through a pool-riffle unit and the dynamics of sediment movement as bedload sheets. A brief introduction to the literature regarding these topic areas is presented next.

5.1 Introduction

The stochastic nature of sediment transport rates in gravel-bed rivers has been observed in both field (*Ehrenberger*, 1931; *Einstein*, 1937; *Cudden and Hoey*, 2003; *Hassan and Church*, 2001; *Hoey and Sutherland*, 1991; *Jackson and Beschta*, 1982; *Madej and Ozaki*, 1996; *Nanson*, 1974; *Powell et al.*, 2001; *Reid et al.*, 1985; *Wooldridge and Hickin*, 2005) and laboratory (*Dietrich et al.*, 1989; *Iseya and Ikeda*, 1987; *Kuhnle and Southard*, 1988; *Lisle et al.*, 1993; *Kuhnle et al.*, 2006; *Nelson et al.*, 2009; *Recking et al.*, 2009). In gravel-bed rivers, part of this stochasticity has been attributed to the migration of bedload sheets (*Ashmore*, 1991; *Bennett and Bridge*, 1995a; *Drake et al.*, 1988; *Gomez*, 1983; *Kuhnle and Southard*, 1988; *Kuhnle and Willis*, 1998; *Whiting et al.*, 1988; *Madej et al.*, 2009; *Nelson et al.*, 2009; *Pryor et al.*, 2011). *Whiting et al.* (1985) initially coined the term bedload sheets to describe their observations of bed material being organized into waves with distinct coarse fronts. The coarse fronts were only 1 or 2 grains in height and metres in length. A similar phenomenon, referred to as diffuse gravel sheets, had been previously identified in the field by *Smith* (1974) and *Hein and Walker* (1976), who described these sheets as incipient bar features (see also *Prestegaard*, 1987), the sheets were observed to only move during peak flows, and once the flow decreased the sheets were deposited, sometimes leading to the formation of diagonal bars (*Hein and Walker*, 1976).

Whiting et al. (1988) suggested that bedload sheets develop in moderately to poorly sorted sediment potentially as a consequence of coarse and fine grain interaction. The differentiation of bed material into coarse fronts and fine tails was thought to lead to increased mobility of the sediment as a result of smoothing, exposure and collision (*Iseya and Ikeda*, 1987). *Seminara et al.* (1996) attributed the growth of bedload sheets to grain sorting. Following *Iseya and Ikeda* (1987), *Whiting et al.* (1988) proposed that bedload sheet migration in mixed-size sediment is related to a "catch and mobilize" process in which the coarse grains in transport interact with the bed and either slow down or stop. The finer grains in transport pass over and fill in the interstices between the coarse grains, which in turn reduces roughness and increases the drag on the coarse grains, leading to their re-entrainment.

Bedload sheets appear to be directly related to sediment availability in the channel. *Dietrich et al.* (1989) observed that with decreasing sediment supply the spatial segregation of the bed varied. During high feed runs, bedload sheets dominated the surface which manifested in alternating zones of congested (coarse), smooth (fine), and transitional (intermediate) zones, as described by *Iseya and Ikeda* (1987). As sediment feed was reduced, bedload sheets became less frequent and distinct, coarse and inactive zones expanded, and the zone of active sediment transport became a narrow longitudinal fine textured zone.

Two recent papers have brought renewed attention to bedload sheets, *Recking et al.* (2009) focused on the production and migration of bedload sheets, and *Nelson et al.* (2009) focused on the response of bedload sheets to reductions in sediment supply. *Recking et al.* (2009) conducted 20 experiments under constant discharge and feed conditions, with varying mixtures of uniform sediments, and at slopes that ranged from 0.8 to 9%. They found that bedload sheet production and migration was associated with variations in bed slope, bed fining and paving, and bedload. *Recking et al.* (2009) proposed that bedload sheets resulted from vertical and longitudinal grain sorting that results in episodic increases in the transport rate efficiency of the coarser sized fractions of the bed.

Nelson et al. (2009) presented results from two sets of flume experiments, one conducted in the late 1980s at the University of Tsukuba (*Dietrich et al.*, 1989; *Kirchner et al.*, 1990) and another conducted at the UC Berkeley with the purposes of understanding the response of bed surface patchiness to reduction in sediment supply. Sediment patches are homogeneous areas of similar sized sediments on the bed surface of a channel, that may result from variations in shear stress, sediment transport and topographic sorting (*Paola and Seal*, 1995). *Nelson et al.* (2009) extended the terminology of bar types from *Seminara* (1998) to classify patches into three types: free patches, which are zones of sorted material that can move freely, bedload sheets being an example; forced patches, which are areas of sorting forced by topographic controls; and, fixed patches, which are immobile as a result of localized coarsening and can remain persistent through time. In general, they found a direct link between sediment supply and the distribution of free and fixed patches, as well the dynamics of bedload sheets. *Nelson et al.* (2009) attributed substantial increases in sediment flux due to the passage of bedload sheets, and suggest that the migration of the sheets can be the primary cause of the observed short-term fluctuations in sediment transport rates.

For the experiment presented here, the focus was on observations of bedload sheet movement through complex channel morphology, where stable equilibrium conditions were not observed. In addition to gaining insight into the behaviour and downstream movement of these features, their movement downstream allowed visualization of sediment transport paths. In particular, we focussed on the evolution of sediment transport patterns through a pool and riffle sequence over time.

How sediment moves and is sorted through pools and riffles is strongly dependent on the varying shear stress induced by diverging and converging flow conditions related to the downstream variability in bed topography. A number of models have been developed to describe the relationships between the distributions of boundary shear stress with channel topography and the spatial pattern of bedload transport and grain size in a meandering channels.

The following brief description of flow structure in a curved channel comes from *Powell* (1998). In a channel meander, channel curvature results in a depth-dependent, centrifugal force acting in the flow-transverse direction forcing surface water toward the outer bank leading to higher water surface elevation than the inner bank, where the water surface elevation is lowered (super-elevation). The difference between the centrifugal and pressure gradient forces results in outward flow on the surface where centrifugal forces are greater, and an inward flow on the bed where pressure gradient forces are greater (Figure 5.1a). This difference results in the helical secondary circulation. As flow progresses through a meander bend the forces change and this results in the zone of maximum boundary shear stress changing from the inside of the upstream bank to the outside of the downstream bank (Figure 5.1b). This is further enhanced in channels with pool-bar topography, because it alters the near-bed flow velocity, increases the cross-stream variation in shear stress, and promotes rapid shifting of the zone of maximum bed shear stress *Robert* (2003). The path of a particle through a meander bend responds to the forces acting upon it and results in a pattern of sediment sorting that results in coarser sediment moving down the transverse slope of the bar toward the pool as it moves through the meander. How sediment moves through a bend will depend on the relative magnitude of the drag due to the inward-acting secondary flow and the outward-acting gravitational force (Figure 5.1c).

The objectives of this chapter are to:

1. describe the general patterns of sediment transport in a complex flume during a single experimental run; and

2. elucidate how bedload sheets interact with the bed morphology in a complex flume.

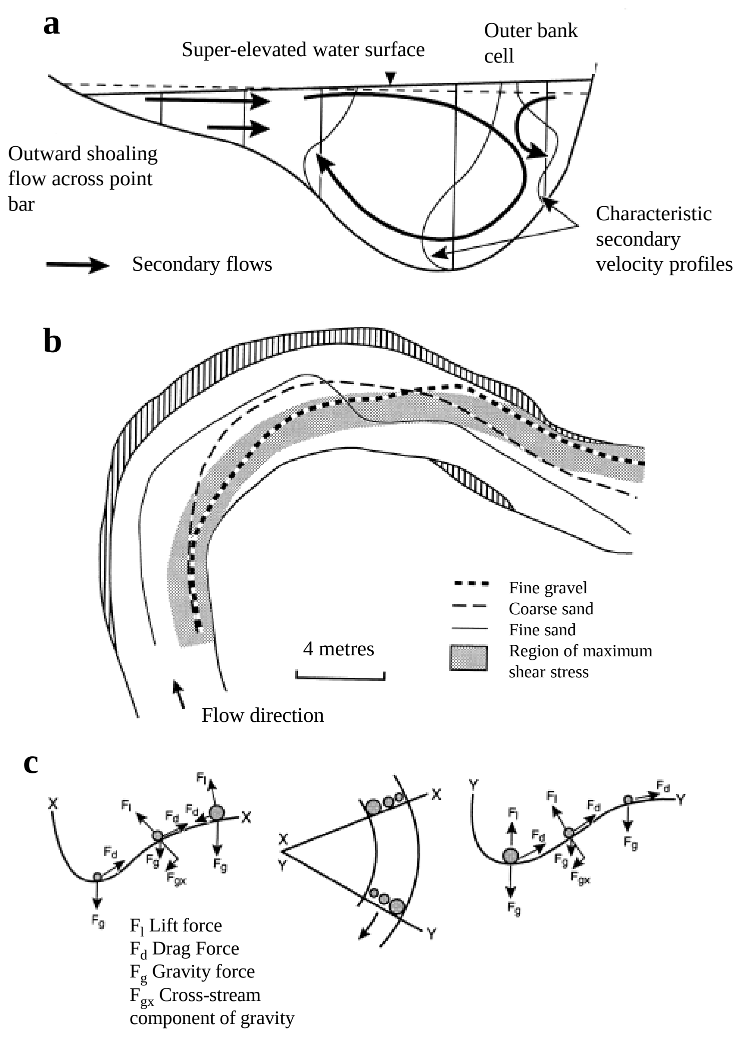

Figure 5.1: This figure contains a) flow structure, b) shifting loci of maximum boundary shear stress and sediment transport pathways, and c) forces acting on a bedload particle in meander bends. From *Powell* (1998).

The approach taken to meet these objectives is essentially qualitative in nature. These objectives emerged from observations made during the experiments, consequently the design of the experiments was not made with them in mind. Thus the data required to quantitatively present these objectives was not collected.

5.2 Experiment

Only the results from Exp. 6, will be discussed in this chapter. The experiment was conducted under conditions of constant flow (2.0 L/s) and sediment feed rate (0.50 g/s). The hydraulic characteristics from this experiment are provided in Table 5.1, as are estimates of the bedload sheet velocity, based on analysis of videos taken during the run.

Table 5.1: Experimental conditions and results

Time (min)	$\overline{U}$ [a] (cm/s)	Slope (m/m)	$\overline{d}$ [b] (cm)	Fr [c]	Q_b (g)	D_{50s} (D_{90s})[d] (mm)	D_{50t} (D_{90t})[e] (mm)	τ_b (Pa)	θ	Bedload Sheet Velocity[f] (cm/s)
300	35.4	0.015	1.67	0.87	9,024	2.70 (5.00)	0.88 (2.12)	2.44	0.056	0.24-1.11
600	35.6	0.015	1.66	0.88	2,953	2.35 (4.74)	1.16 (2.61)	2.44	0.064	0.22-0.69
900	34.5	0.015	1.71	0.84	3,071	2.51 (4.80)	1.12 (2.57)	2.54	0.063	0.26-0.89
1200	34.5	0.016	1.71	0.84	7,046	2.82 (5.38)	1.12 (2.77)	2.65	0.058	0.21-0.99
1500	34.2	0.017	1.73	0.83	6,686	2.70 (5.23)	1.00 (2.50)	2.82	0.065	0.21-0.63
1800	33.4	0.017	1.77	0.80	6,381	3.02 (6.31)	1.04 (2.58)	2.95	0.060	0.15-0.99
2100	33.0	0.017	1.79	0.79	6,952	2.51 (5.09)	0.95 (2.41)	3.02	0.074	0.22-0.77
2400	34.7	0.018	1.70	0.85	7,232	2.49 (5.58)	0.95 (2.58)	2.97	0.074	0.27-1.46

a. $\overline{U}$ is the average spatial harmonic velocity.
b. $\overline{d}$ is the average depth, calculated using continuity $d = Q/(wU)$.
c. $Fr = U/\sqrt{gd}$, where U is the velocity, g is gravitational acceleration, and d is the average depth.
d. D_{50s} (D_{90s}) represents the 50th (90th) percentile of the bed surface grain size distribution.
e. D_{50t} (D_{90t}) represents the 50th (90th) percentile of the transported material grain size distribution.
f. Bedload sheet velocity was determined from videos. The minimum and maximum velocity observed during a 5 hour are given.

5.3 Experimental Observations

5.3.1 General Observations

A total of 648 individual velocity measurements were made during the experiment, which is approximately 16 per hour. The average velocity for the entire experiment was 34.4 cm/s, all individual 300 min intervals were well within one standard deviation of the mean.

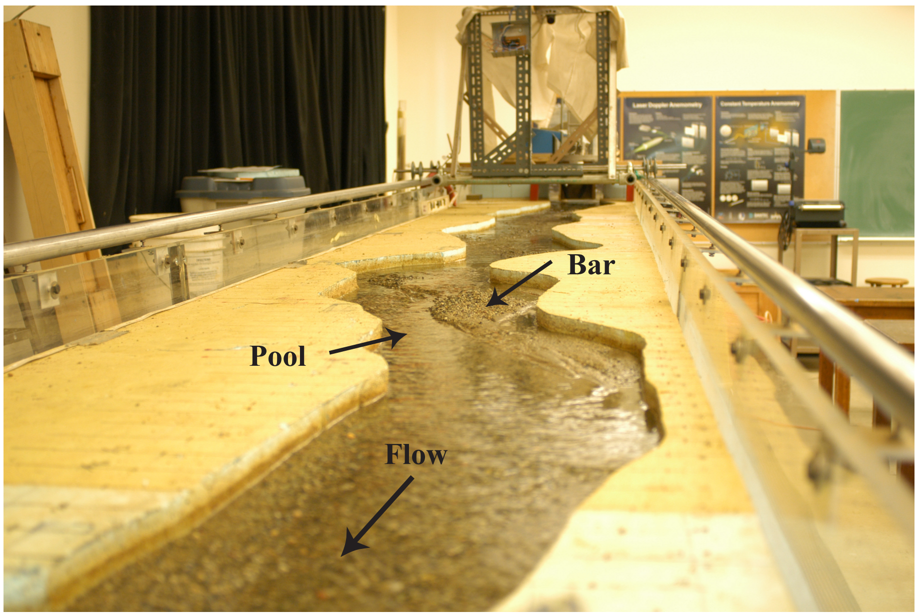

Figure 5.2: Photo of experiment looking upstream during low flow conditions. Emergent bars and pools are identifiable in the image.

Velocity appeared to decrease from the onset of the experiment up until until 2100 minutes (Figure 5.3). The channel aggraded throughout the experiment, as a result channel slope increased from 0.015 to 0.018. Average channel depth, determined using the continuity equation, was approximately 1.7 cm for the experiment. The Froude number was also constant for most of the experiment, at around 0.84. Volumetric sediment output peaked during the first 300 minutes of the experiment, then decreased for the following 600 minutes, and then remained relatively constant for the remaining 1500 minutes.

Changes in the surface grain size distribution were relatively minor over the course of the experiment. The bulk of the adjustments in grain sizes were made during the first 5 hours; recall that the D_{50} and D_{90} of the initial bed sediment and sediment feed was 1.14 mm and 3.28 mm respectively. The average armouring ratio for the experiment was 2.31 for the D_{50} and 1.61 for the D_{90}. For the transported material the average D_{50t} was 1.03 mm, which is slightly smaller than the D_{50} of the feed, and the average D_{90t} was 2.52, which is significantly finer than the feed.

During the conditioning phase of the experiment, small lobes or tongues of fine sediment were observed. These features appear to be similar to those described previously by *Ashmore* (1991). Figure 5.4a shows a colour close up of one such lobe, that was still visible after the experiment had stopped. The lobe is delineated in the photo based on it finer texture relative to the surrounding sediment. In the smaller scale image, the black and white one, additional fine sediment depositional areas can be identified upstream and downstream of the location of the close-up image. In Figure 5.4a the location of four of the ten cross sections monitored during the experiment have been identified. Micro bedform features that had developed during the first 300 min did not seem to be of sufficient size to influence channel hydraulics, even at the local scale. At this flow stage, the planform of the channel appeared to be the dominant influence on flow characteristics. The channel at this stage was fairly uniform, no pools had developed and the fine depositional areas were not topographically significant. Figure 5.6 shows selected cross sections following the conditioning flow, 0 min, and only minor cross section variability is evident. The bed surface sediment, other than the areas of fine deposition, remained fairly similar to the initial condition.

At the start of the experiment active sediment transport was observed to be occurring over 90% of the channel width at some of the observed cross sections. The presence of sediment transport occurring in the active areas was identified by observing either sediment transport as bedload sheets or traction transport.

Within the first 60 minutes of the experiment, channel bars had developed and pools had begun to form. The morphological development of the channel was partly associated with incipient bar features that had been identified following the conditioning run. The downstream progression of some of the sediment lobes had been halted by local flow conditions primarily due to channel hydraulics associated with the planform. Using the terminology of *Nelson et al.* (2009), free patches had become fixed patches. Some of the finer free patches that became fixed, remained fine for long periods. The width of active

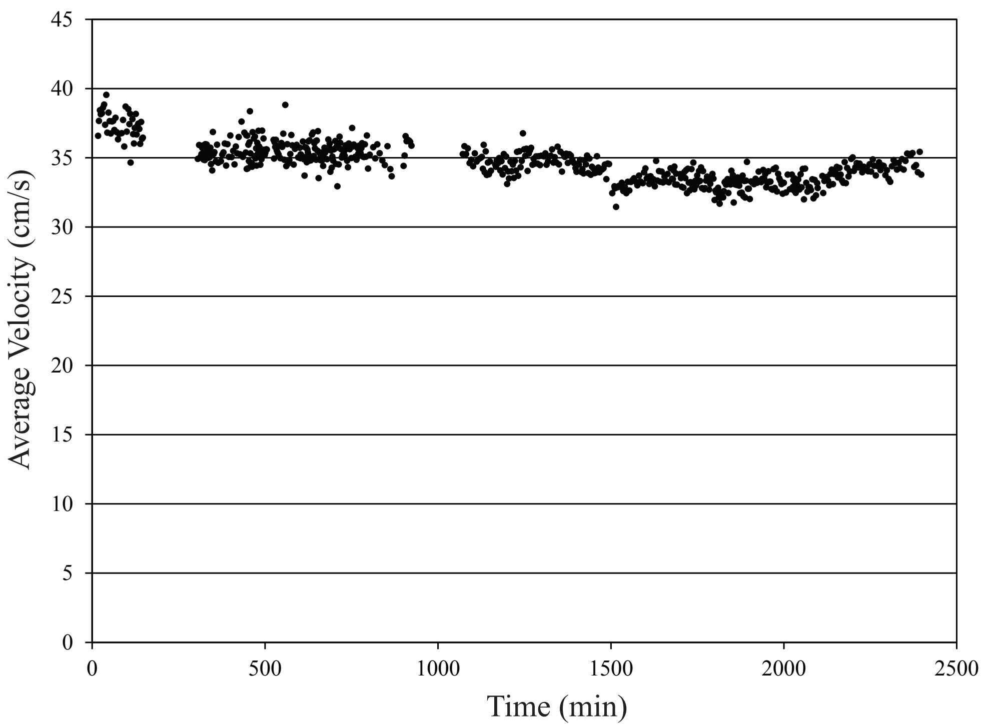

Figure 5.3: Plot showing individual velocity measurements for Exp. 6.

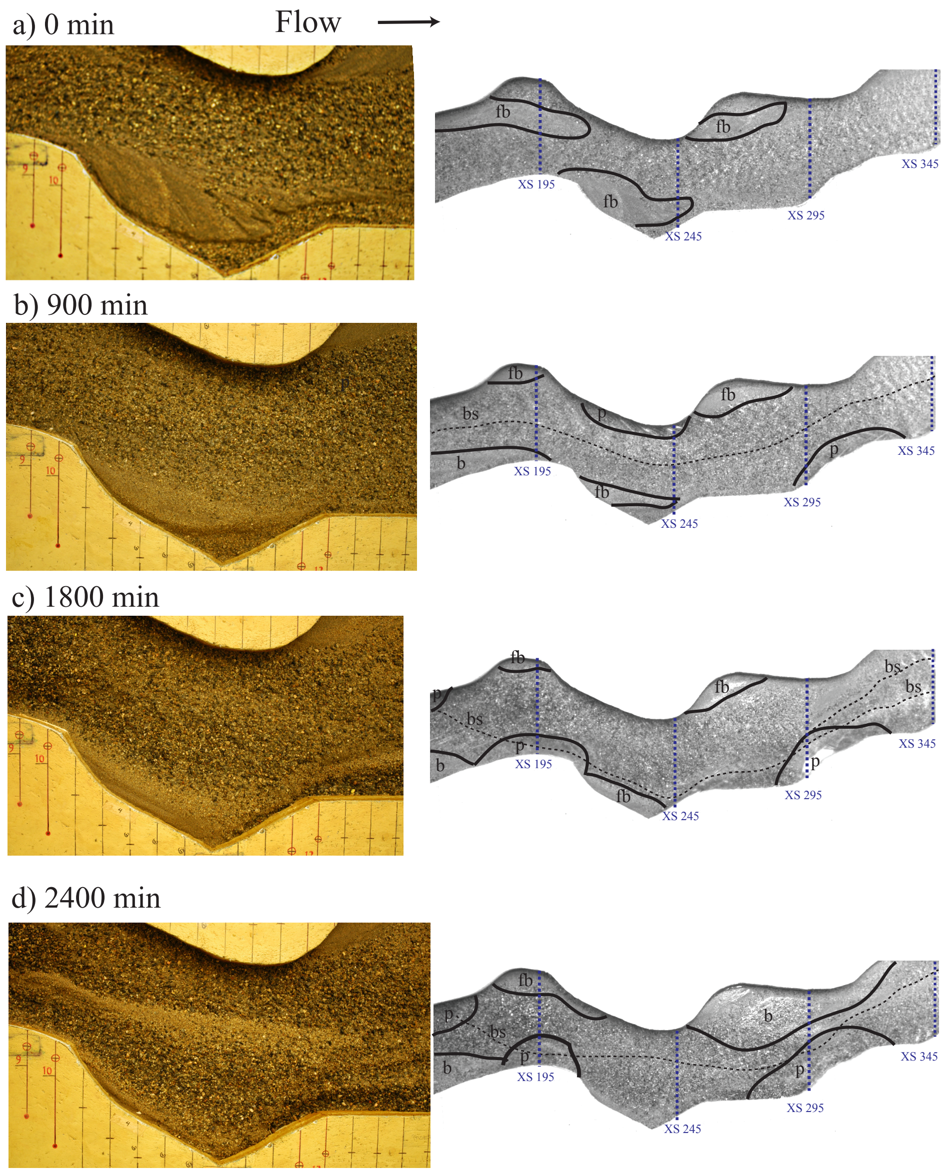

Figure 5.4: Large scale photos taken during periods of no flow and overhead photos taken from video during the experiment are presented at various time intervals: a) 0 minutes, b) 900 minutes, c) 1800 minutes, and d) 2400 minutes. Channel features identified on the maps have been transferred onto the smaller scale images, the following acronyms were used: fb = fine bar; b=bar; p=pool; bs = bedload sheet. Bedload sheets when present on the maps were added as dotted lines on the image. The location of cross sections (XS 195, 245, 295 and 345 presented in Figure 5.6) discussed is shown on overhead photo a).

transport was 100% at some of the cross sections, but on average represented 62 % of the channel width.

After 300 minutes some minor cross sectional adjustment had occurred, except for Figure 5.6d where the channel aggraded. Aggradation of the channel at this cross section was the result of a developing lateral bar, which also resulted in a decrease in the width of active transport by over 50% at this cross section (Figure 5.5b). Other cross sections did not experience such a reduction and overall active transport remained high relative to channel width (78%). The lateral topographic change at this cross section resulted in concentration of the flow, and consequently sediment transport..

As morphological complexity of the channel increased, the width of active sediment transport zone decreased. By 720 minutes, a large bar had developed in the upper section of the flume along the right bank. The development of the bar modified local hydraulics which caused the concentration of sediment transport. Although sediment output remained relatively flat, the variability in the width of active sediment transport appeared to be a direct result of increased morphological complexity.

After 900 minutes, the zone of active transport was mostly confined along the channel centreline (Figure 5.4b). The bed surface appears finer in this image compared to the 0 min image, although this is not reflected in the surface samples (Table 5.1), fine sediment patches along the left and right banks downstream of the channel curves are also evident. The development and growth of bars upstream of XS 195 limited the downstream movement of sediment, and hence the width of active transport following a peak after 800 minutes (Figure 5.5b). As a result of bar formation, highlighted in Figure 5.4b along the upstream right bank, the zone of maximum sediment transport was directed from the right bank downstream toward the left bank, which lead to pool development at XS 245, which then deflected the zone downstream to the right bank, at XS 295, where an additional pool developed. Bedload sheets were mapped and their position of movement is indicated in the figure, and remained in the mid-channel position. Channel cross sectional change after 900 min are most evident at XS 195, 245 and 295 (Figure 5.6a - c).

Following 1800 minutes a pool adjacent to the left bank had developed upstream of XS 195, sediment exited the pool and traversed the channel to a pool located at XS 195 (Figure 5.4c). The width of the active transport zone declined after 1400 minutes (Figure 5.5b) to 35%. It is interesting to note that although sediment feed rates, sediment output, and the surface grain sizes following the first 300 min were fairly constant, the zone of active transport continually evolved which is directly related to the morphology of the channel. In Figure 5.4c the pool at XS 295 scoured to the bottom of the flume, water depth was greater than 6 cm. Sediment that exited the pool took one of two paths Figure 5.4c. The origin of the sediment that exited the pool determined which path the sediment would more likely take: the mid-channel path was mainly sediment the came from the eroding transverse bed slope of the pool, related to additional lateral pool scour and growth; and, the path closer to the right bank was sediment that mainly came from upstream. In Figure 5.6 maximum pool depths occurred at both XS 195 (4 cm) and XS 295 at 1800 minutes.

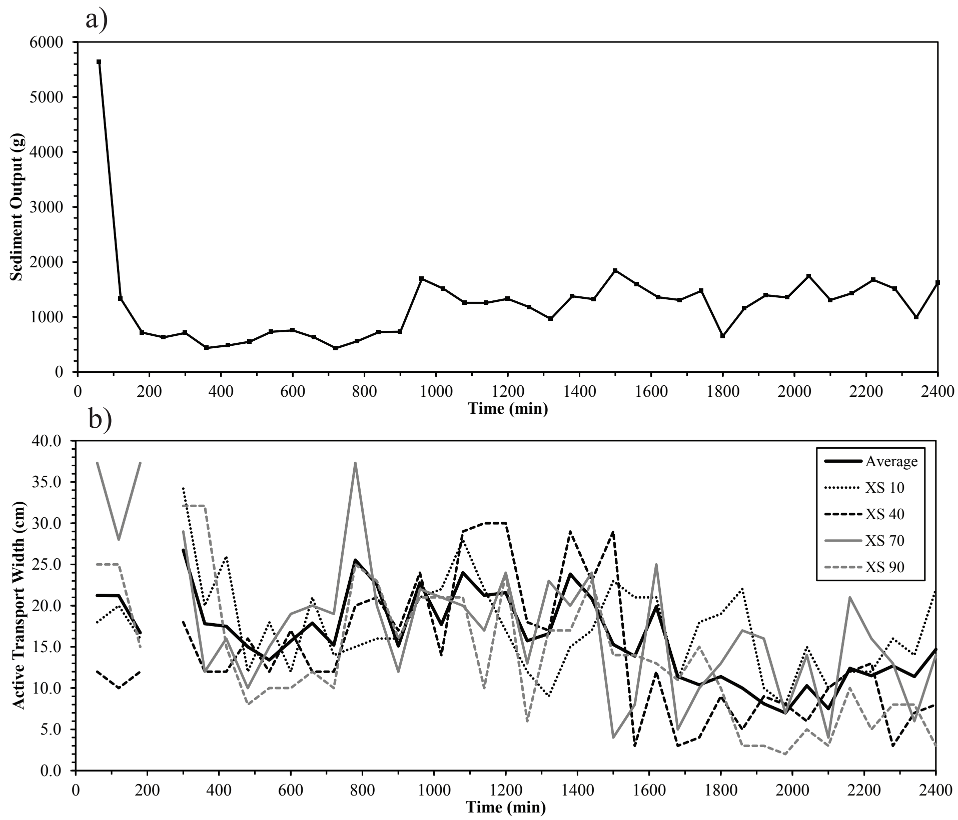

Figure 5.5: a) Cumulative sediment output (g) at 60 minute intervals is shown on the primary axis over time. b) The average width of active sediment transport of all ten cross sections during the experiment and from four individual cross sections. Note that no observations were made at 240 minutes.

After 2040 minutes a similar situation occurred with the pool located at XS 195, that is two separate sheets exited the pool at the same time.

After 2400 minutes a bar developed between XS 245 and XS 345 along the left bank (Figure 5.4d). The presence of the bar altered the path of bedload sheet migration as the dimensions of the pool at XS 195 expanded. As sediment emerged from the pool it fanned out over the downstream riffle, with the finer sediments remaining near the right bank and in the middle of the channel, and the coarse material moving in between these two zones. The colour picture in Figure 5.4d) shows this result clearly, with a fine sediment ribbon close to the right bank, and another ribbon seen in the mid-channel. Coarse sediment movement was associated with the bedload sheets as well as traction transport in between the bedload trails visible in the photo. The width of active transport declined after 1800 minutes to an average low of 20% at 1980 minutes, by 2400 minutes it had risen to 45% (Figure 5.5b). Infilling of pools is evident in Figure 5.6, for XS 195 to XS 295.

Overall, the experimental design successfully produced pool-riffle morphology in the flume. The use of fixed irregular banks created complex morphology and patterns of sediment transport, not unlike those observed in nature. Surface coarsening of the channel occurred relatively early on in the experiment, although morphological evolution of the channel continued throughout. This result suggests that the development and interaction of morphologic units is more important to channel form and sediment transport processes than channel armouring, especially under high flow conditions, similar to the conditions produced in these experiments.

The importance of bedload sheets was also highlighted by this experiment. The presence of sheets not only aided in identifying sediment transport pathways, but was also an indicator of in-channel sediment supply and morphological change. Bedload sheets will be discussed further in the following section.

5.3.2 Bedload Sheets

Most observations of bedload sheets in flumes have been made using straight walled flumes with plane bed morphology (for example, *Iseya and Ikeda*, 1987; *Dietrich et al.*, 1989; *Kuhnle and Southard*, 1988; *Nelson et al.*, 2009; *Recking et al.*, 2009). It is possible that these conditions promote the abrupt segmentation of smooth versus congested zones (*Iseya and Ikeda*, 1987). Topographically complex conditions with lateral cross sectional diversity, due to the presence of channel bars and pools, introduced more complex behaviour in bedload sheets than observed previously. Bedload sheets were observed to grow and their migration rate increase in pools or topographically convergent areas, generally sediment in these areas is more mobile during higher flow events. In topographically divergent areas, such as riffles, bedload sheets can sometimes lose velocity and disperse and other times not.

Bedload sheet migration velocity was highly variable during the experiment. Table 5.1 shows the range in observed velocities for each 300 minute period. On average the

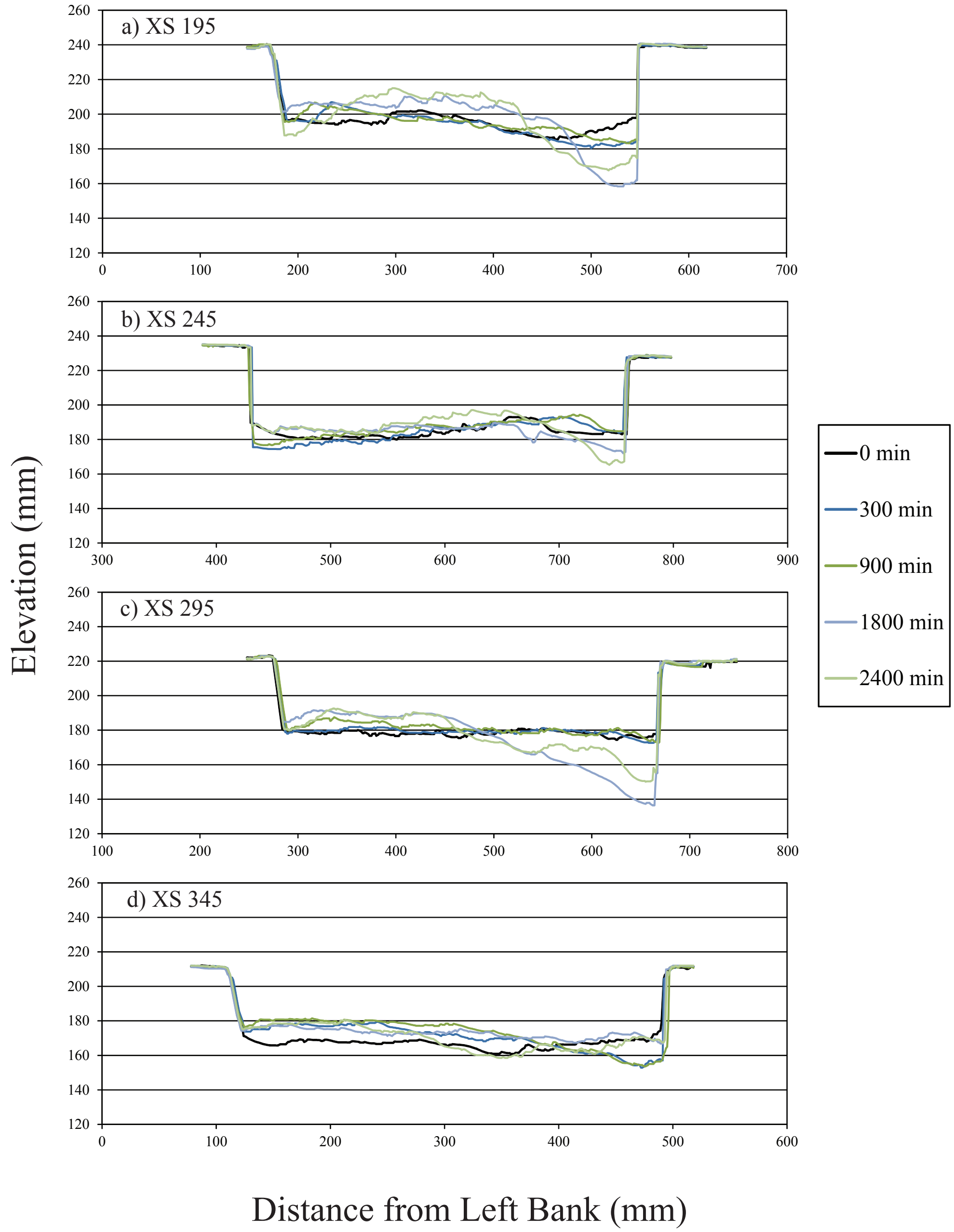

Figure 5.6: Selected cross sections from laser scans of the bed for: a) XS 195; b) XS 245; c) XS 295; d) XS 345. Data is presented at 300 minute intervals, when scans were completed while experiment was not running.

observed velocities for bedload sheet migration ranged from 0.15 - 1.46 cm/s in this experiment. Comparatively, *Recking et al.* (2009) found velocities from 0.6-1.4 cm/s; *Kuhnle and Southard* (1988) measured 0.5 - 1 cm/s; *Iseya and Ikeda* (1987) measured 0.36-1.13 cm/s; and, *Madej et al.* (2009) found velocities of 1 - 2 cm/s. *Recking et al.* (2009) suggested that variability in his experiments was partly attributable to channel slope. Variability in the velocities observed here appeared to be partly due to the availability of sediment, with high velocities and frequency at the beginning of the experiment and during periods of pool scour and growth, and channel morphology. During periods of high sediment availability, bedload sheet velocities were high. It should be noted that migration velocities were determined based on a limited observation window, between XS 195 and XS 245 in Figure 5.4. Similar to *Kuhnle et al.* (2006) coarser grains appeared to travel faster than the finer fractions of the bedload sheet. It would be expected that bedload sheet migration velocities would be high in an area of convergent flow (i.e., a pool) compared to an area of divergent flow (a riffle). The variability may also suggest that bedload sheets interact with the zone of maximum shear stress (assumed to be approximately where with the highest concentration of sediment in transport was observed), and when the sheet is in the zone velocities are higher than when they are not.

Figure 5.7 is an image from the overhead camera during the experiment. In the upstream edge of the image a single bedload sheet can be seen as it entered the pool, near the right bank in the image (as indicated by the thicker arrow). The upstream sheet can be identified in the image by its smoother texture and lighter hue of grey, in contrast to the coarser textured, darker tone surface of the non bedload sheet bar toward the left bank. At the downstream end of the pool, two bedload sheets exit the pool. The bedload sheet adjacent to the right bank followed an existing ribbon of fine sediment, evident in the photo. The sheet was relatively narrow, less than 5 cm wide, and the sediment that composed it appeared slightly finer than that which entered the pool. The bedload sheet near the left bank emerged from the pool onto a mid-channel riffle. The coarse-surfaced riffle caused the sheet to diverge as the particles within the sheet moved through the riffle. The result of the riffle, diverging flow, and divergence of the sheet resulted in a width of 15 cm. The coarse and finer sediments interacted with the coarse bed sediment as the bedload sheet moved through the riffle, however the majority of the sediment maintained downstream momentum. It was difficult to quantify in the video if the interaction of the bedload sheet with the riffle actually resulted in lower velocity for the upper bedload sheet, however, it did appear to. The two bedload sheets converged prior to entering the next pool downstream.

Recking et al. (2009) proposed a model of periodical bedload production, in which aggradation on the bed continued until a critical slope was reached. Once the slope was attained it results in increased gravel mobility and strong local erosion, producing a bedload sheet. Here, sheet production was observed to occur during morphological scouring events. For example, in Figure 5.7, as the pool expanded laterally, the sediment from the eroding face, exited the pool as a bedload sheet. This suggests that sediment supply may be a more

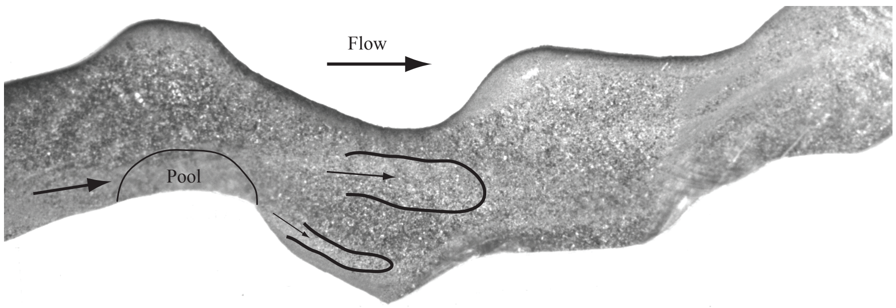

Figure 5.7: Image showing two bedload sheets emerging from the same pool. As the sheet entered the pool it diverged into two separate sheets. The coarse leading fronts of the two sheets are indicated in the image. The arrows highlight the direction of movement of the bedload sheet.

critical component of bedload sheet production. Even local sources such as pool scour, or a bank erosion event in a field setting, could result in bedload sheet production.

Bedload sheets are commonly associated with fluctuations in bedload transport, previous researchers have suggested that the large, short-term variations in sediment flux are associated with bedload sheets (*Nelson et al.*, 2009). Although, the resolution of the data presented here were not collected at a scale fine enough to delineate individual bedload sheet pulses in the output data, it is clear that morphological adjustments, scour and fill, were the predominant cause of large short-term variability in sediment flux.

Bedload sheets have been categorized as bedforms (*Whiting et al.*, 1988; *Bennett and Bridge*, 1995a; *Kuhnle et al.*, 2006) and/or patches (*Nelson et al.*, 2009). Some have observed dunes developing from bedload sheets (*Kuhnle and Southard*, 1988; *Whiting et al.*, 1988; *Wilcock*, 1992). In this experiment gravel bars developed from bedload sheets, this may be similar to what *Ashmore* (1991) observed in his experiments. This suggests that bedload sheets may be pseudo bedforms. In these experiments, bedload sheets appear to be more of a sediment transport pathway, in which they develop in response to excess local sediment supply in order to move the excess sediment downstream in a rapid manner.

5.3.3 Observations of sediment transport

The observations of sediment transport and bedload sheet movement during the experiment and in the videos, allowed visualization of sediment transport pathways. From these observations, inferences into flow and sediment transport through the channel were made. Models of flow and sediment transport and sorting through bends differ primarily in how they account for the relative magnitude and importance of the components of the downstream and cross-stream force balance in channels (*Whiting*, 1997). *Whiting* (1997) found that these distinctions were related to differences in either flow stage or magnitude of topographic relief, with the convective acceleration term being more important in channels with greater topographic relief and lower stages. Topographic relief evolved during these experiments and the stage was relatively high; it is anticipated that aspects of both models will be observed.

Figure 5.8 illustrates the flow processes and sediment pathways and sorting through a meander following *Dietrich and Smith* (1984). In the *Bridge* (1992) model the cross-stream component of particle weight is balanced by the fluid drag from secondary circulation, suggesting a static balance of forces as the particle travels through the bend. For Bridge's model the coarse sediment follows the zone of maximum shear stress downstream through the bend, but no net cross-stream transport occurs, therefore particle size differentiation does not occur through the meander. *Dietrich and Smith* (1984) suggested that sediment transport through a meander is the result of a dynamic balance of forces. Shoaling flow from the bar causes outward sediment transport that forces the zone of maximum bedload transport rate to track the outward-shifting zone of maximum shear stress (Figure 5.8). The outward-directed flow over the bar balances the spatial variation in shear stress with the convergent sediment transport (*Powell*, 1998). This implies that as coarse and fine particles move through the meander they cross paths due to inward-acting secondary flow, which moves fine particles up the transverse bed slope, and the outward-acting gravitational flow, which moves coarse particles down the transverse bed slope toward the pool.

Both models were developed for equilibrium conditions, and thus assumptions of stable morphology were made. In this experiment the pool at which sediment movement was observed was not in equilibrium and changed during the course of the experiment. Additionally, the morphology of the experimental channel is not equivalent to the meander pattern described in either of the two models. Most importantly, the bar adjacent to the pool was a lateral bar and not a point bar, which may have implications for the magnitude of the outward shoaling flow across the bar.

If we can assume that observations of bedload sheet movement through a pool are representative of sediment pathways and sorting, then this experiment can offer new insight into this process. From observations made during this experiment three particle pathways and sorting outcomes were identified. These outcomes appeared to depend upon the morphology of the pool and its hydraulic connection to upstream and downstream morphological units. The three outcomes are:

1. sediment entered the pool, travelled along the transverse bed slope and exited with little to no evidence of sorting;

2. sediment entered the pool and exited pool with evidence of sorting; and,

3. sediment entered the pool, travelled through the maximum pool depth and exited pool with little evidence of sorting;

The first item represents sediment movement through the pool in a manner similar to the scenario described by *Bridge* (1992). This outcome appeared to be predicated by pool dimensions that created conditions where gravitational and convective forces were balanced. Coarse particles were visually tracked as they entered the pool and they appeared to maintain a consistent elevation through the pool. The relation of the coarser grains to the finer grains did not appear to be altered as the sheet travelled through the pool. An important factor appeared to be the angle at which the bedload sheet entered the pool. If the downstream trajectory of the sheet was parallel to the bar face and the overall orientation of the pool, its movement through the pool was not altered. This suggests that the morphology was conducive to the balance of forces between shoaling and secondary flows.

The second item represents sediment movement and sorting through the pool similar to that described by *Dietrich and Smith* (1983), where the shoaling induced outward flow and secondary flows sort the sediment particles as they moved through the pool. This was observed when the transverse bed slope of the bar was at a low angle and the pool was generally wider and more fully developed. The bedload sheet shown in Figure 5.4d) is an

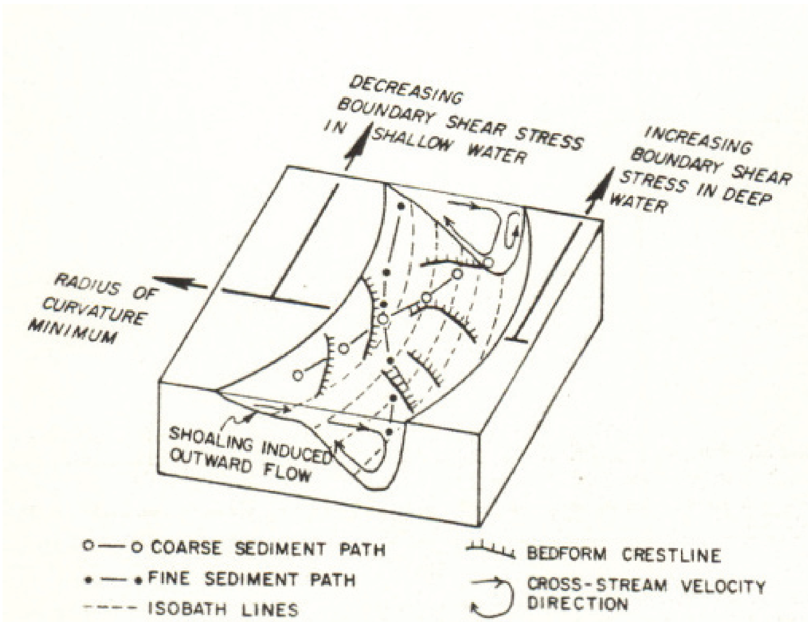

Figure 5.8: Flow processes controlling morphology and sediment sorting in a river meander. Flow direction is from the lower to upper end of the figure. From *Dietrich and Smith* (1984).

illustration of this. The cross-section of the pool at 2400 min can be seen in Figure 5.6a, the combination of a deep pool and relatively gentle transverse bed slope encouraged the outward shoaling flow. The magnitude of the secondary flow circulation is also reflected by the change in the downstream angle of the bedload sheet trajectory as it entered the pool relative to the angle it had when it entered the pool.

Lastly, the bedload sheet entered the pool as a coherent line and travelled through the deepest part of the pool and exited with very little sorting or alteration of its downstream trajectory. Figure 5.4c provides an example of this, the angle of the bedload sheet relative to downstream flow is unaltered as it travels through the pool-bar unit. The cross-section at 1800 minutes (Figure 5.6a) shows a deep pool with a steep transverse bed slope. The angle at which the bedload sheet entered the pool (Figure 5.4c) took the sediment through the centre of the pool. In addition to the magnitude of the transverse bed slope, the orientation of the zone of maximum sediment transport relative to the downstream orientation of the pool appears to influence how sediment moves through the pool-bar unit.

5.4 Discussion and Conclusions

A complex channel planform was used to replicate pool-riffle morphology in a mountain gravel-bed river. Experimental observations, hand drawn maps, still images and videos were used to describe sediment transport processes and pathways during Exp. 6. The development of an experimental channel under conditions of constant discharge and sediment feed was discussed and linkages were made between sediment transport and the morphological development of the channel. The width of active sediment transport was found to be variable throughout the experiment, but generally declined overtime. The reduction in width was related to increased lateral variability in the channel, which appeared to concentrate sediment movement into a smaller percentage of the channel width. This reduction in the width of active transport was not due to reduced sediment transport as had been identified previously (for example, *Lisle et al.*, 1993). The reduction suggests that the channel became more efficient in transporting sediment over time. Similar volumes of material were being moved through the channel, but it occurred over a relatively smaller portion of the channel. Channel cross sections evolved from a simple featureless plane-bed morphology to a topographically complex system exhibiting characteristics of pool-riffle morphology.

Previously, observations of bedload sheets in laboratory settings have been mainly done under simplified morphologic conditions: this experiment allowed observations of bedload sheet movement and production to be made in a topographically and planimetrically complex environment. Unfortunately, the frequency of sediment sampling at the output prevented direct measurement of variability in sediment output rates due to bedload sheet migration.

Flow and sediment transport characteristics were inferred from observations of bedload sheet movement in the experimental channel. Existing models of sediment movement and sorting through a channel are based on the assumption of equilibrium conditions, which may or may not occur in many gravel-bed rivers in glaciated regions. The pool-bar unit presented here was not in equilibrium and changed over the course of the experiment. The development of the outward-directed shoaling flow and the inward-directed secondary circulation were dependent on pool dimensions and the angle of the transverse bed slope. The angle of the transverse bed into the pool was an important topographic characteristic that influenced both flow and sediment sorting. Additionally, the relative orientation of the incoming bedload sheet relative to the downstream orientation of the pool appeared to influence sediment movement and sorting through the pool.

Chapter 6

Conclusions

The aim of this research was to investigate long-term channel development and response under conditions of constant discharge and sediment supply. A Froude scaled physical model was constructed using Fishtrap Creek, a gravel-bed stream in the interior of British Columbia, as a field prototype. Eight experiments were conducted holding sediment feed rate and water discharge constant within each experiment, but varying the magnitudes between experiments. A ninth experiment was conducted with no sediment feed and water discharge held constant. A final experiment was conducted to see how sediment mobility responded to increased discharge with no sediment feed. Design flows used in the experiments were based on conditions in the field prototype, corresponding to flow conditions having return periods ranging from the 2-yr to greater than 150-yr. As the purpose of the experiments were to investigate long-term channel response, a sediment-feed protocol was employed. A novel approach to the design of the flume was undertaken in order to focus the experiments on intermediate-sized gravel-bed rivers in forested environments. An irregular meandering planform was built to reflect the planform observed in the prototype. The flume design successfully produced both pool-riffle and plane-bed morphologies, both of which are present in the prototype.

Specifically, this research investigated:

- the effects of varying sediment supply and discharge on bed surface and transported sediment characteristics;
- the effects of varying sediment supply and discharge on channel storage and channel morphology; and,
- sediment transport processes and pathways.

In Chapter 3 the effects on the characteristics of the bed surface and transported sediment under differing regimes of discharge and sediment feed were investigated. Experiments focused on channel formative flows employing discharges ranging from the 2-yr to over 150-yr return period events. The results indicate that even with discharges exceeding the 10-yr flood full mobility was not observed. This slight but persistent size-selectivity produces long-term aggradation and surface coarsening, as the larger grain sizes are left on the surface. This size-selectivity occurred when the sediment feed had the same grain size distribution as the bed material. These results are compared with a reanalysis of previously published data from a generic model of small gravel-bed streams with erodible bed and banks. Those channels exhibit a similar size-selectivity, which seems to be critical for maintaining stable channel banks, with full mobility potentially being related to a shift from a stable single thread channel that does not aggrade to an unstable channel that does aggrade over time.

In Chapter 4 the effects of varying sediment supply and discharge on channel storage and morphology were explored. The results showed that sediment transport rates varied both spatially and temporally. This variability was found to be more dependent upon changes in the morphology of the channel, rather than adjustments in the surface grain size distribution. The primary self-adjusting mechanism in the experimental channel was to adjust channel form. Adjustments to bed surface texture, tended to be a short-term and immediate response to the high flows. The development of surface patches appeared to be in response to hydraulics associated with channel topography.

The transport-storage relation originally presented by *Lisle and Church* (2002) and later by *Madej et al.* (2009), *Pryor et al.* (2011) and *Lisle* (2012) employing declining or variable sediment feeds rates was investigated. Similar to the conclusions of *Lisle and Church* (2002), sediment transport capacity was found to be variable and that it changed as the volume of sediment stored in the channel changed. *Madej et al.* (2009) and *Pryor et al.* (2011) observed hysteresis cycles in the relationship between sediment transport rate and sediment storage, which they attributed to morphological responses to changes in the feed rate. Unlike these studies, the analysis presented here indicates that these cycles occurred when transport rates were approximately equal to the feed rates (i.e., when the channel was near equilibrium). Cycles of aggradation-degradation were observed to occur without changes in either sediment supply or flow discharge. It was concluded that the transport-storage relation does not offer a unique relation between transport rates and sediment storage, thus limiting its usefulness in the development of an improved sediment transport model.

The results suggest that the idea of sediment reservoirs is more complex than *Lisle and Church* (2002) had originally envisioned and that these reservoirs are transitional. Additionally, multiple reservoirs may exist within homogeneous reaches as they may scale down to the morphologic unit. Each reservoir may also have a have different time signature in terms of how responsive they are to changes in either flow or sediment supply. This difference is dependent upon flows, sediment supply, and local adjustment to the topography, which in addition to the previous parameters is dependent upon boundary conditions (such as bank stability, bank form and alignment (important in most forested landscapes).

For Chapter 5 a less formal approach was taken to describe the sediment transport processes and pathways observed during the experiments. As similar patterns emerged during each experiment, only information from one of the experiments, Exp. 6, was used for this chapter. A variety of qualitative data sources were used, including experimental notes, hand drawn field maps, width measurements of sediment transport, colour images during dewatered periods, and experimental videos.

The dominance of bedload sheets as a process by which sediment was transported through the reach is one of the key findings in the chapter. Bedload sheets appear to be the conveyor belts of sediment transport. Observations of the movement of bedload sheets through a pool and riffle unit provided further insight in how they behave in more topographically complex settings. For example, single bedload sheets were observed to enter a pool and two bedload sheets emerged. The appearance of multiple sheets emerging from the pool was linked to an additional source of sediment within the pool itself; divergence of the sheet as it exited the pool was influenced by the presence of a riffle, and the sheets appeared to follow the margins of the riffles. When bedload sheets encountered riffles directly, they would disaggregate as the particles moved through the coarser surface and reform into a sheet when downstream of the riffle.

During periods of high sediment mobility the zone of active sediment transport appeared to occupy the entire cross section. During these periods the majority of sediment was being transported in bedload sheets, the movement individual particles was still observed outside of the areas occupied by bedload sheets. The area of the channel in which active transport was observed was not simply a function of sediment supply, increased morphological complexity. The development of a pool-riffle morphology confined sediment transport pathways to the lower elevation portions of the channel cross section.

Ranges in bedload sheets migration velocities observed in Exp. 6 were found to be similar to those of previous experiments (*Iseya and Ikeda*, 1987; *Kuhnle and Southard*, 1988; *Madej et al.*, 2009; *Recking et al.*, 2009). Bedload sheet production seems entirely dependent on sediment availability, which can also include in-channel scour events. The notion that bedload sheets are in themselves a bedform (*Whiting et al.*, 1988; *Bennett and Bridge*, 1995b; *Kuhnle et al.*, 2006) or represent mobile patches (*Nelson et al.*, 2009) needs to be revisited. The observations here suggest that they may actually be a how channels transport sediment downstream, as they appeared to be a robust method to transport excess sediment out of the reach more rapidly than normal transport processes.

Observations of sediment movement through a pool-riffle unit confirmed aspects of sediment sorting models of *Dietrich and Smith* (1984) and *Bridge* (1992). From these experiments the importance of pool dimensions, depth and transverse bed slope of the bar, and local channel hydraulics play an important role in determining not only how sediment enters a pool, but the path it takes as it moves through it and the effectiveness of sorting processes within it. Although not measured in these experiments, pool dimensions appear to determine the relative magnitude of secondary circulation to the primary flow direction, with stronger secondary circulation resulting in more sediment sorting as it moves through the pool. Additionally, the relative downstream velocity and angle of sediment entering the pool relative to the hydraulics within the pool influenced how or if sediment was sorted as it moved through.

6.1 Questions, Observations and Future Research

The experiments provided an opportunity to observe channel evolution under high flow conditions. Whether or not the experimental channels are representative of natural environments may be debatable, but they are channels in and of themselves, and their morphology evolves under the same physics as "real" rivers.

The following itemized list, not in any particular order, provides some additional thoughts, research questions and approaches that emerged as this research was being conducted.

- Channel stability in gravel-bed rivers is likely the result of an interaction between the channel boundaries, armouring of the bed surface and morphological units present. Holding the channel boundaries constant, the relationship between the stability of channel units and the effects of armouring can be investigated in experiments with uniform and graded sediments.

- The stability of the pool-riffle morphology in gravel-bed rivers may also represent an extension of the jammed state theory, similar to the application made to step-pool channels by *Church and Zimmermann* (2007). In a jammed state within granular material, individual grains form force chains that resist movement under directed force due to grain-on-grain structural arrangements and/or strong frictional binding. For step-pool channels, the force chain is established across the channel. The relative scale of flow depth (D/d) to these grains in step-pool channels is small. In pool-riffle channels the relative depth of water to individual grains is much greater. However, it is suggested that channel bars might behave in a similar manner; it is a matter of seeing the bar as a structural arrangement of grains. Bars jam up in the channel in which the stored sediment resists movement, in the sense that they create their own hydraulic environment that can sustains their form over time. This hydraulic environment links bars adjacent in both the upstream and downstream directions.

- Additional research on the role of topographic evolution within channels and its associated effect on sediment transport rates is suggested. It is believed that the topographic signature of the channel plays a dominant role not only in channel hydraulics, and the distribution of shear stresses, but on the development of in-channel surface patches and sediment reservoirs. Linking physical models with numerical models is likely the most productive method to accomplish this task.

- Improved techniques to investigate bedload sheet production, migration and deposition should be undertaken, Experiments specifically designed with this in mind should be conducted. The design approach should utilize a more realistic channel planform as the morphological complexity of the channel influences the behaviour of the sheets. Understanding this linkage is critical to further our understanding their behaviour. Questions to explore could include: What are the relative roles of sediment supply, morphological complexity and surface sediment size in determining bedload sheet migration velocity? Can bedload sheets develop in beds with uniform grain sizes?

- The same intensity of research that was applied to surface armouring should be applied to channel morphologic units, such as bars and pools. This would likely require numerical and physical models. The physical models should be designed with this topic in mind, and therefore would require modified flume designs.

- Additional research should be undertaken regarding the effects of Froude scaling on the sediment size distribution. What are the implications of truncating the smaller size classes? What effect does the truncation have on channel morphodynamics?

- The importance of the largest grains in determining channel morphodynamics has been shown to be important in this research. The link between the larger grains, channel bedforms and channel stability in gravel-bed rivers merits additional research.

- Further research into the variability of sediment supplied to a system and its influence on channel responses. Depending on the geology and geologic history of a basin, a channel in mountainous areas can receive a wide range in the calibre of material delivered to the channel. Coupled numerical and physical model experiments could be set up to explore these effects.

Research in gravel-bed rivers has been mainly focused on the grain scale for the last 30 years, it is suggested that this scale may not be entirely appropriate for understanding the morphology of rivers at the scale of interest to most practitioners.

References

Ackers, P., and F. G. Charlton (1970), Meander geometry arising from varying flows, *Journal of Hydrology*, *11*(3), 230–252.

Andrews, C. (2010), A stream in transition: short-term morphodynamics of Fishtrap Creek following wildfire, Master's thesis, The University of British Columbia.

Andrews, E. D. (1983), Entrainment of gravel from naturally sorted riverbed material, *Geological Society of America Bulletin*, *94*(10), 1225–1231.

Ashmore, P. (1991), Channel morphology and bed load pulses in braided, gravel-bed streams, *Geografiska Annaler. Series A. Physical Geography*, *73*(1), 37–52.

Ashworth, P., J. Best, J. Leddy, and G. Geehan (1994), The physical modelling of braided rivers and deposition of fine-grained sediment, in *Process models and theoretical geomorphology*, edited by M. Kirkby, pp. 115–139, John Wiley and Sons.

Ashworth, P. J., and R. I. Ferguson (1989), Size-selective entrainment of bed load in gravel bed streams, *Water Resources Research*, *25*(4), 627–634.

Barry, J. J., J. M. Buffington, and J. G. King (2004), A general power equation for predicting bed load transport rates in gravel bed rivers, *Water Resources Research*, *40*(10), W10,401, doi:10.1029/2004WR003190.

Bartholdy, J., and P. Billi (2002), Morphodynamics of a pseudomeandering gravel bar reach, *Geomorphology*, *42*(3), 293–310.

Bartley, R., and I. Rutherford (2005), Re-evaluation of the wave model as a tool for quantifying the geomorphic recovery potential of streams disturbed by sediment slugs, *Geomorphology*, *64*(3), 221–242.

Benda, L., and T. Dunne (1997a), Stochastic forcing of sediment routing and storage in channel networks, *Water Resources Research*, *33*(12), 2865–2880.

Benda, L., and T. Dunne (1997b), Stochastic forcing of sediment supply to channel networks from landsliding and debris flow, *Water Resources Research*, *33*(12), 2849–2863.

Bennett, S., and J. Bridge (1995a), An experimental study of flow, bedload transport and bed topography under conditions of erosion and deposition and comparison with theoretical models, *Sedimentology*, *42*(1), 117–146.

Bennett, S., and J. Bridge (1995b), The geometry and dynamics of low-relief bed forms in heterogeneous sediment in a laboratory channel, and their relationship to water flow and sediment transport, *Journal of Sedimentary Research*, *65*(1), 29–39.

Blench, T. (1969), *Mobile-Bed Fluviology*, The University of Alberta Press, Edmonton.

Braudrick, C., W. Dietrich, G. Leverich, and L. Sklar (2009), Experimental evidence for the conditions necessary to sustain meandering in coarse-bedded rivers, *Proceedings of the National Academy of Sciences*, *106*(40), 16,936–16,941.

Bravo-Espinosa, M., W. Osterkamp, and V. Lopes (2003), Bedload transport in alluvial channels, *Journal of Hydraulic Engineering*, *129*(10), 783–795.

Bray, D. (1975), Representative discharges for gravel-bed rivers in Alberta, Canada, *Journal of Hydrology*, *27*(1), 143–153.

Brewer, P., and J. Lewin (1998), Planform cyclicity in unstable reach: complex fluvial response to environmental change, *Earth Surface Processes and Landforms*, *23*(11), 989–1008.

Bridge, J. (1992), A revised model for water flow, sediment transport, bed topography and grain size sorting in natural river bends, *Water Resources Research*, *28*(4), 999–1013.

Brummer, C. J., T. B. Abbe, J. R. Sampson, and D. R. Montgomery (2006), Influence of vertical channel change associated with wood accumulations on delineating channel migration zones, Washington, USA, *Geomorphology*, *80*(3), 295–309.

Buffington, J., and D. Montgomery (1999a), Effects of hydraulic roughness on surface textures of gravel-bed rivers, *Water Resources Research*, *35*(11), 3507–3521.

Buffington, J. M., and D. R. Montgomery (1999b), Effects of sediment supply on surface textures of gravel-bed rivers, *Water Resources Research*, *35*(11), 3523–3530.

Carling, P. (1987), Bed stability in gravel streams, with reference to stream regulation and ecology, in *River Channels: Environment and Process*, edited by K. Richards, p. 321 347, Blackwell, Oxford, UK.

Carling, P. (1988), The concept of dominant discharge applied to two gravel-bed streams in relation to channel stability thresholds, *Earth Surface Processes and Landforms*, *13*(4), 355–367.

Carson, M. A., and G. A. Griffiths (1987), Bedload transport in gravel channels, *Journal of Hydrology (NZ)*, *26*(1), 1–151.

Chorley, R., and B. Kennedy (1971), *Physical Geography - A Systems Approach*, 370 pp., Prentice Hall International Inc.

Church, M. (1992), Channel morphology and typology, in *The Rivers Handbook*, edited by P. Callow and G. Petts, pp. 126–143, Blackwell Science.

Church, M. (1995), Geomorphic response to river flow regulation: case studies and time-scales, *Regulated Rivers Research and Management*, *11*(1), 3–22.

Church, M. (1998), Think globally, learn locally: broadening prespectives of the earth, *Geoscience Canada*, *25*(4), 171–182.

Church, M. (2006), Bed material transport and the morphology of alluvial river channels, *Ann. Rev. Earth Planet. Sci.*, *34*, 325–354.

Church, M., and M. Hassan (2005), Upland gravel-bed rivers with low sediment transport, in *Catchment Dynamics and River Processes. Mediterranean and Other Climate Regions*, edited by C. Garcia and R. Batalia, pp. 141–168, Elsevier.

Church, M., and M. A. Hassan (2002), Mobility of bed material in harris creek, *Water Resources Research*, *38*(11), 1237, doi:10.1029/2001WR000753.

Church, M., and D. Jones (1982), Channel bars in gravel-bed rivers, in *Gravel-bed Rivers*, edited by R. Hey, J. Bathurst, and C. Thorne, pp. 291–338, John Wiley & Sons Ltd.

Church, M., and A. Zimmermann (2007), Form and stability of step-pool channels: Research progress, *Water Resources Res*, *43*, W03,415, doi:10.1029/2006WR005037.

Church, M., M. A. Hassan, and J. F. Wolcott (1998), Stabilizing self-organized structures in gravel-bed stream channels: Field and experimental observations, *Water Resources Research*, *34*(11), 3169–3179.

Cudden, J. R., and T. B. Hoey (2003), The causes of bedload pulses in a gravel channel: the implications of bedload grain-size distributions, *Earth Surface Processes and Landforms*, *28*(13), 1411–1428.

Cui, Y., and G. Parker (2005), Numerical model of sediment pulses and sediment-supply disturbances in mountain rivers, *Journal of Hydraulic Engineering*, *131*(8), 646–656.

Cui, Y. T., G. Parker, T. E. Lisle, J. Gott, M. E. Hansler-Ball, J. E. Pizzuto, N. E. Allmendinger, and J. M. Reed (2003), Sediment pulses in mountain rivers: 1. Experiments, *Water Resources Research*, *39*(9), 1239, doi:10.1029/2002WR001803.

Davies, T. R. H., and A. I. Lee (1988), Physical hydraulic modelling of width reduction and bed level change in braided rivers, *Journal of Hydrology (NZ)*, *27*(2), 113–127.

Dietrich, W., and J. Smith (1984), Bed load transport in a river meander, *Water Resources Research*, *20*(10), 1355–1380.

Dietrich, W., P. Nelson, E. Yager, J. Venditti, M. Lamb, and L. Collins (2005), Sediment patches, sediment supply, and channel morphology, in *River, Coastal and Estuarine Morphodynamics: RCEM 2005*, edited by G. Parker and M. Garcia, pp. 79–90.

Dietrich, W. E., and J. D. Smith (1983), Processes controlling the equilibrium bed morphology in river meanders, in *River Meandering*, pp. 759–769, ASCE.

Dietrich, W. E., J. W. Kirchner, H. Ikeda, and F. Iseya (1989), Sediment supply and the development of the coarse surface layer in gravel-bedded rivers, *Nature*, *340*(6230), 215–217.

Diplas, P., and J. B. Fripp (1992), Properties of various sediment sampling procedures, *Journal of Hydraulic Engineering, ASCE*, *118*(7), 955–970.

Drake, T., R. Shreve, W. Dietrich, P. Whiting, and L. Leopold (1988), Bedload transport of fine gravel observed by motion-picture photography, *Journal of Fluid Mechanics*, *192*, 193–217.

Eaton, B. (2013), Hydraulic geometry: empirical investigations and theoretical approaches, in *Treatise on Geomorphology*, vol. 9, edited by J. Shroder and E. Wohl, Academic Press.

Eaton, B. C., and M. Church (2004), A graded stream response relation for bedload dominated streams, *Journal of Geophysical Research - Earth Surface*, *109*(F03011), doi: 10.1029/2003JF000,062.

Eaton, B. C., and M. Church (2009), Channel stability in bed load-dominated streams with nonerodible banks: Inferences from experiments in a sinuous flume, *Journal of Geophysical Research - Earth Surface*, *114*(F01024), doi: 10.1029/2007JF000,902.

Eaton, B. C., and T. R. Giles (2009), Assessing the effect of vegetation-related bank strength on channel morphology and stability in gravel bed streams using numerical models, *Earth Surface Processes and Landforms*, *34*(5), 712–714.

Eaton, B. C., and M. F. Lapointe (2001), Effects of large floods on sediment transport and reach morphology in the cobble-bed Sainte Marguerite River, *Geomorphology*, *40*(3–4), 291–309.

Eaton, B. C., M. Church, and R. G. Millar (2004), Rational regime model of alluvial channel morphology and response, *Earth Surface Processes and Landforms*, *29*(4), 511–529.

Eaton, B. C., C. A. E. Andrews, T. R. Giles, and J. C. Phillips (2010a), Wildfire, morphologic change and bed material transport at Fishtrap Creek, British Columbia, *Geomorphology*, *118*, 409–424.

Eaton, B. C., R. D. Moore, and T. R. Giles (2010b), Forest fire, bank strength and channel instability: the 'unusual' response of Fishtrap Creek, British Columbia, *Earth Surface Processes and Landforms*, *35*(10), 1167–1183.

Ehrenberger, R. (1931), Direct bedload measurements at the Danube near Vienna and their results to date, *Die Wasserwirtschaft*, *34*, 1–9.

Einstein, H. A. (1937), The calibration of the bedload trap used in the rhine, *Schweuzerische Bauzeitung*, *110*, 29–32.

Emmett, W. W. (1976), Bedload transport in two large, gravel-bed rivers, Idaho and Washington, in *Proceedings of the 3rd Intra-Agency Sedimentation Conference*, pp. 4–101 – 4–114.

Ettema, R., R. Arndt, P. Roberts, and T. Wahl (2000), *Hydraulic modeling: concepts and practice*, no. 97 in Task Committee on Hydraulic Modeling, Environmental and Water Resources Institute, manual of practice no. 97 ed., 390 pp., ASCE Publication.

Ferguson, R. I. (2003), The missing dimension: effects of lateral variation on 1-d calculations of fluvial bedload transport, *Geomorphology*, *56*(1-2), 1–14.

Francalanci, S., S. Solair, M. Toffolon, and G. Parker (2012), Do alternate bars affect sediment transport and flow-resistance in gravel-bed rivers?, *Earth Surface Processes and Landforms*, *37*(8), 866–875.

Friedkin, J. F. (1945), A laboratory study of the meandering of alluvial rivers, *Tech. rep.*, US Waterways Engineering Experimental Station.

Fripp, J., and P. Diplas (1993), Surface sampling in gravel streams, *Journal of Hydraulic Engineering*, *119*(4), 473–490.

Gaeumann, D., J. Schmidt, and P. Wilcock (2005), Complex channel responses to changes in stream flow and sediment supply on the lower Duchesne River, Utah, *Geomorphology*, *64*(3-4), 185–206.

Gilbert, G. (1880), *Report of the Geology of the Henry Mountains*, 170 pp., US Government Printing Office.

Gilbert, G. K. (1914), *The transport of debris by running water*, no. 86 in U.S. Geological Survey Professional Paper 105, 154 pp., U.S. Geological Survey.

Gintz, D., M. Hassan, and K. Schmidt (1996), Frequency and magnitude of bedload transport in a mountain river, *Earth Surface Processes and Landforms*, *21*(5), 433–446.

Gomez, B. (1983), Temporal variations in the particle size distribution of surficial bed material: the effect of progressive bed armouring, *Geografiska Annaler.*, *65*(3–4), 183–192.

Gomez, B., and M. Church (1989), An assessment of bed load sediment transport formulae for gravel bed rivers, *Water Resources Research*, *25*(6), 1161–1186.

Gomi, T., and R. Sidle (2003), Bed load transport in managed steep-gradient headwater streams of southeastern Alaska, *Water Resources Research*, *39*(12), 1336, doi: 10.1029/2003WR002440.

Gran, K., and D. Montgomery (2005), Spatial and temporal patterns in fluvial recovery following volcanic eruptions: Channel response to basin-wide sediment loading at Mount Pinatubo, Philippines., *Geological Society of America Bulletin*, *117*(1–2), 195–211.

Gran, K., D. Montgomery, and D. Sutherland (2006), Channel bed evolution and sediment transport under declining sand inputs, *Water Resources Research*, *42*(10), W10,407, doi:10.1029/2005WR004306.

Haschenburger, J., and P. Wilcock (2003), Partial transport in a natural gravel bed channel, *Water Resources Research*, *39*(1), 1020–1029, doi:10.1029/2002WR001532.

Hassan, M., R. Egozi, and G. Parker (2006), Experiments on the effect of hydrograph characteristics on vertical grain sorting in gravel bed rivers, *Water Resources Research*, *42*(9), doi:10.1029/2005WR004707.

Hassan, M., B. Smith, D. Hogan, D. Luzi, A. Zimmermann, and B. Eaton (2007), Sediment storage and transport in coarse bed streams: scale considerations, in *Gravel-Bed Rivers VI: From Process Understanding to River Restoration*, vol. 11, edited by H. Habersack, H. Piegay, and M. Rinaldi, pp. 473–496, Elsevier.

Hassan, M. A., and M. Church (2000), Experiments on surface structure and partial sediment transport on a gravel bed, *Water Resources Research*, *36*(7), 1885–1895.

Hassan, M. A., and M. Church (2001), Sensitivity of bed load transport in harris creek: Seasonal and spatial variation over a cobble-gravel bar, *Water Resources Research*, *37*(3), 813–825.

Hassan, M. A., M. Church, T. E. Lisle, F. Brardinoni, L. Benda, and G. E. Grant (2005), Sediment transport and channel morphology of small, forested streams, *Journal of the American Water Resources Association*, *41*(4), 853–876.

Hein, F., and R. Walker (1976), Bar evolution and development of stratification in the gravelly, braided, Kicking Horse River, British Columbia, *Canadian Journal of Earth Science*, *14*(4), 562–570.

Hoey, T. (1992), Temporal variations in bedload transport rates and sediment storage in gravel-bed rivers, *Progress in Physical Geography*, *16*(3), 319–338.

Hoey, T., and A. Sutherland (1991), Channel morphology and bedload pulses in braided rivers: a laboratory study, *Earth Surface Processes and Landforms*, *16*(5), 447–462.

Hooke, J. M. (2007), Spatial variability, mechanism and propagation of change in an active meandering river, *Geomorphology*, *84*(3), 277–296.

Iseya, F., and H. Ikeda (1987), Pulsations in bedload transport rates induced by a longitudinal sediment sorting: a flume study using sand and gravel mixtures, *Geografiska Annaler. Series A. Physical Geography*, *69*(1), 15–27.

Jackson, W. L., and R. L. Beschta (1982), A model of two-phase bedload transport in an oregon coast range stream, *Earth Surface Processes and Landforms*, *7*(6), 517–527.

Jackson, W. L., and R. L. Beschta (1984), Influences of increased sand delivery on the morphology of sand and gravel channels, *Water Resources Bulletin*, *20*(4), 527–533.

Jones, C. (1977), Effects of varying discharge regimes on bed-form sedimentary structures in modern rivers, *Geology*, *5*(9), 567–570.

Jones, L. S., and N. F. Humphrey (1997), Weathering-controlled abrasion in a coarse-grained meandering reach of the Rio Grande: implications for the rock record, *Geological Society of America Bulletin*, *109*(9), 1080–1088.

Kasai, M., T. Manutani, and G. Brierley (2004), Channel bed adjustments following major aggradation in a steep headwater setting: Findings from Oyabu Creek, Kyushu, Japan, *Geomorphology*, *14*(4), 199–215.

Kellerhals, R., and M. Church (1989), The morphology of large rivers: characterization and management, *Can. Spec. Publsl Fish. Aquat. Sci*, *106*, 31–48.

Kennedy, R. G. (1895), The prevention of silting in irrigation canals, in *Proc. Inst. of Civ. Engrs.*, vol. 119, pp. 281–290.

Kirchner, J., W. Dietrich, F. Iseya, and H. Ikeda (1990), The variability of critical shear stress, friction angle, and grain protrusion in water-worked sediments, *Sedimentology*, *37*(4), 647–672.

Komar, P. D. (1987), Selective grain entrainment by a current from a bed of mixed sizes: a reanalysis, *Journal of Sedimentary Petrology*, *57*(2), 203–211.

Kuhnle, R. (1996), Unsteady transport of sand and gravel mixtures, in *Advances in Fluvial Dynamics and Stratigraphy*, edited by P. Carling and M. Dawson, pp. 183–201, John Wiley.

Kuhnle, R., and J. Willis (1998), Statistics of sediment transport in Goodwin Creek, *Journal of Hydraulic Engineering*, *124*(11), 1109–1114.

Kuhnle, R., J. Horton, S. Bennett, and J. Best (2006), Bed forms in bimodal-sand-gravel sediments: laboratory and field analysis, *Sedimentology*, *53*(3), 631–654.

Kuhnle, R. A., and J. B. Southard (1988), Bed load transport fluctuations in a gravel bed laboratory channel, *Water Resources Research*, *24*(2), 247–260.

Kuhnle, R. A., and J. B. Southard (1990), Flume experiments on the transport of heavy minerals in gravel-bed streams, *Journal of Sedimentary Research*, *60*(5), 687–696.

Lacey, G. (1930), Stable channels in alluvium, *Proceedings of the Institution of Civil Engineers*, *229*, 259–384.

Lane, E. (1937), Stable channels in erodible material, *Transactions of the American Society of Civil Engineers*, *63*, 123–142.

Lane, E. (1955), Design of stable channels, *American Society of Civil Engineers, Transactions*, *120*, 1234–1260.

Lane, S. N., and K. S. Richards (1997), Linking river channel form and process: time, space and causality revisited, *Earth Surface Processes and Landforms*, *22*(3), 249–260.

Laronne, J., and M. Carson (1976), Interrelationships between bed morpholog and bed-material transport for a small gravel-bed channel, *Sedimentology*, *23*(1), 67–85.

Lenzi, M., V. D'Agostino, and P. Billi (1999), Bedload transport in the instrumented catchment of the Rio Cordon: Part i: Analysis of bedload records, conditions and threshold of bedload entrainment, *Catena*, *36*(6), 171–190.

Leopold, L. B., and T. Maddock (1953), The hydraulic geometry of stream channels and some physiographic implications, *U.S. Geol. Surv. Prof. Pap.*, *252*.

Lewin, J. (1976), Initiation of bed forms and meanders in coarse-grained sediment, *Geological Society of America Bulletin*, *87*(2), 281–285.

Lisle, T. (1995), Particle size variations between bed load and bed material in natural gravel bed channels, *Water Resources Research*, *31*(4), 1107–1118.

Lisle, T. (2012), Transport capacity, bedrock exposure, and process domains, in *Gravel-bed Rivers: Processes, Tools, and Environments*, edited by M. Church, P. M. Biron, and R. A. G., first ed., John Wiley & Sons Ltd.

Lisle, T., F. Iseya, and H. Ikeda (1993), Response of a channel with alternate bars to a decrease in supply of mixed-size bed load: A flume experiment, *Water Resources Research*, *29*(11), 3623–3629.

Lisle, T., J. Pizzuto, H. Ikeda, F. Iseya, and Y. Kodama (1997), Evolution of a sediment wave in an experimental channel, *Water Resources Research*, *33*(8), 1971–1981.

Lisle, T. E. (1982), Effects of aggradation and degradation on riffle-pool morphology in natural gravel channels, northwestern California, *Water Resources Research*, *18*(6), 1643–1651.

Lisle, T. E. (1986), Stabilization of a gravel channel by large streamside obstructions and bedrock bends, Jacoby Creek, northwestern California, *Water Resources Research*, *18*, 1643–1651.

Lisle, T. E. (1989), Sediment transport and resulting deposition in spawning gravels, north coastal California, *Water Resources Research*, *25*(6), 1303–1319.

Lisle, T. E., and M. Church (2002), Sediment transport-storage relations for degrading, gravel bed channels, *Water Resources Research*, *38*(11), 1219, doi: 10.1029/2001WR001086.

Lisle, T. E., and S. Hilton (1992), The volume of fine sediment in pools - an index of sediment supply in gravel-bed streams, *Water Resources Bulletin*, *28*(2), 371–383.

Lisle, T. E., H. Ikeda, and F. Iseya (1991), Formation of stationary alternate bars in a steep chanel with mixed-size bed load: A flume experiment, *Earth Surface Processes and Landforms*, *16*(5), 463–469.

Lisle, T. E., J. M. Nelson, J. Pitlick, M. A. Madej, and B. L. Barkett (2000), Variability of bed mobility in natural, gravel-bed channels and adjustments to sediment load at local and reach scales, *Water Resources Research*, *36*(12), 3743–3755.

Mackin, J. H. (1948), Concept of the graded river, *Geological Society of America Bulletin*, *59*(5), 463 – 512.

Madej, M. (2001), Development of channel organization and roughness following sediment pulses in single-thread, gravel bed rivers, *Water Resources Research*, *37*(8), 2259–2272.

Madej, M., and V. Ozaki (1996), Channel response to sediment wave propagation and movement, redwood creek, california, usa, *Earth Surface Processes and Landforms*, *21*(10), 911–927.

Madej, M. A., D. Sutherland, T. E. Lisle, and B. Pryor (2009), Channel responses to varying sediment input: a flume experiment modeled after Redwood Creek, California, *Geomorphology*, *103*(4), 507–591.

McNamara, J., J. Oatley, D. Kane, and L. Hinzman (2008), Case study of a large summer flood on the north slope of Alaska: bedload transport, *Hydrology Research*, *39*(4), 299–308.

Millar, R. G. (2000), Influence of bank vegetation on alluvial channel patterns, *Water Resources Research*, *36*(4), 1109–1118.

Millar, R. G., and M. C. Quick (1993), Effect of bank stability on geometry of gravel rivers, *Journal of Hydraulic Engineering-ASCE*, *119*(12), 1343–1363.

Milne, A. (1928), *The House at Pooh Corner*, 1988 print ed., Dutton's Children Books.

Montgomery, D., J. Buffington, R. Smith, K. Schmidt, and G. Pess (1995), Pool spacing in forest channels, *Water Resources Research*, *31*(4), 1097–1105.

Montgomery, D. R., and J. M. Buffington (1997), Channel-reach morphology in mountain drainage basins, *Geological Society of America Bulletin*, *109*(5), 596–611.

Montgomery, D. R., and J. M. Buffington (1998), Channel processes, classification, and response, in *River Ecology and Management*, edited by R. Naiman and R. Bilby, pp. 13–42, Springer-Verlag, New York.

Moreton, D., P. Ashworth, and J. Best (2002), The physical scale modeling of braided alluvial architecture and estimation of subsurface permeability, *Basin Research*, *14*(3), 265–285.

Nanson, G. C. (1974), Bedload and suspended-load transport in a small, steep, mountain stream, *American Journal of Science*, *274*(5), 471–486.

Nash, D. (1994), Sediment-transporting discharge from magnitude-frequency analysis, *Journal of Geology*, *102*(1), 79–95.

Nelson, J. M. (1988), Mechanics of flow and sediment transport over non-uniform erodible beds, Ph.D. thesis, University of Washington.

Nelson, P., J. G. Venditti, W. E. Dietrich, J. W. Kirchner, H. Ikeda, F. Iseya, and L. Sklar (2009), Response of bed surface patchiness to reductions in sediment supply, *Journal of Geophysical Research - Earth Surface*, *114*(F02005), doi:10.1029/2008JF001,144.

Nelson, P., W. Dietrich, and J. Venditti (2010), Bed topography and the development of forced bed surface patches, *Journal of Geophysical Research*, *115*, F04,024, doi: 10.1029/2010JF001747.

Nitsche, M., D. Rickenmann, J. Turowski, A. Badoux, and J. Kirchner (2011), Evaluation of bedload transp[ort predictions using flow resistance equations to account for macro-roughness in steep mountain streams, *Water Resources Research*, *47*, W08,513, doi: 10.1029/2011WR010645.

Nordin, C. F. (1985), The sediment loads of rivers, in *Facets of hydrology*, edited by J. C. Rodda, pp. 183–204, Wiley.

Nunnally, N. R. (1985), Application of fluvial relationships to planning and design of channel modifications, *Environmental Management*, *9*(5), 417–426.

Paola, C., and R. Seal (1995), Grain-size patchiness as a cause of selective deposition and downstream fining, *Water Resources Research*, *31*(5), 1395–1407.

Papanicolaou, A., and A. Schuyler (2003), Cluster evolution and flow-frictional characteristics under difference sediment availablilities and specific gravity, *Journal of Engineering Mechanics*, *129*(10), 1206–1219, doi:10.1061/(ASC)0733-9399(2003)129:10(1206).

Parker, G. (1990), Surface-based bedload transport relation for gravel rivers, *Journal of Hydraulic Research*, *28*(4), 417–436.

Parker, G., and P. C. Klingeman (1982), On why gravel bed rivers are paved, *Water Resources Research*, *18*(5), 1409–1423.

Parker, G., and A. W. Peterson (1980), Bar resistance of gravel-bed streams, *Journal of the Hydraulics Division-ASCE*, *106*(Hy10), 1559–1575, american Society of Civil Engineers. New York, NY, United States. 1980. Serial.

Parker, G., and C. M. Toro-Escobar (2002), Equal mobility of gravel in streams: The remains of the day, *Water Resources Research*, *38*(11), 1264, doi:10.1029/2001WR000669.

Parker, G., S. Dhamotharan, and H. Stefan (1982), Model experiments on mobile, paved gravel bed streams, *Water Resources Research*, *18*(5), 1395–1408.

Parker, G., C. M. Toro-Escobar, M. Ramey, and S. Beck (2003), Effect of floodwater extraction on mountain stream morphology, *Journal of Hydraulic Engineering*, *129*(11), 885–895.

Parker, G., M. A. Hassan, and P. Wilcock (2007a), Adjustment of the bed surface size distribution of gravel-bed rivers in response to cycled hydrographs, in *Gravel Bed Rivers 6: From Process Understanding to River Restoration*, vol. 11, edited by H. Habersack, H. Piegay, and M. Rinaldi, pp. 241 – 290, Elsevier.

Parker, G., P. Wilcock, C. Paola, W. Dietrich, and J. Pitlick (2007b), Physical basis for quasi-universal relations describing bankfull hydraulic geometry of single-thread gravel bed rivers, *Journal of Geophysical Research - Earth Surface*, *112*, F04,005, doi: 10.1029/2006JF000549.

Peakall, J., P. Ashworth, and J. L. Best (1996), Physical modelling in fluvial geomorphology: principles applications and unresolved issues, in *The scientific nature of geomorphology: Proceedings of the 27th Binghamton Symposium in Geomorphology*, edited by B. Rhoads and C. Thorn, pp. 221–253, John Wiley & Sons Ltd.

Phillips, J. (2007), Post-fire dynamics of a gravel bed stream: Fishtrap Creek, British Columbia, Msc, The University of British Columbia.

Pickup, G., and R. F. Warner (1976), Effects of hydrologic regime on magnitude and frequency of dominant discharge, *Journal of Hydrology*, *29*(1/2), 51–75.

Pilon, P., and D. Harvey (1993), *CFA - Consolidated Frequency Analysis version 3.1*, Environment Canada, Surveys and Information Systems Branch.

Pitlick, J., E. Mueller, C. Segura, R. Cress, and M. Torizzo (2008), Relation between flow, surface-layer armoring and sediment transport in gravel-bed rivers, *Earth Surface Processes and Landforms*, *33*(8), 1192–1209.

Pizzuto, J. (1994), Channel adjustments to changing discharges, Powder River, Montana, *GSA*, *106*(11), 1494–1501.

Powell, D. M. (1998), Patterns and processes of sediment sorting in gravel-bed rivers, *Progress in Physical Geography*, *22*(1), 1–31.

Powell, M., I. Reid, and J. Laronne (2001), Evolution of bed load grain size distribution with increasing flow strength and the effect of flow duration on the caliber of bed load sediment yield in ephemeral gravel bed rivers, *Water Resources Research*, *37*(5), 1463–1474.

Prestegaard, K. (1987), Sediment tarnsport and depostion zones in braided streams, in *Erosion and Sedimentation in the Pacific Rim*, no. 165 in IAHS Publ., pp. 411–412.

Pryor, B., T. Lisle, D. Montoya, and S. Hilton (2011), Transport and storage of bed material in a gravel-bed channel during episodes of aggradation and degradation: a field and flume study, *Earth Surface Processes and Landforms*, *36*, 2028–2041, doi:10.1002/esp.2224.

Recking, A. (2010), A comparison between flume and field bed load transport data and consequences fro surface-based bed load transport prediction, *Water Resources Research*, *46*, WO3518, doi:10.1029/2009WR008007.

Recking, A., P. Frey, A. Paquier, and P. Belleudy (2009), An experimental investigation of mechanisms involved in bed load sheet production and migration, *Journal of Geophysical Research*, *114*, F03,010, doi:10.1029/2008JF000990.

Reid, I., L. Frostick, and J. Layman (1985), The incidence and nature of bedload transport during flood flows in coarse-grained alluvial channels, *Earth Surface Processes and Landforms*, *10*, 33–44.

Robert, A. (2003), *River Processes: An Introduction to Fluvial Dynamics*, 214 pp., Arnold.

Ryan, S., L. Porth, and C. Troendle (2005), Coarse sediment transport in mountain streams in Colorado and Wyoming, USA, *Earth Surface Processes and Landforms*, *30*, 269–288.

Schuerch, P., A. Densmore, B. McArdell, and P. Molnar (2006), The influence of landsliding on sediment supply and channel change in a steep mountain catchment, *Geomorphology*, *78*(3), 222–235.

Schumm, S. (1977), *The Fluvial System*, 338 pp., John WIley & Sons.

Schumm, S., and R. Lichty (1965), Time, space, and causality in geomorphology, *American Journal of Science*, *263*, 110–119.

Schumm, S. A. (1969), River metamorphosis, *Journal of the Hydraulics Division-ASCE*, *95*(HY1), 255–273.

Schumm, S. A., and H. R. Khan (1972), Experimental study of channel patterns, *Geological Society of America Bulletin*, *83*, 1755–1770.

Seminara, G. (1998), Stability and morphodynamics, *Meccanica*, *33*, 59–99.

Seminara, G., M. Colombini, and G. Parker (1996), Nearly pure sorting waves and formation of bedload sheets, *Journal of Fluid Mechanics*, *312*, 253–278.

Shvidchenko, A., and Z. D. Kopaliani (1998), Hydraulic modeling of bed load transport in gravel-bed Laba River, *Journal of Hydraulic Engineering*, *124*(8), 778–785.

Simon, A. (1992), Energy, time, and channel evolution in catastrophically disturbed fluvial systems, *Geomorphology*, *5*(3), 345–372.

Simon, A., and C. Hupp (1986), Channel evolution in modified Tennessee channels, in *Proceedings of the Fourth Federal Interagency Sedimentation Conference: March 24-27, 1986, Las Vegas, Nevada*, vol. 2, pp. 71–82, Subcommittee on Sedimentation of the Interagency Advisory Committee on Water Data, US Government Printing Office.

Sklar, L., W. E. Dietrich, E. Foufoula-Georgiou, B. Lashermes, and D. Bellugi (2006), Do gravel bed river size distributions record channel network structure?, *Water Resources Research*, *42*(W06D18), doi:10.1029/2006WR005,035.

Smith, B. J. (2004), Relations between bed material transport and storage during aggradation and degradation in a gravel bed channel, Master's thesis, Humboldt State University.

Smith, N. (1974), Sedimentology and bar formation in the Upper Kicking Horse river, a braided outwash stream, *The Journal of Geology*, *82*(2), 205–223.

Tal, M., and C. Paola (2007), Dynamic single-thread channels maintained by the interaction of flow and vegetation, *Geology*, *35*(4), 347–350.

Talbot, T., and M. Lapointe (2002), Modes of response of a gravel bed river to meander straightening: The case of the Sainte-Marguerite River, Saguenay Region, Quebec, Canada, *Water Resources Research*, *38*(6), 1073, doi:10.1029/2001wr000324.

Thompson, C., and J. Croke (2008), Channel flow competence and sediment transport in upland streams in southeast austalia, *Earth Surface Processes and Landforms*, *33*, 329–352.

Venditti, J., W. Dietrich, P. Nelson, M. Wydzga, J. Fadde, and S. L. (2010), Effect of sediment pulse grain size on sediment transport rates and bed mobility in gravel bed rivers, *Journal of Geophysical Research*, *115*, 2003–2012, doi:10.1029/2009JF001418.

Waldon, M. (2004), Estimation of average stream velocity, *Journal of Hydraulic Engineering*, *130*(11), 1119–1122.

Warburton, J. (1992), Observations of bed load transport and channel bed changes in a proglacial mountain stream, *Arctic snd Alpine Research*, *24*(3), 195–203.

Warburton, J., and T. Davies (1994), Variability of bedload transport and channel morphology in a braided river hydraulic model, *Earth Surface Processes and Landforms*, *19*, 403–421.

Wathen, S., R. Ferguson, T. Hoey, and A. Werritty (1995), Unequal mobility of gravel and sand in weakly bimodal river sediments, *Water Resources Research*, *31*(8), 2087–2096.

Whiting, P., W. Dietrich, L. Leopold, and L. Collins (1985), The variability of sediment transport in a fine-gravel stream (abs), in *International Fluvial Sedimentology Conference, 3rd*, p. 38, Colorado State University Press.

Whiting, P., W. Dietrich, L. Leopold, T. Drake, and R. Shreve (1988), Bedload sheets in heterogeneous sediment, *Geology*, *16*(2), 105–108.

Whiting, P., J. Stamm, D. Moog, and R. Orndorff (1999), Sediment-transporting flows in headwater streams, *GSA Bulletin*, *111*(3), 450–466.

Whiting, P. J. (1997), The effect of stage on flow and components of the local force balance, *Earth Surface Processes and Landforms*, *22*, 517–530.

Wilcock, P. (1992), Experimental investigation of the effect of mixture properties on transport dynamics, in *Dynamics of Gravel-bed Rivers*, edited by P. Billi, R. Hey, C. Thorne, and P. Tacconi, pp. 109–139, John Wiley & Sons Ltd.

Wilcock, P. (2001a), Toward a practical method for estimating sediment-transport rates in gravel-bed rivers, *Earth Surface Processes and Landforms*, *26*(13), 1395–1408, doi: 10.1002/esp.301.

Wilcock, P. (2001b), The flow, the bed, and the transport: interaction in flume and field, in *Gravel-bed Rivers V*, edited by M. Mosley, pp. 181–220, New Zealand Hydrological Society, Wellington, New Zealand.

Wilcock, P., and B. McArdell (1993), Surface-based fractional transport rates: mobilization thresholds and partial transport of a sand-gravel sediment, *Water Resources Research*, *29*(4), 1297–1312.

Wilcock, P., and B. McArdell (1997), Partial transport of a sand/gravel sediment, *Water Resources Research*, *33*(1), 235–245.

Wilcock, P., and J. Southard (1989), Bed load transport of mixed size sediment: fractional transport rates, bed forms, and the development of a coarse bed surface layer, *Water Resources Research*, *257*, 1629–1641.

Wilcock, P., S. Kenworthy, and J. Crowe (2001), Experimental study of the transport of mixed sand and gravel, *Water Resources Research*, *37*(12), 3349–3358.

Wittenberg, L., and M. D. Newson (2005), Particle clusters in gravel-bed rivers: an experimental morphological approach to bed material transport and stability concepts, *Earth Surface Processes and Landforms*, *30*, 1351–1368.

Wolman, M. G., and J. P. Miller (1960), Magnitude and frequency of forces in geomorphic processes, *Journal of Geology*, *68*, 54 – 74.

Wong, M., and G. Parker (2006), One-dimensional modeling of bed evolution in a gravel bed river subject to a cycled flood hydrograph, *Journal of Geophysical Research*, *111*, doi:10.1029/2006JF000478.

Wooldridge, C., and E. Hickin (2005), Radar architecture and evolution of channel bars in wandering gravel-bed rivers: Fraser and Squamish Rivers, British Columbia, Canada, *Journal of Sedimentary Research*, *75*, 844–860.

Yalin, S. M. (1971), On the formation of dunes and meanders, in *Proceedings of the 14th Congress of the International Association of Hydraulic Research*, Paper C13, pp. 1–8.

Young, W., and J. Warburton (1996), Principles and practice of hydraulic modeling of braided gravel-bed rivers, *Journal of Hydrology, New Zealand*, *35*(2), 175–198.